THE UNIVERSITY *of* EDINBURGH

This thesis has been submitted in fulfilment of the requirements for a postgraduate degree (e.g. PhD, MPhil, DClinPsychol) at the University of Edinburgh. Please note the following terms and conditions of use:

- This work is protected by copyright and other intellectual property rights, which are retained by the thesis author, unless otherwise stated.
- A copy can be downloaded for personal non-commercial research or study, without prior permission or charge.
- This thesis cannot be reproduced or quoted extensively from without first obtaining permission in writing from the author.
- The content must not be changed in any way or sold commercially in any format or medium without the formal permission of the author.
- When referring to this work, full bibliographic details including the author, title, awarding institution and date of the thesis must be given.

Study into a role for Aar2p in U5 snRNP biogenesis

Vanessa Solange Fernandes de Oliveira Cristão

A thesis presented for the degree of Doctor of Philosophy

The University of Edinburgh
2010

DECLARATION

I hereby declare that I alone composed this thesis and that the work presented here is my own, except where stated otherwise.

September 2010

Acknowledgements

Thank you to Jean for accepting me as a member of her lab, for all the helpful suggestions and for being so caring and understanding.

I am grateful to Fundação Calouste Gulbenkian, Instituto Gulbenkian de Ciência and Fundação para a Ciência e a Tecnologia for funding my studies and making this thesis possible.

To past and present members of the Beggs lab thank you for all the help when things didn't go as planned and for teaching me how to do loads of thing in the lab. Thank you for making the Beggs lab a great place to work.

Thanks to: Josefin Fernius for the help with experiments; Flávia Alves and Juri Rappsilber for the mass spectrometry analysis; Janusz Bujnicki for helpful suggestions; Patricia Fabrizio for antibodies and yeast strain; Patricia Rischitor for plasmids; the Tyers lab for yeast strains; the Tollervey lab for kindly sharing material and reagents.

To my family and friends thank you for all the care, support and encouragement.

To Hugo, I could never make it without you. Thank you for everything.

Abstract

Aar2p is an essential yeast protein involved in pre-mRNA splicing and component of a U5 snRNP precursor form. It has been suggested that the mature U5 snRNP and U4/U6.U5 tri-snRNP assemble from the Aar2p-U5 core particle that is formed in the cytoplasm. After nuclear import, Aar2p would be displaced from its interaction with Prp8p in the Aar2p-U5 particle and the mature U5 snRNP would be formed by interaction of Brr2p with Prp8p. In one model, Aar2p acts as a transport factor either for nuclear import of the Aar2p-U5 particle, or for nucleocytoplasmic shuttling of Prp8p. As a non-mutually exclusive alternative, Aar2p can function as a chaperone, regulating the Prp8p/Brr2p interaction.

In this thesis I investigate the role of Aar2p in U5 snRNP biogenesis. I demonstrate by fluorescence microscopy that Aar2p is not required for nuclear localisation of the U5 snRNP components Snu114p and Prp8p. By a yeast two-hybrid (Y2H) assay I establish that $Prp8p_{1649-2413}$ interacts with $Aar2p_{1-170}$ but not with $Aar2p_{150-355}$. I also show for the first time that Aar2p is phosphorylated in five aminoacids: S253, T274, Y328, S331 and T345. In my Y2H system S253 phosphorylation disrupts the Aar2p/Prp8p interaction. This suggests a mechanism whereby formation of the mature U5 snRNP and activation of Brr2p by Prp8p may be regulated through phosphorylation. Surprisingly, when the S253A and S253E mutations are inserted into genomic *AAR2* there is no change in the amount of Prp8p and U5 snRNA immunoprecipitated by Aar2p.

Finally, using $Aar2p_{1-170}$ as bait for a Y2H screen, a variety of new Aar2p interactors are revealed. The obtained preys include the other half of Aar2p itself, proteins involved in DNA damage repair, chromatin-binding, ubiquitin-binding and membrane proteins. Overall these results suggest that besides modulating splicing, Aar2p is involved in several other important cellular processes.

Table of contents

Common Abbreviations

˚C	Degree Celsius
aa	Aminoacid(s)
3AT	3-amino-triazole
ATP	Adenosine-5'-triphosphate
bp	Base-pair
BSA	Bovine serum albumin
Da	Dalton
DNA	Deoxyribonucleic acid
dNTP	Deoxynucleoside triphosphate
DTT	Dithiothreitol
ECL	Enhanced Chemi-Luminescence
EDTA	Ethylenediaminetetraacetic acid
EGTA	Ethylene glycol tetraacetic acid
g	Gram(s)
h	Hour(s)
HEPES	4-(2-hydroxyethyl)-1-piperazineethanesulfonic acid
Ig	Immunoglobulin
kb	Kilobase
L	Litre(s)
M	Molar (moles per litre)
min	Minute(s)
mRNA	Messenger RNA
o/n	Over/night
OD	Optical density
ORF	Open Reading Frame
PCR	Polymerase Chain Reaction
Prp8p-CTF	C-terminal fragment of Prp8p, $Prp8p_{1806-2413}$ that contains part of the RNaseH and Jab1/MPN domains
RNA	Ribonucleic acid
rpm	Revolutions per minute
s	Second(s)
SDS	Sodium Dodecyl Sulphate
snRNA	Small nuclear RNA
Ss	Splice site
TCA	Trichloroacetic acid
Tris	Tris(hydroxymethyl)aminomethane
V	Volt(s)
v/v	Volume unit per volume
w/v	Weight unit per volume

CHAPTER 1 - Introduction

1.1 Pre-mRNA splicing

Pre-mRNA (precursor of messenger RNA) is the immediate product of transcription by RNA polymerase II, enclosing all the information encoded on DNA. Pre-mRNA is composed of introns (non-coding sequences) and exons (the sequences retained in the mature mRNA – usually coding sequences).

Introns are a substantial component of genomes and can be divided into several groups according to their mechanism of removal: group I, group II, nuclear precursor messenger RNA (pre-mRNA) and tRNA introns (Stoltzfus, 2001). If the gene contains one or more introns, in order to serve as a template for translation, the pre-mRNA has to be processed - the introns have to be removed and the flanking exons have to be joined by a process designated splicing (Berget *et al.*, 1977; Chow *et al.*, 1977). Despite showing extremely divergent sequences, three short regions of consensus sequence identify pre-mRNA introns and are active agents in the splicing reaction: the 5' splice site, the branchpoint and the 3' splice site.

Splicing is a basic process, conserved across eukaryotes and its disruption can lead to various serious diseases (Wang & Cooper, 2007). The majority of higher eukaryote genes contain more that one intron. This feature permits exons to be joined in multiple combinations, by a process denominated alternative splicing (Leff *et al*., 1986). Alternative splicing adds an extra level to the eukaryotic proteome complexity, allowing different protein isoforms to be expressed from the same genomic sequence. All this is due to a change in the splice-site recognition that can be mediated by several factors (Keren *et al*., 2010).

One of the most widely used model organisms to study pre-mRNA splicing is the budding yeast, *Saccharomyces cerevisiae*. Found in only a small percentage of genes in *S. cerevisiae* (approximately 4%), budding yeast introns are usually relatively short and are generally located near the pre-mRNA 5' end (Beggs, 2001). Only a few *S. cerevisiae* genes have two introns (Miura *et al*., 2006).

1.2 The splicing reaction

Intron removal and simultaneous exon ligation are accomplished by two sequential transesterification reactions. First the 2’ hydroxyl group of the intron branchpoint adenosine causes a nucleophilic attack to the phosphate at the 5’ splice site resulting in cleavage of the phosphodiester bond. From this appear: a free 3’ hydroxyl in exon 1; and a covalent ligation (2’–5’ phosphodiester bond) between the 5’ end of the intron and the branchpoint adenosine, resulting in an intron–exon 2 branched lariat structure. Secondly, the free 3’ hydroxyl of exon 1 brings about a nucleophilic attack at the 3’ splice site and cleaves it. A 3’–5’ phosphodiester bond joins the exons at the same time the intron is released, with messenger RNA being formed (Figure 1.1).

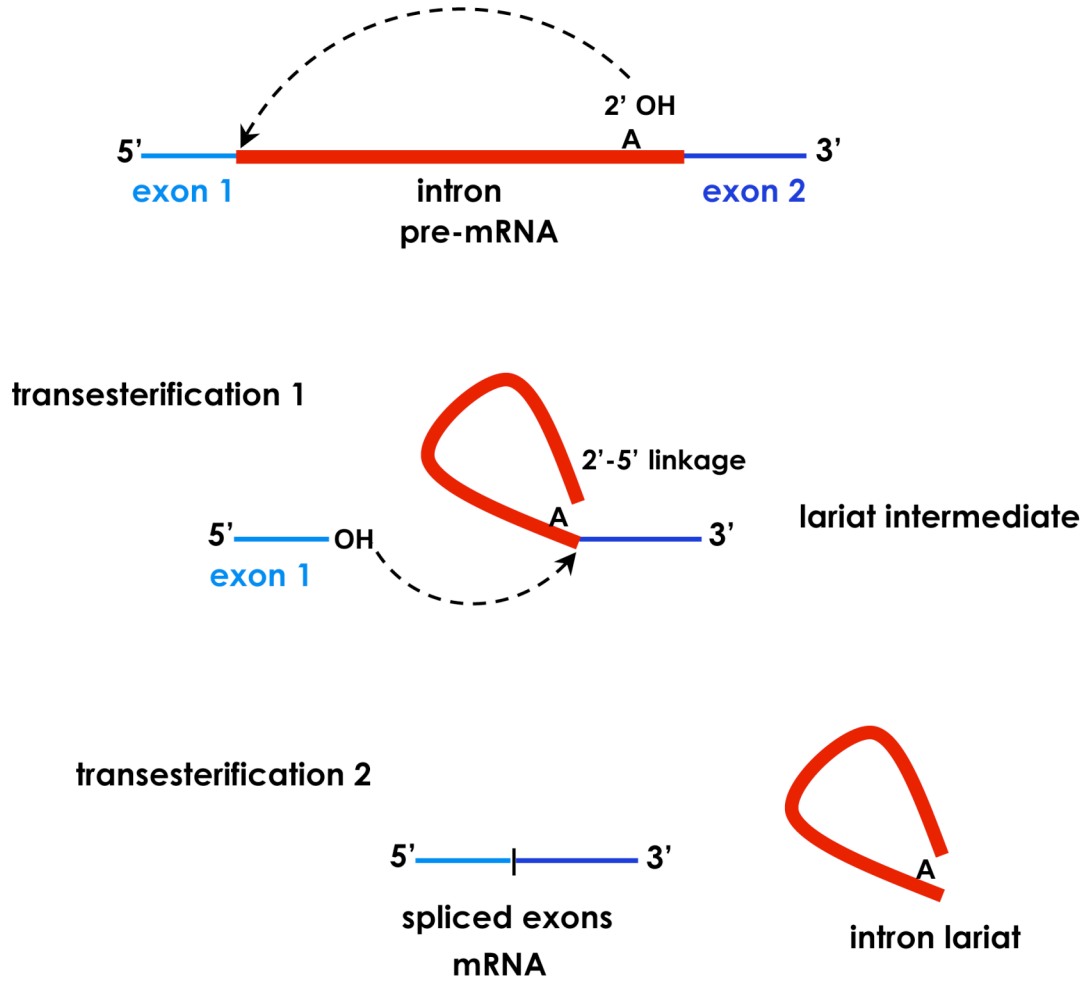

Figure 1.1. The splicing reaction. The intron is removed and the exons are joined by two sequential transesterification reactions.

1.3 The splice sites

The 5' splice site, the branch point and the 3' splice site are one of the few segments of conserved sequences on pre-mRNA introns. They were identified in 1982 (Mount, 1982) by yeast and mammalian intron sequence comparison.

In yeast the 5' splice site consensus sequence is R/GUAUGU (the cleavage site is indicated by / and R represents a purine); the branchpoint sequence is UACUAAC (the underlined A represents the branchpoint adenosine); and the 3' splice site is Y_nYAG (Y represents a pyrimidine) and is preceded by a pyrimidine-rich sequence (Green, 1986).

1.4 The spliceosome

In yeast and metazoa, pre-mRNA splicing is catalysed by the spliceosome; a large ribonucleoprotein complex formed by the ordered association of five small ribonucleoprotein particles (snRNPs) U1, U2, U5, U4/U6 onto each intron (Wahl *et al*., 2009). Non-snRNP proteins also take part in spliceosome assembly (Jurica & Moore, 2003). Through spliceosome assembly and the splicing process itself, several conformational rearrangements of RNA/RNA, RNA/protein and protein/protein interactions occur; the specificity, accuracy and efficiency of which are protein-regulated (Staley & Guthrie, 1998).

1.4.1 Spliceosome assembly

Spliceosome assembly is a highly dynamic and complex process that requires ATP hydrolysis (Staley & Guthrie, 1998). There are also numerous conformational rearrangements before and during pre-mRNA splicing catalysis (Fabrizio *et al*., 2009; Warkocki *et al*., 2009).

Commitment Complex (CC) formation is the first step in spliceosome assembly (Figure 1.2). It takes place co-transcriptionally and consists of U1 association with the 5' splice site and Bbp1 (Branchpoint Binding Protein) interaction with the branchpoint region (Kotovic *et al.*, 2003; Gornemann *et al*., 2005; Lacadie & Rosbash, 2005). Watson-Crick base-pairing between the U2 snRNP and the branchpoint sequence forms the complex A. As there is incomplete complementation between the two sequences, the branchpoint adenosine is projected

from the U2 snRNA/pre-mRNA duplex. This feature later boosts the characteristic first splicing step nucleophilic attack. Next, the Nineteen complex proteins (NTC) and the U4/U6.U5 triple snRNP associate with complex A giving rise to complex B. After unwinding of the U4/U6 base pairing, U2/U6 interaction and U1 and U4 dissociation from the spliceosome, the catalytically active B* complex is formed. This complex catalyses the first splicing step, after which the spliceosome changes conformation to complex C, proceeding to the second splicing step (Konarska 2008; Wachtel & Manley, 2009; Wahl *et al.*, 2009; Hogg *et al.*, 2010).

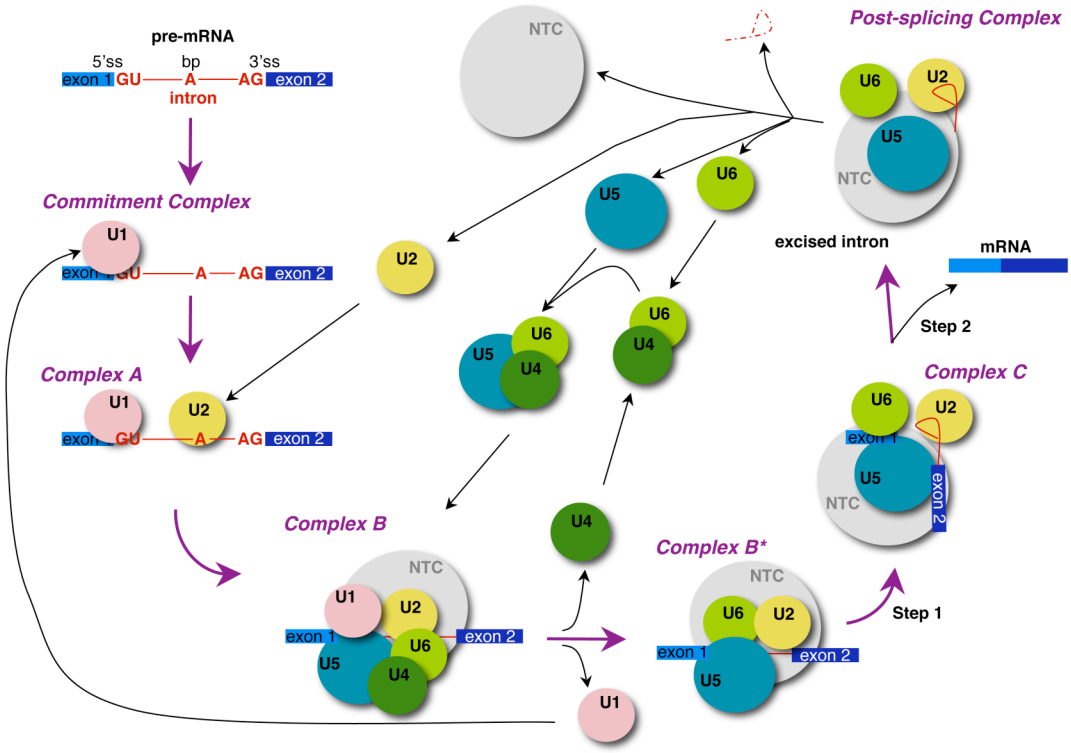

Figure 1.2. Spliceosome assembly in pre-mRNA splicing – figure adapted from Hogg *et al.* (2010). The U1, U2 and U4/U6.U5 tri-snRNP associate in a sequential manner onto the pre-mRNA to assemble the spliceosome. A series of rearrangements occur and the spliceosome adopts different conformations throughout the splicing reaction (Complexes A, B, B* and C). The Nineteen complex of proteins (NTC) is recruited to the spliceosome along with the snRNPs and is essential for the conformational rearrangements in both splicing steps 1 and 2. It is believed that the snRNPs are recycled after each round of splicing to carry out subsequent splicing reactions. The mauve arrows represent the spliceosome transition to the next conformational state; the black arrows indicate the addition or removal of components from the spliceosome.

It is believed that the spliceosome needs to be re-assembled for each new round of splicing and its components are recycled from previous splicing reactions (Makarov *et al*., 2002).

1.5 snRNPs

The snRNPs (small nuclear Ribonucleoprotein Particles) were described as being involved in splicing in 1980 (Lerner *et al*., 1980). They are *trans*-acting factors composed of RNA and protein, receiving their name according to the spliceosomal small nuclear RNA (snRNA) they contain (Lerner & Steitz, 1979). snRNAs are vital in splice sites alignment and are thought to contribute to the spliceosome catalytic core together with some of their associated proteins (Wachtel & Manley, 2009). Two groups of proteins associate with snRNAs in the snRNPs: snRNA-specific proteins, and Sm proteins (B, D1, D2, D3, E, F and G).

1.5.1 snRNPs biogenesis

Most of the actual knowledge on snRNP biogenesis (Figure 1.3) comes from studies in Metazoan species (reviewed in Will & Luhrmann, 2001; Kiss, 2004; Patel & Bellini, 2008).

The U1, U2, U4 and U5 snRNAs are transcribed by RNA polymerase II in the nucleus. Export factors CRM1 and PHAX together with nuclear cap-binding proteins assist in the snRNAs nuclear export (Hamm & Mattaj, 1990; Izaurralde *et al*., 1995, 1997; Fornerod *et al*., 1997; Ohno *et al*., 2000). Once in the cytoplasm snRNP assembly is initiated. The hetero-heptameric Sm protein complex, required for snRNA metabolic stability, 5' cap hypermethylation, 3' end processing and snRNA nuclear import, is assembled on the snRNAs. Importin β, Snurportin1 and the SMN complex are responsible for snRNP nuclear import via interaction with the Sm complex and with the snRNA m_3G cap (Fischer *et al*., 1997; Palacios *et al*., 1997; Huber *et al*., 1998). The snRNP maturation is only completed with the association of snRNP-specific proteins.

Most of what is known for snRNP biogenesis comes from studies in *Xenopus* oocyte and mammalian cells, regarding U1 and U2 snRNPs (Will & Luhrmann, 2001; Kiss, 2004; Patel & Bellini, 2008). Specific U1 and U2 proteins associate at

nuclear Cajal bodies with the core-snRNP. The nuclear import of these proteins is autonomous from the snRNAs import (Jantsch & Gall, 1992; Romac *et al*., 1994; Hetzer & Mattaj 2000; Nesic *et al*., 2004). In *Xenopus* oocytes, U5 snRNP precursor nuclear import is independent from m_3G cap (Fischer *et al*., 1991) and is not known when it associates with U5-specific proteins.

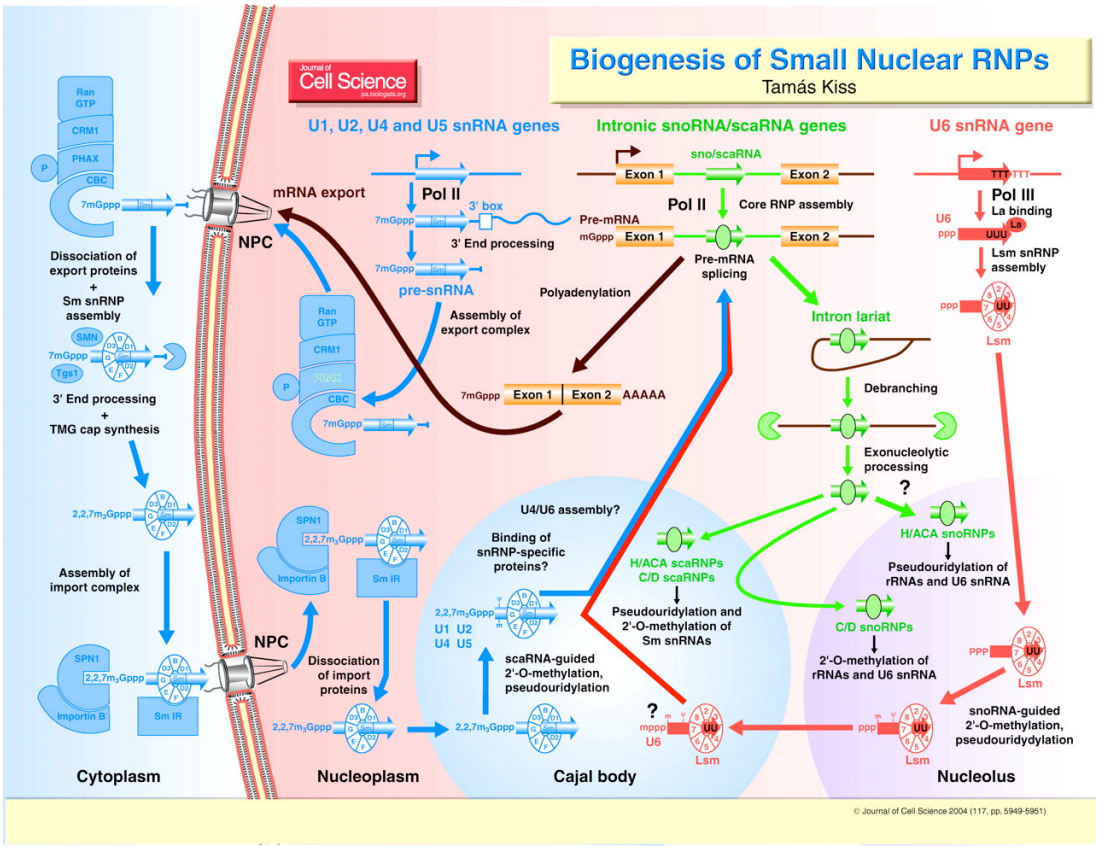

Figure 1.3. Schematic overview of snRNPs biogenesis in high eukaryotes. Figure from Kiss (2004).

The U6 does not bind to Sm proteins but is associated with seven Lsm (Sm-like) proteins. U6 snRNA is an RNA polymerase III product and it is kept in the nucleus after 5' γ-monomethyl phosphate capping (Will & Lührmann, 2001; Kiss, 2004; Beggs, 2005).

Saccharomyces cerevisiae snRNP biogenesis has not been extensively studied. For instance, there are no described orthologs for PHAX export factor or Snurportin1 import factor in budding yeast. Nevertheless, data from Boon *et al*. (2007) show that U5 snRNP has a cytoplasmic stage and its nuclear import is dependent on Prp8p, a

specific U5-snRNP protein and component of the U4/U6.U5 tri-snRNP. The same authors suggest that this Prp8p-dependent U5 nuclear import might be conserved in other species, explaining why in *Xenopus* oocytes U5 import is m_3G cap independent.

1.6 U5 snRNP

The U5 snRNP is one of the spliceosome main components. It contacts the exon sequence adjacent to the 5' splice site prior to the first step of splicing and then maintains its hold, later aligning the ends of the two exons for ligation in the second step (Grabowski & Sharp, 1986; Frilander & Steitz, 2001; Wahl *et al.*, 2009).

U5 snRNA loop 1, an invariant 9-nucleotide sequence, enabled U5 snRNA encoding gene identification - *SNR7* in *S. cerevisiae* (Patterson & Guthrie, 1987). The U5 loop 1 together with the U5 snRNP protein Prp8p are vital for alignment of the exon ends for the second splicing step, Figure 1.4 (Umen & Guthrie, 1995; O'Keefe & Newman, 1998; Grainger & Beggs, 2005).

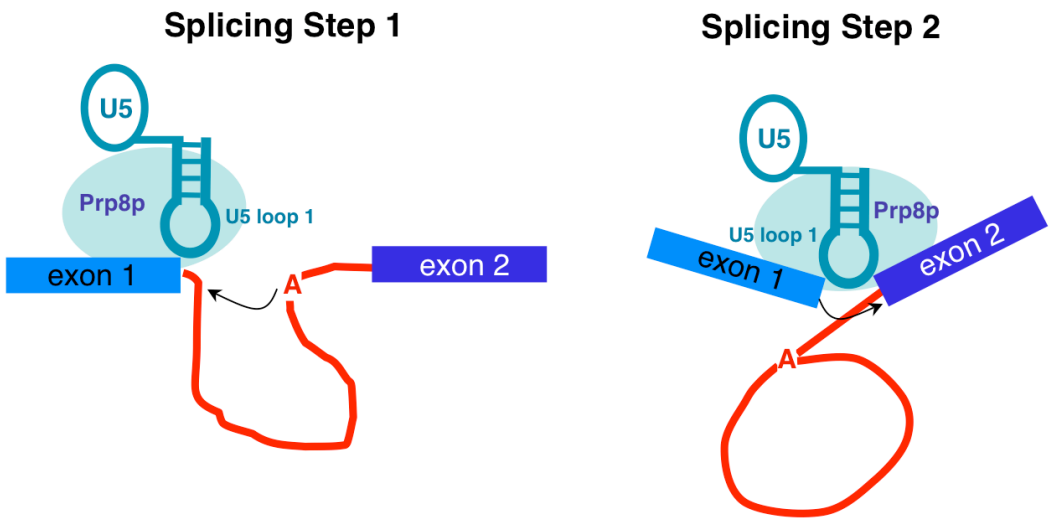

Figure 1.4. U5 snRNA loop 1 and Prp8p align the exons for the second splicing step. Both Prp8p protein and U5 snRNA loop 1 are essential to align the exons for the second splicing step after which the intron is removed and the exons are joined to form mRNA. The red A represents the branchpoint adenosine.

There are two U5 snRNA forms differing in 3' end length U5S (short) and U5L (long). RNase III catalyzes U5-3' end processing and is responsible for this phenomenon (Chanfreau *et al.*, 1997). Both U5S and U5L are found in spliceosomes.

Two U5 snRNP forms were found in *S. cerevisiae*. The mature and functional form contains the U5 snRNA, Sm proteins, Prp8p, Snu114p, Brr2p, Prp28p, Snu40p and Dib1p (Stevens *et al.*, 2001). A form with unknown function that contains U5 snRNA, Sm proteins, Prp8p, Snu114p and Aar2p has been proposed as a precursor or intermediate in U5 snRNP biogenesis and/or recycling (Gottschalk *et al.*, 2001).

A model for U5 snRNP maturation was proposed (Figure 1.5) in which the Aar2p-U5 snRNP complex is an intermediate particle in U5 snRNP biogenesis and is formed in the cytoplasm (Boon *et al.*, 2007). Once in the nucleus, the Prp8p/Aar2p interaction is disrupted allowing Brr2p to interact with Prp8p to form the mature and active U5 snRNP. In this model, Prp8p/Aar2p and Prp8p/Brr2p interactions are likely to be mutually exclusive.

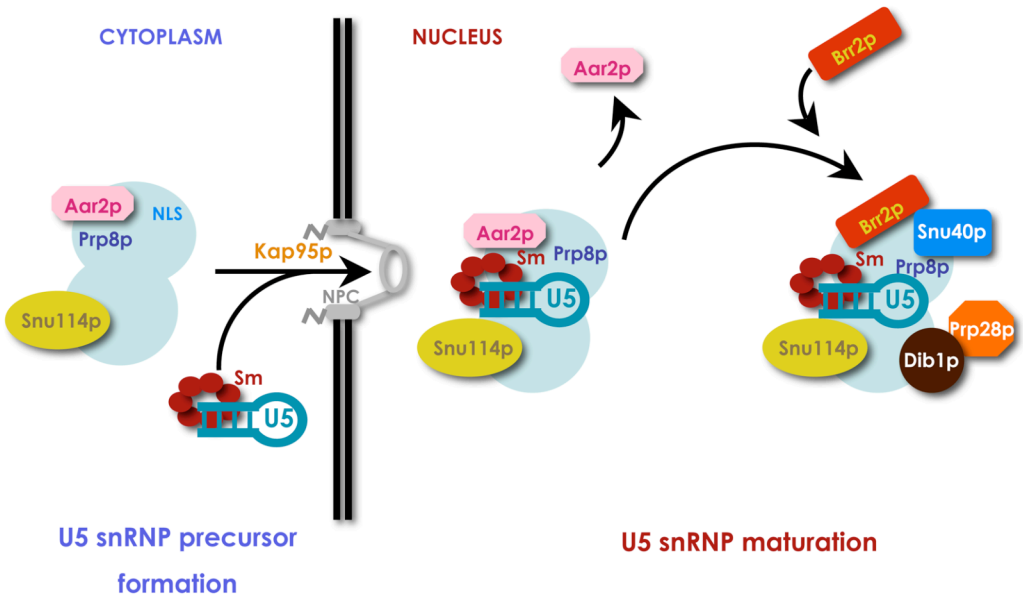

Figure 1.5. The U5 snRNP maturation model – figure adapted from Boon *et al.* (2007). Boon *et al.* (2007) proposed a model for U5 snRNP maturation in which the Aar2p/Prp8p and Brr2p/Prp8p interactions are mutually exclusive. The Aar2p/Prp8p/Snu114p/U5 precursor form is assembled in the cytoplasm and subjected to nuclear import dependent on Kap95p. Once in the nucleus, the mature U5 snRNP would be formed, replacing Aar2p with Brr2p in the Prp8p/Snu114p/U5 complex. As a result, it is expected that an equilibrium will be established between the Aar2p/Prp8p/Snu114p/U5 and Brr2p/Prp8p/Snu114p/U5 complexes in the nucleus.

1.6.1 Major U5 snRNP proteins

One of the most important steps in the spliceosome activation, the U4/U6 dimer unwinding, is dependent on U5 snRNP proteins: Prp8p (Kuhn *et al*., 1999), Brr2p (Raghunathan & Guthrie, 1998; Kim & Rossi, 1999; van Nues & Beggs, 2001) and Snu114p (Bartels *et al*., 2002, 2003; Brenner & Guthrie, 2005). These three proteins form a stable complex at the core of U5 snRNP and remain associated throughout the entire splicing reaction (Achsel *et al.*, 1998; Fabrizio *et al*., 2009).

Prp8p

RNA8 (*PRP8*) was first identified in 1967 from a genetic screen to isolate temperature-sensitive mutations in *S. cerevisiae* (reviewed in Grainger and Beggs, 2005). Due to its essential contribution to pre-mRNA processing, *RNA8* was renamed *PRP8* (Vijayraghavan *et al.*, 1989). Several studies contributed to the comprehension of *PRP8* function, mainly immunodepletion and immunoprecipitation experiments done with antibodies raised against different Prp8p domains (Lossky *et al.*, 1987; Jackson *et al.*, 1988; Anderson *et al.*, 1989; Whittaker *et al.*, 1990; Brown & Beggs, 1992; Hinz *et al.*, 1996; Luo *et al.*, 1999). These experiments demonstrated that Prp8p joins the spliceosome very early and remains through both the first and second splicing steps. It is also found together with the excised intron in the post-splicing complex.

Prp8p requirement for splicing is ubiquitous, although in humans its expression level is higher in cardiac and skeletal muscle (Luo *et al.*, 1999). It is the largest (280-kDa in budding yeast) and most highly conserved splicing factor (Grainger & Beggs, 2005) and regulates several conformational rearrangements in the spliceosome. Numerous Prp8p interactions with other proteins were identified (van Nues & Beggs, 2001; Grainger & Beggs, 2005; Boon *et al*, 2006). Amongst these, are interactions with Snu114p and Brr2p.

It was thought that alignment of the exon ends during the splicing reaction was the responsibility of U5 snRNA loop 1 (O'Keefe *et al.*, 1996). Nevertheless it was shown that splicing still occurs in the absence of U5 loop 1 (Segault *et al*., 1999); moreover, it is necessary just for the second splicing step in yeast extracts (O'Keefe *et al.*, 1996; O'Keefe & Newman, 1998). Besides, both pre-mRNA 5' and 3' splice

sites contact Prp8p (Whittaker & Beggs, 1991; Teigelkamp *et al.*, 1995); and in U5 loop 1 absence, Prp8p cross-links to 3' splice sites (Dix *et al.*, 1998). This indicates that Prp8p together with U5 loop 1 are crucial anchoring factors in spliceosome/exons interactions and may contribute to exon end alignment for the second splicing step (Dix *et al.*, 1998; O'Keefe & Newman, 1998). Prp8p gets destabilized with mutations on U5 loop 1 affecting pre-mRNA splicing. This can be one of the reasons why U5 loop 1 sequence is so conserved (Kershaw *et al*., 2009).

Prp8p is a large protein composed of several domains (Grainger & Beggs, 2005; see Figure 1.6). Basically it contains a nuclear localization signal (NLS) at the N-terminus, an RNA recognition motif (RRM) at the centre, an RNaseH and a Jab1/MPN domain at the C-terminus (Maytal-Kivity *et al*., 2002; Grainger & Beggs, 2005; Pena *et al*., 2007; Pena *et al*., 2008). From the RNaseH domain a β-hairpin finger similar to the ones found in ribosomal proteins is projected, which helps in stabilizing the RNA structure in the ribosome (Yang *et al*, 2008).

Prp8p NLS is located between amino acids 96-117 and Kap95p is responsible for its nuclear uptake (Boon, 2005; Boon *et al*., 2007). When this NLS is deleted, Prp8p, which is normally concentrated in the nucleus, is delocalized to the cytoplasm together with U5 snRNA and Snu114p. An increased association of Prp8ΔNLSp with Aar2p was also observed, and lower levels of Prp8ΔNLSp associated with Brr2p and U4 and U6 snRNAs. This suggests a deficiency in mature U5 snRNP and tri-snRNPs formation, probably due to retention of precursor U5 snRNP in the cytoplasm that might need Prp8p for translocation into the nucleus (Boon *et al*., 2007).

Crystal structures of the human and yeast Prp8p RNase H domain showed that it is conserved between species. This domain interacts with the key sequences on the pre-mRNA: the 5' ss, the branchpoint and the 3' ss. It also interacts with the U4/U6 di-snRNP and with Brr2p (Pena *et al*., 2008). The same study suggests that this domain contributes to the assembly and stabilization of the catalytic core of the spliceosome and can also contribute to splicing catalysis (Pena *et al*., 2008).

Mutational analysis showed Prp8p β-finger to be involved in the transition from the first to the second splicing step and also in the U4/U6 unwinding (Kuhn *et al*., 2000; Liu *et al*., 2007).

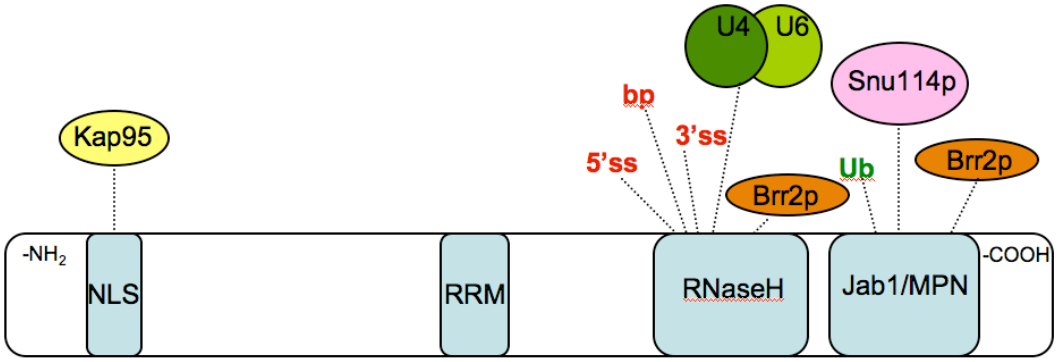

Figure 1.6. Schematic representation of Prp8p domains and their main interactors (see main text for detailed description). NLS - nuclear localization signal; RRM - RNA recognition motif; 5' ss - 5' splice site; bp - branch point; 3' ss - 3' splice site; Ub - ubiquitin.

Prp8p C-terminal Jab1/MPN domain was shown to bind ubiquitin (Bellare *et al*., 2006), Snu114p and Brr2p (Pena *et al*., 2007). The crystal structure confirmed Jab1/MPN domain organization to be typical for deubiquitinating enzymes (Pena *et al*., 2007). Furthermore, Prp8p-ubiquitin conjugates were isolated within the U4/U6.U5 tri-snRNP, insinuating a role for ubiquitination in pre-mRNA splicing regulation (Bellare *et al*., 2008). Pena and colleagues suggest that the Jab1/MPN is a pseudoenzyme that during evolution was converted into a protein-protein interaction domain (Pena *et al*., 2007)**.**

Snu114p

Snu114p is homologous to the ribosomal translocase elongation factor G (EF-G in prokaryotes/EF2 in eukaryotes) and so far is the only GTPase identified in the spliceosome. This suggests that Snu114p might be responsible for spliceosomal rearrangements through GTP hydrolysis (Fabrizio *et al.*, 1997). Snu114p comprises eight domains, three of which (III-V) are expected to reorganize as a result of GTP hydrolysis (Brenner & Guthrie, 2005). Snu114p together with U5 loop 1 is required for Prp8p stabilization within the spliceosome (Brenner & Guthrie, 2006; Kershaw *et al*., 2009).

Several studies point to a requirement for Snu114p in the assembly of U5 with U4/U6 and afterwards for U4/U6 unwinding and U1 release (Bartels *et al.*, 2002, 2003; Brenner & Guthrie, 2005).

Work from the Staley lab (Small *et al.*, 2006) suggests that Snu114p is involved in both spliceosome activation and disassembly. The authors showed that GDP represses post-splicing U2/U6.U5.intron complex disassembly; and that this can be reverted by GTP and analogs without hydrolysis in the presence of Brr2p (Small *et al.*, 2006). They suggest an innovative mechanism for Snu114p function. Going against the general consensus, Small *et al.* (2006) suggest that Snu114p works as a G protein and not as a classic GTPase. They propose that Snu114p, by GTP binding, regulates Brr2p unwinding activity towards U4/U6 (and probably U2/U6 too). Their suggestion is that Snu114p is a signal-dependent switch that controls Brr2p along several steps of the splicing reaction, explicitly those of spliceosome activation and disassembly. Brr2p would then be responsible for U4/U6 and U2/U6 unwindings via ATP hydrolysis, as a conventional helicase. This Snu114p control over Brr2p can be either direct or indirect (since no direct interaction between Snu114p and Brr2p was shown until now), with two putative candidates for the third component being U5 snRNA and Prp8p.

More recently it was proposed that the Snu114p G-domain (GTP binding and hydrolysis) detects the U4/U6 and U2/U6 snRNAs base pairing state. Subsequently, by its C-terminal domain Snu114p would control Brr2p, which in turn triggers RNA/RNA rearrangements in the spliceosome (Frazer *et al*., 2009).

Brr2p

Brr2p was first identified as being involved in pre-mRNA splicing in a screen for splicing defective cold-sensitive mutants (Noble & Guthrie, 1996). It is a DExH-box RNA helicase, composed of an N-terminal domain and two helicase modules (one N-terminal and the other C-terminal). Each helicase module is composed of a helicase domain followed by a Sec63 domain (Hahn & Beggs, 2010). Brr2p N-terminal helicase module is required for U4/U6 unwinding due to its ATPase activity (Raghunathan & Gutrie, 1998; Kim & Rossi, 1999). The C-terminal helicase module is believed to be responsible for interactions with other proteins and

also for controlling the activity of the first helicase domain (reviewed in Hahn & Beggs, 2010).

As mentioned above, Brr2p activity is vital for U4/U6 unwinding and is controlled by Snu114p (Frazer *et al*., 2009). Snu114p-GTP activates Brr2p and Snu114p-GDP represses it. By its GTP and phosphorylation states, Snu114p is thought to regulate Brr2p activity in spliceosome disassembly in unwinding of U2/U6 (Small *et al*., 2006; Frazer *et al*., 2008).

Prp8p also regulates Brr2p helicase activity (Kuhn *et al*., 1999). It was shown that the C-terminal fragment of Prp8p (Prp8p-CTF, $Prp8p_{1806-2413}$ that contains part of the RNaseH and Jab1/MPN domains) represses Brr2p ATPase activity but stimulates its helicase activity (Maeder *et al*., 2009).

It was observed that disruption of ubiquitin recognition blocks splicing by acceleration of U4/U6 unwinding and consequent imbalance in the U4/U6.U5 tri-snRNP level. The evidence that Prp8p-ubiquitin is co-purified with the tri-snRNP further suggests that ubiquitinated Prp8p mediates Brr2p U4/U6 unwinding activity (Bellare *et al*., 2008).

1.7 Retinitis Pigmentosa

About 1 in 4000 people worldwide suffer from serious visual impairment due to Retinitis Pigmentosa (RP) (Wang & Cooper, 2007). The disease is named after the accumulation of intra-retinal pigment deposits during the later stages of the disease. RP encloses a group of progressively incapacitating, hereditary disorders that cause terrible retinal damage, affecting the retina in a centripetal way. The rods (retinal photoreceptors responsible for dim light vision) are the first and main RP targets; the patients acquire tunnel vision and night-vision is also disturbed. As a consequence, the cones (daylight vision photoreceptors) start to die and ultimately central vision is lost. In parallel, the retinal vasculature gets weakened and the characteristic intra-retinal deposits of rhodopsin accumulate (Kennan *et al.*, 2005).

Approximately 31 RP-causing genes were identified so far and 13 are related to autosomal dominant forms of RP (adRP). Amongst these, five are splicing factors: *PRPF3, PRPF8, PRPF31, SNRNP200* and *PAP-1* (reviewed in Kennan *et al.*, 2005; Mordes *et al*., 2006; and Hahn & Beggs, 2010). With the exception of PAP-1, all

have orthologs in *S. cerevisiae* and are tri-snRNP components. This suggests a link between adRP and spliceosome assembly, more specifically tri-snRNP formation.

It is interesting how mutations in ubiquitously expressed splicing factors can lead to a retina-specific disease with a late onset. A possible explanation is that the retina is a highly metabolically active tissue with an elevated turnover. In the case of splicing factors with RP mutations the splicing levels of an important retinal protein such as rhodopsin are compromised, resulting in a reduced number or defective transcripts that are not enough for the retinal metabolic demands. Additionally defective and non-functional protein can aggregate inducing *wt* protein aggregation. This is a cumulative effect with time and the visual abilities of the patient will get worse progressively (Kennan *et al.*, 2005; Mordes *et al*., 2006; Kosmaoglou *et al*., 2008).

Regarding *PRPF8*, adRP-causing mutations were identified in a 14 codon-stretch in the last exon. The altered aminoacid residues are highly conserved from humans to *S. cerevisiae* (McKie *et al.*, 2001). Several studies have shown a link between RP mutations in hPrp8p (protein encoded by *PRPF8* in humans) and Prp8p (protein encoded in *S. cerevisiae* by the budding yeast ortholog of *PRPF8*), Prp8p/Snu114p/Brr2p complex formation and U5 snRNP maturation (Boon *et al*., 2007; Pena *et al*., 2007; Maeder *et al*., 2009; reviewed in Newman & Nagai, 2010).
It was observed that RP mutations in the hPrp8p C-terminal deteriorate interactions between this region, hSnu114p and hBrr2p (Pena *et al*., 2007).

After showing that *S. cerevisiae* Prp8p-CTF interacts with Brr2p, stimulating its ATP-dependent unwinding activity towards a U4/U6 duplex, Maeder and colleagues observed that Brr2p activity was strongly affected if the same Prp8p fragment contained an RP mutation. As a result, Prp8p RP mutations will have an effect on spliceosome activation (Maeder *et al*., 2009).

Furthermore, RP mutations lead also to a defect in U5 snRNP maturation in yeast. Prp8p RP mutations caused the Aar2p-U5 snRNP precursor form to accumulate at the same time as a decrease in Brr2p-U5 snRNP mature form was detected. In consequence a reduction in the U4/U6.U5 tri-snRNP level and splicing defects were also observed (Boon *et al.*, 2007).

Recent studies showed a connection between mutations in hBrr2p and RP (Zhao *et al*., 2009; Li *et al*., 2009). The same mutations in budding yeast lead to a deficient U4/U6 unwinding but do not affect the tri-snRNP levels, implying therefore U5 snRNP maturation defects (Zhao *et al*., 2009).

1.8 Aar2p

Aar2p is an essential protein, and component of the U5 snRNP (required for both *in vivo* and *in vitro* splicing) but not of the U4/U6.U5 tri-snRNP (Gottschalk *et al.*, 2001). It has been suggested that Aar2p has a role in snRNP recycling since its depletion has a negative effect on later rounds of splicing.

It is suggested that the yeast mature U5 snRNP and U4/U6.U5 tri-snRNP assemble from a putative Aar2p-U5 core particle (Gottschalk *et al*., 2001; Boon *et al*., 2007).

Nakazawa *et al*. (1991) first described Aar2p as being required for *MATa1* pre-mRNA splicing but not for *ACT1* splicing. In the same paper, both *aar2-1* and *aar2-2* mutants led to severe growth defects and *AAR2* disruption seems to be lethal. By primer extension it was verified that there is a defect in splicing the two *MATa1* pre-mRNA short introns in both mutants and disrupted *AAR2*. Introducing an intronless *MATa1* restores the alpha mating type but not the growth phenotype. This suggests that *AAR2* is required also for splicing of gene(s) essential for cell growth. Aar2p sequence comparison revealed a leucine zipper structure between aminoacids 261-282 that can be implicated in homo- or heterodimerization. There is also an acidic region between aminoacids 332-341. The authors suggested that the level of *AAR2* transcript is very low in the absence of appropriate mating pheromone induction. This is suggested because there is one copy of a pheromone-responsive element (5'-TGAAACA-3') at positions -398 to -392, and three copies of inverted sequences of this element with incomplete matches at positions -98 to -92, -294 to -288, and -416 to -410 of *AAR2*. Also, these authors could not detect *AAR2* transcript in logarithmic growth phase (Nakazawa *et al*., 1991 - data not shown).

Gottschalk *et al*. (2001) found that Aar2p is specifically associated with U5 but not with the tri-snRNP (IPs from total cell extracts with αAar2p and Northern blot analysis of coprecipitated RNAs; plus, a complementary experiment followed by

glycerol gradient assaying each fraction by Northern and Western blots). There is a fraction of Aar2p at the top of the gradient that is thought to be unbound Aar2 protein. Aar2p-U5 was invariably coisolated with U1, regardless of the purification protocol used by these authors (P_{GAL1}-*AAR2*-His strain, total cell extract and 2-step affinity purification). They verified that Aar2p is required for pre-mRNA splicing *in vivo* but not *in vitro* of U3 or *ACT-1* pre-mRNAs. Removal of Aar2p resulted in a reduction of 25S tri-snRNP levels, which are still sufficient to support *in vitro* splicing. Aar2p depletion interferes with later rounds of splicing and recombinant Aar2p partially complemented the Δ*aar2* splicing defect. These last results led to the suggestion that Aar2p has a role in snRNP recycling (Gottschalk *et al*., 2001).

The splicing reaction is thought to be under quality control by a putative discard pathway. If aberrant complexes are formed throughout the splicing reaction, the discard pathway is activated to remove them (Konarska and Query, 2006). The DEAH box ATPase Prp43p is one of the main responsibles for this process (Pandit *et al*., 2006; Mayas *et al*., 2010). In a suppressor screen to identify components the discard pathway (Pandit *et al*., 2006) an *AAR2* mutant allele D281N=aar2G841A that acts as a *prp38-1* suppressor was identified. The *prp38-1* mutants are *ts* (temperature-sensitive) due to splicing impairment at an early stage of the reaction – slow U1 and U4 release. So, for D281N=aar2G841A to suppress this effect, Aar2p has to be either a factor that enhances splicing efficiency or that is involved in defective spliceosome turnover. This later alternative is more plausible since it was shown that Aar2p depletion has a negative effect in later rounds of splicing (Gottschalk *et al*., 2001).

Regarding Aar2p physical interaction with components of the intermediate U5 snRNP, it was observed that disruption at $Prp8p_{2173}$ interferes with Prp8p association with Aar2p. In the same study, the amount of Aar2p associated with $Prp8p_{771-2413}$ was increased compared to the full-length Prp8p (Boon *et al*., 2006).

Kutach (Guthrie lab, unpublished data – personal communication) purified Prp8p-CTF from yeast and identified one co-purifying protein - Aar2p - and no Brr2p. An *in vitro* mixture of Aar2p, Brr2p and Prp8p-CTF resulted in the formation of a Prp8p/Aar2p/Brr2p complex. Prior binding of Brr2p to Prp8p does not inhibit interaction of Aar2p with Prp8p-CTF. Pre-binding an excess of Aar2p to CTF

inhibits binding of Brr2p. CTF binds to Aar2p with a higher affinity than CTF-N in a direct competition, even though he did not detect a direct interaction between the first two. He suggests that Aar2p binds to CTF-N and clamps down the CTF-C impairing Brr2p binding to this region.

With reference to other aspects that might help in understanding Aar2p mechanism, Albuquerque *et al*. (2008) identified Aar2p as being phosphorylated at S331. Aar2p phosphorylation state may well control Aar2p activity and also regulate its interaction with other proteins. Ptacek *et al*. (2005) identified Aar2p, Lsm12p and Prp40p as *in vitro* substrates for Prr2p kinase using proteome chip technology. Another kinase - Gcn2p - was identified as a physical interactor of Aar2p, Brr2p, Prp4p, Prp6p, Prp8p, Prp31p, Sun66p and Snu114p in a genome-wide screen (Gavin *et al*., 2006).

Aar2p was found as a prey in two independent yeast two-hybrid assays. The first one used Psf2p as bait (Hazbun *et al*., 2003). Psf2p is a GINS complex component responsible for DNA replication machinery assembly to replication origins (Takayama *et al*., 2003; Kanemaki *et al*., 2003). In the second screen (Yeast Resource Center, Fields S. – unpublished data) the bait was Rgd2p, which is a Cdc42p and Rho5p GTPase activating protein (RhoGAP) (Roumanie, *et al*., 2001).

Despite the data gathered around Aar2p its exact role in pre-mRNA splicing is still unclear.

1.9 Aim of this work

As described above, U5 snRNP biogenesis is a relevant step for spliceosome assembly and its disruption leads to splicing defects in general and can lead to diseases like retinitis pigmentosa in humans in particular. Hence there is an increased interest in understanding how this essential process is regulated.

To gain a better understanding of U5 snRNP biogenesis, in this work I investigate the role of an understudied protein - Aar2p - in this process. The obtained results are put into context with the proposed U5 snRNP maturation model (Boon *et al*., 2007). According to this model, the balance between the mutually exclusive Aar2p/Prp8p and Brr2p/Prp8p interactions is thought to be vital for correct U5 snRNP maturation (Boon *et al*., 2007).

I use *S. cerevisiae* as a model system as the overall splicing mechanism is conserved relative to higher eukaryotes. Also, its undemanding lab manipulation makes it a perfect model to study Aar2p *in vivo* using a combination of molecular biology techniques, biochemical assays and live imaging.

CHAPTER 2 - Materials and Methods

2.1 Chemicals and reagents

General chemicals were acquired from Sigma, Amersham, Thermo-Scientific, Roche, Invitrogen, Pierce, Biorad.

Reagents for yeast media were purchased from Formedium.

All restriction enzymes were bought from New England Biolabs; DNA polymerases from Promega and Roche.

2.1.1 Oligonucleotides

Oligonucleotides were either purchased from Sigma or Invitrogen.

Name	Sequence 5'-3'	Notes
U5-7wtsmnr	AAGTTCCAAAAAATATGGCAAGC	Boon 2005 U5 snRNA probe
BamHI-Aar2-1-F	CGCGGATCCGCGATGAATACTGTACCATTTAC	Genomic AAR2 amplification
XhoI-Aar2-170-R	CCGCTCGAGCGGTTAATCTTCATTCTTGGCTTCC	Genomic AAR2 amplification
BamHI-Aar2-150-atg-F	CGCGGATCCGCGATGAATGAGCTGCTAAAATCCAG	Genomic AAR2 amplification
PstI-Aar2-355R	CCGCTGCAGCGGTTATGGCCTTTGGTAATAGAGAC	Genomic AAR2 amplification
R-seq-pBTM116-1	GCCGGCATGCCGGTAGAGGTG	Sequencing
SDM3-Aar2-S253E-F	GATCGAACTGATATGTTCAGAAGCTACGGTGCC	SDM
SDM3-Aar2-S253E-R	CATATGTTTAGGCACCGTAGCTTCTGAACATATC	SDM
SDM3-Aar2-T274E-F	CGAAATCTTATATTATCAGATAAAGGAATTGCCTGAAC	SDM
SDM3-Aar2-T274E-R	CTGAGTATTGTTCAGGCAATTCCTTTATCTG	SDM
SDM3-Aar2-Y328E-F	GAAGACGACGCTCTTATTGAAGGTATCAGTG	SDM
SDM3-Aar2-Y328E-R	CTTTCTTCATCACTGATACCTTCAATAAGAGCG	SDM

SDM3-Aar2-S331E-F	CGCTCTTATTTACGGTATCGAAGATGAAGAAAG	SDM
SDM3-Aar2-S331E-R	CGTCATCCCTTTCTTCATCTTCGATACCG	SDM
SDM3-Aar2-T345E-F	GATGATGAGCACAACCCTGAAATTGTTGGC	SDM
SDM3-Aar2-T345E-R	GTAATAGAGACCGCCAACAATTTCAGGGTTGTGC	SDM
SDM3-Aar2-S253A-F	GATCGAACTGATATGTTCAGCCGCTACGGTGCC	SDM
SDM3-Aar2-S253A-R	CATATGTTTAGGCACCGTAGCGGCTGAACATATC	SDM
SDM3-Aar2-T274A-F	CGAAATCTTATATTATCAGATAAAGGCCTTGCCTGAAC	SDM
SDM3-Aar2-T274A-R	CTGAGTATTGTTCAGGCAAGGCCTTTATCTG	SDM
SDM3-Aar2-Y328A-F	GAAGACGACGCTCTTATTGCCGGTATCAGTG	SDM
SDM3-Aar2-Y328A-R	CTTTCTTCATCACTGATACCGGCAATAAGAGCG	SDM
SDM3-Aar2-S331A-F	CGCTCTTATTTACGGTATCGCCGATGAAGAAAG	SDM
SDM3-Aar2-S331A-R	CGTCATCCCTTTCTTCATCGGCGATACCG	SDM
SDM3-Aar2-T345A-F	GATGATGAGCACAACCCTGCCATTGTTGGC	SDM
SDM3-Aar2-T345A-R	GTAATAGAGACCGCCAACAATGGCAGGGTTGTGC	SDM
F-seq-SDM-Aar2	CTTCAAATCTAGAGAAGCCATAAGG	Sequencing
R-seqAar2	TTATGGCCTTTGGTAATAGAG	Sequencing
FAar2-pGID	ATGCCATGTTTTTTGGTAACTACGGGTCGAGTTTGCAATGGCATGCTATG	Infusion cloning
RAar2-pGID	CCATAGGCATCAAGTCAAATACGTTTGATGATAGCGCCGCACGATGATCGACTAGTGGATCTGATATCATCGATGAA	Infusion cloning
F-seq-pGID3	GCTTCGTACGCTGCAGGTCGAC	Sequencing
F-Aar2-genSDM	GAGTTTGCAATGGCATGCTATG	Genomic insertion
R-infAar2SDM	ATTAACCCGGGGATCCTTATGGCCTTTGGTAATAGAG	Genomic insertion

F-Snu114-GFP	AGCGCTGAATTATACGCTCAATTAAGAGA AAATGGCTTAGTACCGCGGATCCCCGGGT TAATTAA	GFP cassette amplification, C-terminal insertion
R-Snu114-GFP	AAAAATATTGTGGACATATTGCTTAATTCT TATGCGCCAAGATTTGAATTCGAGCTCGTT TAAAC	GFP cassette amplification, C-terminal insertion
F-Snu114-Ycol	GCAATCCCAATTTTATTGG	YCPCR
F2-PRP8	GCGGGGGACGAAGAGTTAGAGGCCGAAC AAATCGATGTATTTAGCCGGATCCCCGGGT TAATTAA	Boon, 2005 GFP cassette amplification, C-terminal insertion
R1-PRP8	ATATCTATGAAATAACAGATTCCAGTTTAT TGGGGAATATATTCAGAATTCGAGCTCGTT TAAAC	Boon, 2005 GFP cassette amplification, C-terminal insertion
F-PRP8-6876	AATTTTTTCCACCCCGGGAT	Boon, 2005 YCPCR
R-pTEF	GGATGTATGGGCTAAATGTAC	R. Grainger, Beggs lab. YCPCR
pACTIIseqF	GGCTTACCCATACGATGTTC	R. Grainger, Beggs lab. Sequencing clones Y2H screen
pACTIIseqR	TGAGATGGTGCACGATGG	R. Grainger, Beggs lab. Sequencing clones Y2H screen
R-seq-pBTM116-1	GCCGGCATGCCGGTAGAGGTG	this study

2.1.2 Plasmids

Plasmid	Description	Source
pGEX4T1-Aar2	Bacterial expression vector with GST-Aar2p	Gottschalk et al., 2001
pFA6a-GFP-KAN	CEN-GFP-KAN	P. Rischitor, Hardwick lab
pACTII-stop	2μ, LEU2	Fromont-Racine et al., 1997
pACTII-stop-E1	pACTII-stop with $Prp8p_{1649-2413}$	van Nues & Beggs, 2001

pACTII-stop-E3	pACTII-stop with Prp8p$_{2010-2413}$	van Nues & Beggs, 2001
pACTII-stop-E3H	pACTII-stop with Prp8p$_{2010-2413}$-prp8-52	van Nues & Beggs, 2001
pBTM116-1	2μ, TRP1	M. Fromont-Racine
pBTM116-1-Aar2	pBTM116-1 with Aar2p full length	this study
pBTM116-1-Aar2$_{1-170}$	pBTM116-1 with Aar2p$_{1-170}$	this study
pBTM116-1-Aar2$_{150-355}$	pBTM116-1 with Aar2p$_{150-355}$	this study
pBTM116-1-Aar2-253A	pBTM116-1 with Aar2p full length, and aa substitution S253A	this study
pBTM116-1-Aar2-253E	pBTM116-1 with Aar2p full length, and aa substitution S253E	this study
pBTM116-1-Aar2-274A	pBTM116-1 with Aar2p full length, and aa substitution S274A	this study
pBTM116-1-Aar2-274E	pBTM116-1 with Aar2p full length, and aa substitution S274E	this study
pBTM116-1-Aar2-328A	pBTM116-1 with Aar2p full length, and aa substitution S328A	this study
pBTM116-1-Aar2-328E	pBTM116-1 with Aar2p full length, and aa substitution S328E	this study
pBTM116-1-Aar2-331A	pBTM116-1 with Aar2p full length, and aa substitution S331A	this study
pBTM116-1-Aar2-331E	pBTM116-1 with Aar2p full length, and aa substitution S331E	this study
pBTM116-1-Aar2-345A	pBTM116-1 with Aar2p full length, and aa substitution S345A	this study

pBTM116-1-Aar2-345E	pBTM116-1 with Aar2p full length, and aa substitution S345E	this study
pGID3	NAT cassette for genomic insertion	Decourty et al., 2008
pGID3-wt	pGID3 with $AAR2_{717-1068}$	this study
pGID3-253A	pGID3 with $AAR2_{717-1068}$ and aa substitution S253A	this study
pGID3-253E	pGID3 with $AAR2_{717-1068}$ and aa substitution S253E	this study
pGID3-274A	pGID3 with $AAR2_{717-1068}$ and aa substitution S274A	this study
pGID3-274E	pGID3 with $AAR2_{717-1068}$ and aa substitution S274E	this study
pGID3-328A	pGID3 with $AAR2_{717-1068}$ and aa substitution S328A	this study
pGID3-328E	pGID3 with $AAR2_{717-1068}$ and aa substitution S328E	this study
pGID3-331A	pGID3 with $AAR2_{717-1068}$ and aa substitution S331A	this study
pGID3-331E	pGID3 with $AAR2_{717-1068}$ and aa substitution S331E	this study
pGID3-345A	pGID3 with $AAR2_{717-1068}$ and aa substitution S345A	this study
pGID3-345E	pGID3 with $AAR2_{717-1068}$ and aa substitution S345E	this study

2.1.3 *E. coli* strains

Strain	Genotype	Source
DH5α	lacZM15 (lacZYA-argF) recA1 endA1 hsdR17 (rk^-, mk^+) phoA supE44 thi gyrA96 relA1	Invitrogen
BL21	F^-, ompT, hsdSB, (r_B^-, m_B^-), gal dcm (DE3)	Stratagene

2.1.4 Yeast strains

Strain	Genotype	Source
AGY8	trp1-Δ; his3Δ; ura3-52; lys2-801; ade2-101; aar2Δ::URA3+pRS314-GAL1::AAR2-10xHis, ARS, CEN, TRP1	Gottschalk et al., 2001
L40ΔG	MATa; ade2; trp1-901; leu2-3; -112; lys2-801am; his3Δ200; LYS2::$(lexAop)_4$-HIS3; URA3::$(lexAop)_8$-lacZ; Δgal4::$KANA^R$	Fromont-Racine
BY4741	MATa; his3Δ1; leu2Δ0; met15Δ0; ura3Δ0	EUROSCARF
BY4742	MATα; his3Δ1; leu2Δ0; lys2Δ0; ura3Δ0	EUROSCARF
W303α	MATα; leu2-3,112; trp1-1; kan1-100; ura3-1; ade2-1; his3-11,15	R. Rothstein
JF191	W303α with SPC105:13Myc-kanMX6	J. Fernius, Hardwick lab
ΔPRR2	BY4741; MATa; his3Δ1; leu2Δ0; met15Δ0; ura3Δ0; YDL214c::kanMX4	EUROSCARF
ΔGCN2	BY4741; MATa; his3Δ1; leu2Δ0; met15Δ0; ura3Δ0; YDR283c::kanMX4	EUROSCARF
VCY1	AGY8; PRP8-GFP::kanMX6	this study
VCY2	AGY8; SNU114-GFP::kanMX6	this study
VCY3	L40ΔG+pBTM116-1+pACTII-stop-E1	this study
VCY4	L40ΔG+pBTM116-1+pACTII-stop-E3	this study
VCY5	L40ΔG+pBTM116-1+pACTII-stop-E3H	this study
VCY6	L40ΔG+pBTM116-1+pACTII-stop	this study
VCY7	L40ΔG+pBTM116-1-Aar2+pACTII-stop-E1	this study
VCY8	L40ΔG+pBTM116-1-Aar2+pACTII-stop-E3	this study
VCY9	L40ΔG+pBTM116-1-Aar2+pACTII-stop-E3H	this study
VCY10	L40ΔG+pBTM116-1-Aar2+pACTII-stop	this study

VCY11	L40ΔG+pBTM116-1-Aar2$_{1-170}$+pACTII-stop-E1	this study
VCY12	L40ΔG+pBTM116-1-Aar2$_{1-170}$+pACTII-stop-E3	this study
VCY13	L40ΔG+pBTM116-1-Aar2$_{1-170}$+pACTII-stop-E3H	this study
VCY14	L40ΔG+pBTM116-1-Aar2$_{1-170}$+pACTII-stop	this study
VCY15	L40ΔG+pBTM116-1-Aar2$_{150-355}$+pACTII-stop-E1	this study
VCY16	L40ΔG+pBTM116-1-Aar2$_{150-355}$+pACTII-stop-E3	this study
VCY17	L40ΔG+pBTM116-1-Aar2$_{150-355}$+pACTII-stop-E3H	this study
VCY18	L40ΔG+pBTM116-1-Aar2$_{150-355}$+pACTII-stop	this study
VCY19	L40ΔG+pBTM116-1-Aar2-253A+pACTII-stop-E1	this study
VCY20	L40ΔG+pBTM116-1-Aar2-253A+pACTII-stop-E3	this study
VCY21	L40ΔG+pBTM116-1-Aar2-253A+pACTII-stop-E3H	this study
VCY22	L40ΔG+pBTM116-1-Aar2-253A+pACTII-stop	this study
VCY23	L40ΔG+pBTM116-1-Aar2-253E+pACTII-stop-E1	this study
VCY24	L40ΔG+pBTM116-1-Aar2-253E+pACTII-stop-E3	this study
VCY25	L40ΔG+pBTM116-1-Aar2-253E+pACTII-stop-E3H	this study
VCY26	L40ΔG+pBTM116-1-Aar2-253E+pACTII-stop	this study
VCY27	L40ΔG+pBTM116-1-Aar2-274A+pACTII-stop-E1	this study
VCY28	L40ΔG+pBTM116-1-Aar2-274A+pACTII-stop-E3	this study
VCY29	L40ΔG+pBTM116-1-Aar2-274A+pACTII-stop-E3H	this study
VCY30	L40ΔG+pBTM116-1-Aar2-274A+pACTII-stop	this study
VCY31	L40ΔG+pBTM116-1-Aar2-274E+pACTII-stop-E1	this study
VCY32	L40ΔG+pBTM116-1-Aar2-274E+pACTII-stop-E3	this study
VCY33	L40ΔG+pBTM116-1-Aar2-274E+pACTII-stop-E3H	this study
VCY34	L40ΔG+pBTM116-1-Aar2-274E+pACTII-stop	this study
VCY35	L40ΔG+pBTM116-1-Aar2-328A+pACTII-stop-E1	this study
VCY36	L40ΔG+pBTM116-1-Aar2-328A+pACTII-stop-E3	this study
VCY37	L40ΔG+pBTM116-1-Aar2-328A+pACTII-stop-E3H	this study
VCY38	L40ΔG+pBTM116-1-Aar2-328A+pACTII-stop	this study

VCY39	L40ΔG+pBTM116-1-Aar2-328E+pACTII-stop-E1	this study
VCY40	L40ΔG+pBTM116-1-Aar2-328E+pACTII-stop-E3	this study
VCY41	L40ΔG+pBTM116-1-Aar2-328E+pACTII-stop-E3H	this study
VCY42	L40ΔG+pBTM116-1-Aar2-328E+pACTII-stop	this study
VCY43	L40ΔG+pBTM116-1-Aar2-331A+pACTII-stop-E1	this study
VCY44	L40ΔG+pBTM116-1-Aar2-331A+pACTII-stop-E3	this study
VCY45	L40ΔG+pBTM116-1-Aar2-331A+pACTII-stop-E3H	this study
VCY46	L40ΔG+pBTM116-1-Aar2-331A+pACTII-stop	this study
VCY47	L40ΔG+pBTM116-1-Aar2-331E+pACTII-stop-E1	this study
VCY48	L40ΔG+pBTM116-1-Aar2-331E+pACTII-stop-E3	this study
VCY49	L40ΔG+pBTM116-1-Aar2-331E+pACTII-stop-E3H	this study
VCY50	L40ΔG+pBTM116-1-Aar2-331E+pACTII-stop	this study
VCY51	L40ΔG+pBTM116-1-Aar2-345A+pACTII-stop-E1	this study
VCY52	L40ΔG+pBTM116-1-Aar2-345A+pACTII-stop-E3	this study
VCY53	L40ΔG+pBTM116-1-Aar2-345A+pACTII-stop-E3H	this study
VCY54	L40ΔG+pBTM116-1-Aar2-345A+pACTII-stop	this study
VCY55	L40ΔG+pBTM116-1-Aar2-345E+pACTII-stop-E1	this study
VCY56	L40ΔG+pBTM116-1-Aar2-345E+pACTII-stop-E3	this study
VCY57	L40ΔG+pBTM116-1-Aar2-345E+pACTII-stop-E3H	this study
VCY58	L40ΔG+pBTM116-1-Aar2-345E+pACTII-stop	this study
VCY59	BY4742; AAR2:NAT	this study
VCY60	BY4742; aar2:S253A:NAT	this study
VCY61	BY4742; aar2:S253E:NAT	this study
VCY62	BY4742; aar2:T274A:NAT	this study
VCY63	BY4742; aar2:T274E:NAT	this study
VCY64	BY4742; aar2:Y328A:NAT	this study
VCY65	BY4742; aar2:Y328E:NAT	this study
VCY66	BY4742; aar2:S331A:NAT	this study

VCY67	BY4742; aar2:S331E:NAT	this study
VCY68	BY4742; aar2:T345A:NAT	this study
VCY69	BY4742; aar2:T345E:NAT	this study
VCY70	W303α; AAR2:NAT	this study
VCY71	W303α; aar2:S253A:NAT	this study
VCY72	W303α; aar2:S253E:NAT	this study
VCY73	W303α; aar2:T274A:NAT	this study
VCY74	W303α; aar2:T274E:NAT	this study
VCY75	W303α; aar2:Y328A:NAT	this study
VCY76	W303α; aar2:Y328E:NAT	this study
VCY77	W303α; aar2:S331A:NAT	this study
VCY78	W303α; aar2:S331E:NAT	this study
VCY79	W303α; aar2:T345A:NAT	this study
VCY80	W303α; aar2:T345E:NAT	this study

2.1.5 Bacterial and yeast growth media

All the media solutions were autoclaved and kept at room temperature. For solid media 2% (w/v) bacto agar was added before autoclaving. For the Y2H assays 3-Amino-1,2,4-triazole (3AT) was added to drop-out media after autoclaving.

Medium	**Composition**
Luria-Broth (LB)	1 % (w/v) bacto-tryptone, 0.5% (w/v) yeast extract, 0.5% (w/v) NaCl, pH 7.2
YPDA	1% (w/v) yeast extract, 2% bacto-peptone, 2% (w/v) glucose, 0.003% (w/v) adenine sulphate
YPGR	1% (w/v) yeast extract, 2% bacto-peptone, 2% (w/v) galactose, 2% (w/v) raffinose, 0.003% (w/v) adenine sulphate
YMM drop-out	0.67% yeast nitrogen base without aminoacids, 2% (w/v) glucose, drop-out powders were added according to manufacturer instructions and pH adjusted with 0.1g NaOH per 500 mL

2.1.6 Commonly used buffers

Buffer	Composition/Litre
PBS	8g NaCl, 0.2g KCl, 1.44g Na_2HPO_4, 0.24g KH_2PO_4, pH 7.4
20x MOPS	1 M MOPS (3-N-morpholine) propane sulfonic acid, 1M Tris, 2% (w/v) SDS, 20.5 mM EDTA
50x TAE	2 M Tris, 0.05 M EDTA, 5.7% (v/v) acetic acid
5x TBE	54g Tris base, 27.5g boric acid, 20 mL 0.5 M EDTA
10x Western transfer buffer	200 mM Tris base, 1.5 M glycine
20x SSC	3 M NaCl, 0.3 M sodium citrate, pH 7.0
Church buffer	1% BSA, 1 mM EDTA, 0.5 M NaPO4 pH 7.2, 7% SDS
IPP_{150}	6 mM HEPES pH 7.9; 150 mM NaCl; 2.5 mM MgCl2; 0.05 % (v/v) Nonidet P40
Sample buffer	0.5M Tris-HCl pH 6.8, 5% glycerol, 2% SDS, 100 mM DTT

2.1.7 Markers

Marker	Range
1 kb plus DNA Ladder – Invitrogen	100 bp - 12 kb
SeeBlue® Plus2 Pre-stained Standard - Invitrogen	4-250 kDa

2.1.8 Antisera

Antibody	Description	Source
α8.6 (R1689)	Anti-Prp8p aa2-35, rabbit IgG, primary	Boon et al., 2006
αAar2p	rabbit IgG, primary and immunoprecipitation	Gottschalk et al., 2001
αAar2p (R5725)	rabbit IgG, immunoprecipitation	This work

αBrr2p	rabbit IgG, primary	O. Cordin, Beggs lab
αHis-HRP	His- Horseradish Peroxidase conjugate sc-803, primary	Santa Cruz Biotechnology
αMyc (9E10)	C-Myc sc-40 mouse monoclonal IgG, immunoprecipitation	Santa Cruz Biotechnology
αMyc (A-1F)	C-Myc sc-789 rabbit polyclonal IgG, primary	Santa Cruz Biotechnology
αLexA (2-12)	LexA sc7544 mouse monoclonal IgG, immunoprecipitation	Santa Cruz Biotechnology
αLexA Rbp	Ab to Lex A DNA binding region ab14553-50, primary	AbCam
αHA (F-7)	HA sc-7392 mouse monoclonal IgG, immunoprecipitation	Santa Cruz Biotechnology
αHA (Y-11)	HA sc-805 rabbit polyclonal IgG, primary	Santa Cruz Biotechnology
αPhospho-serine	αPhospho-serine p5747 mouse monoclonal, primary	Sigma
αPhospho-tyrosine (PY99)	αPhospho-tyrosine sc-7020 mouse monoclonal, primary	Santa Cruz Biotechnology
αPhospho-threonine (42H4)	αPhospho-threonine mouse mAb Cell Signaling Technologies	New England Biolabs
αrabbit-HRP	αrabbit IgG Horseradish Peroxidase linked F(ab')2 fragment from donkey, secondary	GE healthcare
αrabbit-IR Dye	αrabbit-IR Dye 800CW 926-32213 from donkey, secondary	LiCor-Odyssey
αmouse-HRP	αmouse IgG Horseradish Peroxidase conjugated NA931 from goat, secondary	Amersham Biosciences

2.2 Microbiology protocols

2.2.1 Propagation, storage and bacteria transformation

Growth, storage, preparation and transformation of competent *E. coli* were performed as described in Sambrook & Russel, 2001.

2.2.2 Propagation, storage and yeast transformation

Growth and *S. cerevisiae* storage were performed as described in Methods in Yeast Genetics, 2000. The lithium acetate method was used for yeast transformation (Gietz *et al*., 1991).

2.3 Molecular Biology protocols

2.3.1 DNA sequencing

PCR reactions for DNA sequencing were prepared with appropriate oligos for each situation and with BigDye® Terminator Cycle Sequencing Ready Reaction from Applied Biosystems. Samples were sequenced by the SBS Sequencing Service, Ashworth Laboratories, University of Edinburgh.

2.3.2 Site-directed mutagenesis

Site-directed mutagenesis (SDM) was used to generate the Aar2p phosphomutations. Each oligonucleotide pair containing the desired mutation was designed to be complementary of the pBTM116-1-Aar2p plasmid. *PFU* DNA polymerase from PROMEGA was used in the PCR reaction. For the 50 μL PCR reaction were used: 36 μL H_2O, 5 μL *PFU* 10x Buffer, 2.5 μL dNTP mix (10 mM each), 2.5 μL of each of the two complementary oligonucleotides (10 mM stock), 0.5 μL plasmid DNA template and 1 μL *PFU* DNA polymerase. PCR conditions use were as follow:

1. Denaturing 1 92˚C, 2 min
2. Denaturing 2 92˚C, 30 s
3. Annealing 60˚C, 40 s
4. Extension 68˚C, 8 min
5. Repeat steps 2-4, 25 times
6. Final extension 68˚C, 10 min

The PCR products were treated with *Dpn*I for 3 h to 10 h. After the digestion the reactions were cleaned with Wizard Gel and PCR cleaning kit from PROMEGA. The mutated plasmids were used to transform competent DH5α *E. coli*. The obtained clones were isolated and the mutations confirmed by DNA sequencing.

2.3.3 Nucleic acids techniques

Sambrook & Russel, 2001 was used a general guide for nucleic acids techniques: ethanol precipitation, deproteinisation, endonuclease DNA digestion, DNA ligation, DNA agarose gel electrophoresis and *E. coli* plasmid DNA isolation.

2.3.4 Genomic integration of phospho-mutations

The plasmids obtained from step 2.3.2 were used as templates to clone fragment of phospho-mutated *aar2* into the pGID3 plasmid. This plasmid includes a prMFα2Nat^R cassette for NAT selection and is a tool to insert the phospho-mutations into genomic *AAR2* by homologous recombination. Due to the lack of compatible restriction sites between pBTM116-1 and pGID3 plasmids, In-Fusion® PCR cloning system from Clontech was used to transfer mutant *aar2* sequences (containing each phospho-mutation) from the pBTM116-1-Aar2 templates to the pGID3 plasmid. The *aar2* fragments were amplified from pBTM116-1 by PCR, using oligos designed to promote the fusion between the ends of each PCR fragment to the linearized ends of pGID3.

After the phospho-mutant sequences were inserted immediately 5' to the prMFα2Nat^R cassette in pGID3, a second PCR was preformed to amplify *aar2* with the cassette. These PCR products were integrated into yeast cells by homologous recombination, replacing part of the *AAR2* genomic sequence with each mutant *aar2* fragment plus prMFα2Nat^R cassette. The genomic integration was confirmed by Yeast colony PCR followed by sequencing. This was done with appropriate sets of oligos to verify cassette integraton into the correct locus and confirm the presence of each phospho-mutation in the different transformants.

2.4 Biochemical protocols

2.4.1 Crude yeast extract

3 OD units (OD_{600}) of a yeast strain grown until stationary phase were spun down and the pellet was resuspended in 500 μL of 0.2 M NaOH and incubated on ice for 10 min. Then, 50 μL of 50% TCA were added and the sample left on ice for further 10-30 min. The mixture was spun down at 14000 rpm for 5 min. The pellet was resuspended in 35 μL of dissociation buffer (100 mM Tris pH 6.8; 4 mM EDTA pH 8.0; 4% SDS; 20% glycerol; 2% β-mercaptoethanol and some bromophenol blue). The sample pH was adjusted by the addition of 15 μL of 1M Tris buffer (non-adjusted pH). Sample was boiled for 10 min at 95˚C. At this point samples were either loaded in a gel or stored at -20˚C.

2.4.2 Yeast genomic DNA preparation

3 OD units (OD_{600}) of a yeast strain grown until stationary phase were spun down. Cells were resuspended in 300 μL of lysis solution (4.22 μL H_2O; 100 μL Triton X-100; 500 μL 10% SDS; 125 μL 4 M NaCl; 50 μL 1M Tris-HCl pH 8.0; 10 μL 0.5M EDTA). Approximately 300 mg of zirconia beads were added together with 300 μL of phenol:chloroform:isoamyl alcohol solution and the mixture was vortexed for 6 min at 4˚C. After that the sample was spun for 5 min at 13000 rpm. 200 μL of the top aqueous layer were transferred to a new tube and 180 μL of isopropanol + 20 μL of 3 M sodium acetate pH 5.3 solution were added. The sample was left for 5-30 min at -80˚C to precipitate and then spun for 15 min at 4˚C. Pellet was air dried and resuspended in 100 μL of H_2O. 150 ng of this DNA sample were used as template for 50 μL PCR solutions.

2.4.3 Aar2p antibody production

Aar2p-GST was expressed in *E. coli* (BL21) from pGEX4T1-Aar2-GST plasmid (Gottschalk *et al*., 2001). For this the cells were induced with IPTG at a final concentration of 0.75 mM and grown at 23˚C for 4 h. Cells were collected spinning at 3500 rpm for 5 min at 4˚C.

Cells pellets were resuspended in lysis buffer A (50 mM Tris-HCl pH7.5; 250 mM NaCl; 10 % (v/v) glycerol) with added lysozyme to a final concentration of 0.2 mg/mL and the mixed on ice for 45 min. Triton-X 100 was added to a final concentration of 0.1% (v/v) and mixed on ice for 5 min more. The mixture was centrifuged at 10000 rpm for 10 min at 4˚C in a Beckman centrifuge rotor JA25.5. The supernatant was kept at -80˚C.

Once thawed, the supernatant was incubated for 1h at 4˚C with 1 mL of Gluthatione Sepharose 4B from Amersham (previously washed in PBS). After this, the mixture was placed in a Biorad polyprep chromatography column. The sample was washed three times with wash buffer (50 mM Tris-HCl pH7.5; 250 mM NaCl; 10 % (v/v) glycerol) and eluted from the column with elution buffer (50 mM Tris-HCl pH7.5; 250 mM NaCl; 10 % (v/v) glycerol; 40 mM glutathione). The eluate was dialysed for 4 h against 2 L of dialysis buffer (20 mM Tris-HCl pH 8.0; 100 mM NaCl; 20% (v/v) glycerol) in a dialysis membrane (Slide-A-Lyser 7 kDa cut-off from Pierce).

After dialysis the total volume of protein eluate and the corresponding protein band was gel purified in a denaturing protein gel. The band corresponding to Aar2p was excised from the gel, grinded with liquid nitrogen, resuspended in PBS and sent to Genosphere Biotech, Paris for rabbit inoculation.

Immune-serum from two rabbits was obtained and tested. Serum from the rabbit R5725 proved to be efficient for Aar2p detection by Western blot of crude yeast protein extracts and was used in this study.

2.4.4 λ phosphatase assay

A 50 mL culture of AGY8 cells were grown to early log phase OD_{600}=0.6 approximately, and spun down. The pellet was resuspended in 300 μL lysis buffer (50 mM HEPES pH 7; 75 mM KCl; 1 mM $MgCl_2$ 10 mM EGTA; 20 mM EDTA; 0.1% (v/v) Triton-X 100; 1 mM Na_2VO_4; 50 mM NaF; and for each 10 mL of lysis buffer, 1 mini pellet EDTA-free protease inhibitor and 1 pellet PhoSTOP, both from ROCHE) and 300 μL small glass beads were added. The mixture was homogenized in the rybolizer mixer 3 x 20 s cycles, cooling 1 min on ice between cycles. The lysate was clear at 13 rpm for 10 min at 4˚C. The supernatant was incubated with 20

μL of NiNTA agarose from QIAGEN (previously washed in lysis buffer) for 45 min at 4˚C. The beads were washed 3x with lysis buffer changing tubes once. The beads were washed once with 150 μL of λ phosphatase buffer (New England Biolabs) and the sample was split in half. One half was incubated with 1 μL of λ phosphatase and the other half was treated with buffer only for 30 min at 30˚C (50 μL reactions). The samples were finally spun down. The supernatant removed, the beads resuspended in 30 μL of sample buffer and boiled at 95˚C for 15 min. At this point the samples were either stored at -20˚C or immediately loaded in a 12% SDS-acrylamide denaturing gel and ran in for 20 h at 60 V. A Western blot was preformed to transfer the bands to a PVDF membrane. The membrane was blocked for 1h in blocking solution (PBS-Tween 20 0.01% (v/v); 5% (w/v) skimmed milk). After this the membrane was incubated o/n in blocking solution containing αAar2p (R5725) rabbit anti-serum at a final concentration of 1:3000. The membrane was washed 3x in PBS-Tween 20 0.01% (v/v) and incubated for 1 h in blocking solution containing 1:10000 αrabbit antibody HRP conjugated The membrane was washed in PBS-Tween 20 and incubated with Pierce® ECL Western Blotting substrate for 2 minutes. The membrane was exposed to Kodak medical X-ray blue film.

2.4.5 Phosphoantibodies Western blots

Cell extracts and pulldowns were performed in the same way as in 2.4.4 with the exception of the λ phosphatase treatment. The samples were run in a denaturing gel 4-12 % PAGE gel (1x MOPS buffer) and blotted. For the αPhospho-threonine and αPhospho-tyrosine Western blots the membranes were blocked, and incubated with primary and secondary αmouse antibodies as indicated above. 10 μL of αPhospho-threonine was used in 5 mL of blocking solution and 50 μL of αPhospho-tyrosine in 5 mL blocking solution.

For the α-Phospho-serine western blot the membrane was blocked in PBS-Tween 20 0.01% with 5% (w/v) BSA for 1 h. After that the membrane was incubated o/n with 11.4 μL of αPhospho-serine antibody in 5mL of a solution PBS-Tween20 0.01%, 5% (w/v) BSA. The secondary αmouse antibody was

incubated for 1 h in the PBS-Tween 20 0.01%, 5% (w/v) BSA at a concentration of 1:10000.

2.4.6 Immunoprecipitations

Immunoprecipitations were carried out binding mouse antibodies to protein G Dynabeads (Invitrogen) and rabbit antibodies to protein A Dynabeads according to manufacturer instructions. 10 μL of Dynabeads conjugated with 4 μL of antiserum antibody were used to immunoprecipitated each sample.

Cell extracts were prepared as follow. 60 ODs of cells in log phase were used for experiments in Figures 4.6B and 4.7; 120 ODs for experiments in Figures 4.8, 5.3 and 5.4. Cells were spun down at 4000 rpm for 10 min at 4˚C; washed in 10 mL cold PBS; spun down at again at 4000 rpm for 5 min at 4˚C. All the PBS was carefully removed and the cell pellets were snap frozen in liquid nitrogen. The samples were then kept at -80˚C until needed.

Cell pellets (both 60 and 120 ODs) were thawed on ice and resuspended in 700 μL of lysis buffer (50 mM HEPES pH 7.5; 100 mM NaCl; 1 mM $MgCl_2$; 0.3% (v/v) Triton X-100; 1 mM DTT; for 20 mL of buffer 1 pellet EDTA-free protease inhibitor and 1 pellet PhoSTOP, both from ROCHE, were added). 300 μL of zirconia beads were added and the mixture was vortexed 3x1 min, resting on ice for 1 min between each vortex. The extracts were spun at 4000 rpm for 5 min at 4˚C. The supernatant was transferred to a clean eppendorf tube and spun at 14000 rpm for 20 minutes at 4˚C. The top layer was transferred to a new eppendorf and used immediately for the immunoprecipitations (1-2% of this input lysate was kept for further analysis; 10% for experiment 5.4). The lysate was mixed with the Dynabeads previously bound to antibody and incubated in a rotating wheel at 4˚C. This incubation step was carried out for 45 min in the experiments from Figures 4.6B and 4.7. For the experiments in Figures 4.8, 5.3 and 5.4 the extracts were incubated with the beads for 3 h. After this the tubes were placed in a magnet, the non-bound fraction was removed and 2% of this solution was kept for further analysis (the non-bound fraction was not kept for experiment 5.4). The beads were washed 3x with 200 μL of cold PBS 0.02% Tween 20. 100 μL of the same PBS solution was added to the tubes and the samples were transferred to a clean eppendorf. The tubes were finally placed in the magnet, the

supernatant removed and the beads resuspended in 20 μL of sample buffer. At this point the samples were either stored at -20˚C or boiled at 95˚C for 10 min, loaded in a denaturing 4-12% PAGE (1x MOPS buffer was used) gel together with the 2% input and 2% non-bound fractions for Western blot.

For the experiments illustrated in Figure 4.6B the immunoprecipitations were done using mouse αLexA. Western blot was performed as described above using rabbit αHA and rabbit αPrp8p 8.6 simultaneously as primary antibodies at a concentration of 1:3000. As a secondary antibody sheep αrabbit HRP conjugated was used at a concentration of 1:10000.

The immunoprecipitation in Figure 4.7 was done with mouse αHA and the Western blot with rabbit αLexA and rabbit αBrr2p simultaneously as primary antibodies at a concentration of 1:3000. As secondary antibody fluorescent goat αrabbit was used at a concentration of 1:10000.

For the immunoprecipitations in Figures 4.8, 5.3 and 5.4 rabbit αAar2p (Gottschalk *et al*., 2001) serum was used, since αAar2p serum raised from this study is not efficient for Aar2p pulldown in a *wt* yeast strain (see Figure 2.1).

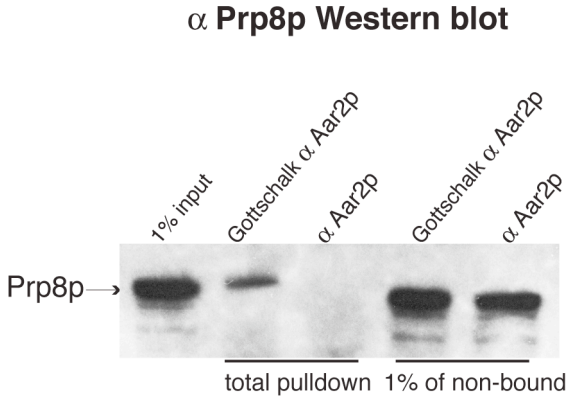

Figure 2.1. Gottschalk *et al*., 2001 αAar2p antibody pulls down Prp8p in Aar2p immunoprecipitation, but my αAar2p antibody does not. Cell extracts from W303 yeast strain were immunoprecipitated in parallel with my αAar2p and Gottschalk *et al*., 2001 rabbit serums. Rabbit αPrp8p antibody was used for the Western blot. The Gottschalk *et al*., 2001 antibody efficiently pulls down Prp8p while the antibody raised by this study does not.

It is not possible to show Aar2p western for this experiment since Aar2p is 42 kDa, and therefore will be masked by the IgG heavy chain.

For the Western blots in Figures 2.1, 4.8 and 5.3 a non-protein blocking buffer has to be used to reduce the high background. Protein-Free (TBS) Blocking Buffer from Thermo scientific was used both for blocking the membrane and for incubation with the primary and secondary antibodies. As primary antibody αPrp8p antiserum was used at 1:3000 dilution. For Figure 2.1 sheep αrabbit HRP was used as secondary antibody at 1:10000 dilution. For Figures 4.8 and 5.3 fluorescent goat αrabbit was used as secondary antibody at a 1:10000 dilution.

2.4.7 Northern blot

For the Northern blot in Figure 5.4, RNA was extracted from the beads after immunoprecipitation, from the input and non-bound fractions.

The beads were washed 2x with IPP_{150}. After that 200 μL of RNA extraction buffer (50 mM Tris pH 7.5; 2% (w/v) SDS; 5 mM EDTA) together with 200 μL of phenol-chloroform iso-amyl alcohol (25:24:1) was added to the washed beads and input samples. The samples were vortexed and spun down at 14000 rpm for 5 min at RT. The top aqueous layer was kept and mixed with 200 μL NaAc 3M pH 5.3 plus 1 μL glycogen and 400 μL ethanol. The RNA was left to precipitate for 20 min to o/n at -20˚C. After this step the samples were spun at 14000 for 30 min at 4˚C. The pellets were washed with ethanol 70% and dried. Finally the samples were resuspended in 10 μL H_2O plus 10 μL formamide loading buffer (formamide; 0.1 M EDTA; trace amounts of bromophenol blue and xylene cyanol), boiled at 95˚C for 3 min, cooled on ice and loaded in an acrylamide gel (Sequagel mixture 6% prepared according to manufacturer instructions) and ran at 23 W for approximately 1 h in 1x TBE.

The RNA was transferred to a Hybond-N nylon membrane at 60 V for 1 h in 0.5x TBE. The RNA was then cross-linked to the membrane in a UV crosslinker.

The membrane was pre-incubated for 30 min at 37˚C in 50 ml Church buffer. Then 50 μL of U5 probe were added and let to incubate o/n (see U5 probe preparation bellow). After that was the membrane was washed in 6x SSC buffer for 10 min at 37˚C; and washed again in 2x SSC for 10 min at 37 ˚C. Finally the

membrane was exposed to autoradiographic film to visualize the results and to phosphor screen for quantification in the PhosphorImager.

For the U5 probe preparation were mixed: 0.5 μL of 10 μM U5 oligonucleotide; 1 μL 10x PNK buffer; 5.5 μL H_2O; 2 μL [γ-^{32}P]ATP (3000 Ci/mmol) and 1 μL kinase T4 polynucleotide (PNK). The reaction was left at 37˚C for 1 h and then incubated at 65˚C for 5 min to inactivate the kinase. Finally were added 40 μL H_2O and the mixture was purified in a spin purification column.

2.4.8 Sample preparation for mass spectrometry

Yeast extracts from P_{GAL1}-*AAR2-His* strain grown in 2% galactose were prepared and a pulldown with NiNTA beads was made as explained above. Samples were run in a denaturing acrylamide 4-12% PAGE gradient gel and the gel stained for 1 h with Coomassie Brilliant Blue R250 from Pierce (Thermo Scientific). In-gel digests with trypsin, elastase, proteinase K, and thermolysin were performed independently according to Schlosser *et al*. (2005) plus 10 μL of acetonitrile in a final digestion volume of 100 μL.

2.5 Live cell imaging

Strains AGY8, VCY1 and VCY2 were grown overnight in 2% galactose. In the morning the strains were diluted to OD_{600}=0.2 and grown in 2% galactose and 2 % glucose in parallel for 8h in log phase. 50 μL of each cell culture were spin down and resuspended in 150 μL of fresh media. From here 50 μL were spread on a poly-lysine coated microscope slide (Polysine, VWR, 631-0107) together with mounting solution containing DAPI. Prp8p-GFP and Snu114p-GFP localisation was verified on live cells by fluorescence microscopy with a Leica FW4000 microscope, 100x magnification. This microscope is equipped with a narrowband filter wheel that detects GFP and DAPI fluorescence (gfp - 489 nm excitation and 508 emission; A4 - 354 nm excitation and 461 emission). Regarding the exposure times, these were 200 to 500 milliseconds to GFP and 50 to 100 milliseconds for DAPI. Because live cells are constantly moving only one z-section was recorded for each snapshot. A CoolSNAP camera (Roper Scientific) with Leica FW4000 V1.1.1 software was used to capture the images.

2.6 Yeast two-hybrid (Y2H) assay and screens

Both Y2H assay and screen were performed according to Fromont-Racine *et al.* (2002).

In the Y2H assay Aar2p full-length, $Aar2p_{1-170}$ and $Aar2p_{150-355}$ were cloned in pBTM116-1 plasmid and used as baits. $Prp8p_{1649-2413}$, $Prp8p_{2010-2413}$ and $Prp8p_{2010-2413}$-prp8-52 fragments previously cloned in pACTII-stop vector (van Nues and Beggs, 2001) were used as preys.

For the Y2H screens the $Aar2p_{1-170}$ and $Aar2p_{150-355}$ fragments already cloned in pBTM116-1 plasmid were used as baits against a *S. cerevisiae* prey library from J. C. Rain, Hybrigenics, Paris.

CHAPTER 3 - Aar2p phosphorylation

3.1 Introduction

A question emerging from the proposed U5 snRNP maturation model (Boon *et al*., 2007) concerns the mechanism that triggers Aar2p release from the precursor U5-snRNP (see Figure 1.5). If Aar2p and Brr2p compete for binding to Prp8p, there must be a signal leading to Aar2p departure from the U5 snRNP, thereby allowing Brr2p to bind Prp8p as one of the required steps for U5 snRNP maturation. One possibility is a post-translational modification that elicits Aar2p release from the U5 snRNP. A common post-translational modification is phosphorylation (Cohen, 2000). In fact, several of the conformational rearrangements that occur during the splicing reaction are controlled by phosphorylation and dephosphorylation events (Misteli, 1999). For example, the PP1/PP2A phosphatases elicit transition from first to second step of splicing having SAP155 and U5-116kDa as major substrates in human spliceosomes (Shi *et al*., 2006). Another relevant event that requires phosphorylation is the integration of the tri-snRNP into the human spliceosome due to PRP28 phosphorylation (Mathew *et al*., 2008). Still in humans, the tri-snRNP proteins PRP6 and PRP31 are phosphorylated by PRP4 kinase during spliceosomal complex B formation (Schneider *et al*., 2010). Accordingly, it is plausible that a phosphorylation/dephosphorylation event might also regulate Aar2p interaction with the U5 snRNP.

Following this hypothesis I investigate the phosphorylation state of Aar2p. All the assays described in this chapter are performed with yeast strain AGY8 (Gottschalk *et al*., 2001) kindly provided by P. Fabrizio. In this strain, the genomic *AAR2* is disrupted by insertion of *URA3* as a marker and it carries a plasmid that produces Aar2p with histidine tag under control of the *GAL1* promoter.

This study shows for the first time that Aar2p is indeed phosphorylated and it identifies five phosphorylated aminoacids: S253, T274, Y328, S331 and T345.

3.2 λ phosphatase assays

The first experiment carried out is a band mobility shift assay after incubation in the presence or absence of λ phosphatase. This enzyme dephosphorylates

phosphorylated serines, threonines and tyrosines (the most frequently phosphorylated amino acids in eukaryotes) in a Mn^{2+}-dependent way (Zhuo *et al*., 1993). If Aar2p is phosphorylated in any of these residues the phosphatase will release the phosphate groups. Under these conditions, the dephosphorylated Aar2p will migrate faster in a denaturing gel than non-treated Aar2p. Cell extracts were prepared from the AGY8 strain (P_{GAL1}-*AAR2-his6*) grown on 0.3%, 0.5% or 2% (w/v) galactose plus 3.7%, 3.5% and 2% (w/v) raffinose respectively in order to produce cell extracts containing different amounts of Aar2p. A pulldown with Ni-NTA beads was done. Half of each sample was treated with λ phosphatase and the other half was treated with λ phosphatase buffer only under the same conditions. The samples were run in a denaturing 12% (w/v) acrylamide gel and a Western blot was carried out, probing for Aar2p (Figure 3.1A). Yeast strain JF191 (kindly provided by J. Fernius) was used as a positive control for λ phosphatase activity and mobility shift in this experiment (Figure 3.1B). In this strain Spc105p, that is a subunit of a kinetochore-microtubule binding complex (Nekrasov *et al.*, 2003), is Myc tagged. Spc105p is known to be phosphorylated at T356 and S380 (Li *et al.*, 2007).

Figure 3.1 shows that when samples are incubated with λ phosphatase, Aar2p mobility in the denaturing gel is affected. The treated samples run faster than the untreated ones demonstrating that Aar2p is indeed phosphorylated *in vivo* in budding yeast.

3.3 Assays with phospho-specific antibodies

Acknowledging that Aar2p is phosphorylated, the next question is which residue(s) is(are) phosphorylated. This can be addressed by using anti-phosphopeptide antibodies (Sefton and Shenolikar, 2001).

Cell extracts were prepared in the same way as for the band shift experiment, but without the λ phosphatase treatment. The samples were run in a denaturing gel and the Western blots were probed with αPhospho-serine, αPhospho-threonine or αPhospho-tyrosine antibodies (Figure 3.2). The results show that some serine and tyrosine residues of Aar2p are phosphorylated. The absence of signal detected with αPhospho-threonine indicates that most likely there are not phosphorylated threonines in Aar2p under the conditions used.

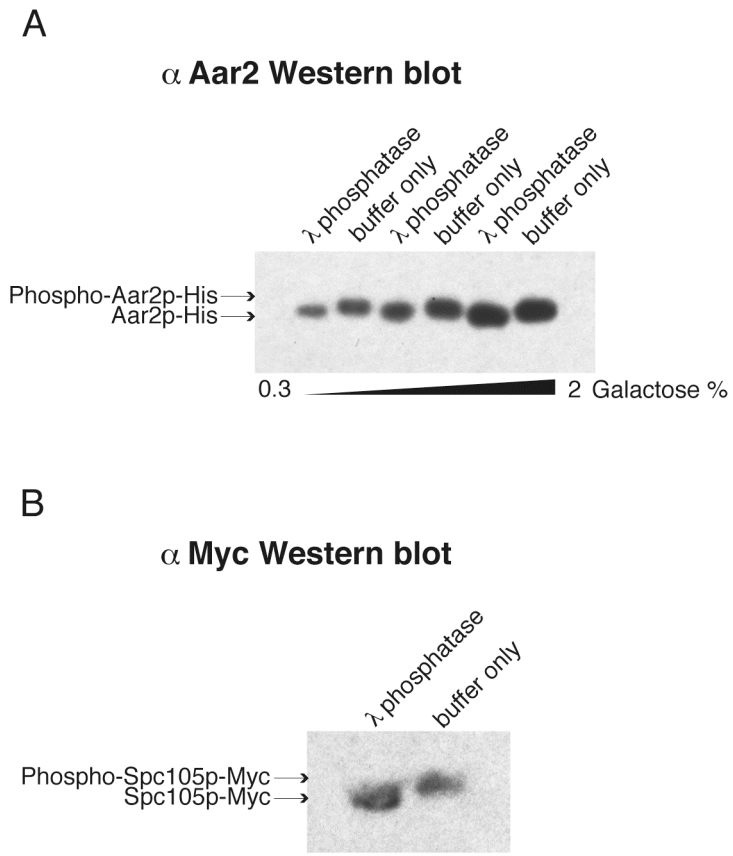

Figure 3.1. Aar2p is phosphorylated in budding yeast. A) Western blot showing Aar2p band-shift after treatment with λ phosphatase. AGY8 cells were grown in 0.3%, 0.5% and 2% galactose (w/v) plus 3.7%, 3.5% and 2% raffinose (w/v) respectively, and collected at OD_{600}=0.6. Cell extracts were prepared and incubated with NiNTA beads to pulldown Aar2p-His_6. The beads-Aar2p-His_6 complexes were split in two equal parts: one was incubated for 30 minutes with λ phosphatase, and the other half was incubated with buffer only. The samples were run in a denaturing 12% acrylamide gel, blotted and probed with anti-Aar2p antibody. All the extracts treated with λ phosphatase show a mobility shift (around 0.45 kDa) when compared with the non-treated ones, indicating that Aar2p is phosphorylated *in vivo*. **B**) Positive control Spc105p-Myc_{13} for band-shift experiment. The cells were collected and treated with λ phosphatase as described for AGY8. Pulldown was made with mouse αMyc antibody and the blot was probed with rabbit αMyc antibody. The band shift observed indicates that the conditions used for the λ phosphatase assay are efficient and the enzyme is active.

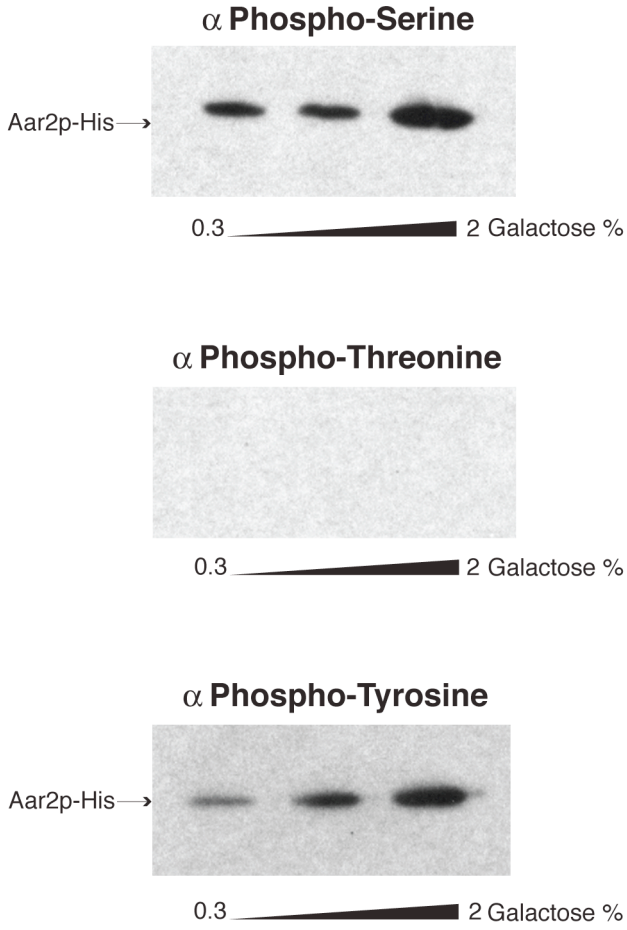

Figure 3.2. Aar2p has phosphorylated serine(s) and tyrosine(s). Western blots showing Aar2p-His_6 detected with αPhospho-serine and αPhospho-tyrosine antibodies. No Aar2p-His_6 was detected with αPhospho-threonine. AGY8 cells were grown in 0.3%, 0.5% and 2% galactose (w/v) plus 3.7%, 3.5% and 2% raffinose (w/v) respectively, and collected at OD_{600}=0.6. Cell extracts were prepared and incubated with NiNTA beads to pulldown Aar2p-His_6. The samples were run in a denaturing SDS-acrylamide 4-12% PAGE gel blotted and probed with αPhospho-Serine, αPhospho-Tyrosine and αPhospho-Threonine antibodies. These results imply that Aar2p has phosphorylated serine(s) and tyrosine(s) *in vivo*.

3.4 Mass-spectrometry results

Mass-spectrometry is a powerful technique in the study of post-translational modifications, enabling identification of phosphorylated aminoacids within a protein (reviewed in Salzano and Crescenzi, 2005). In order to map the exact position of the phosphorylated aminoacids in Aar2p, extracts from the AGY8 strain were prepared and analysed by mass-spectrometry.

Yeast extracts from AGY8 grown in 2% (w/v) galactose plus 2% (w/v) raffinose were prepared as described for previous experiments, and a pulldown with NiNTA beads was done. Samples were run in a denaturing acrylamide 4-12% PAGE gel and the gel stained with Coomassie brilliant blue (Figure 3.3).

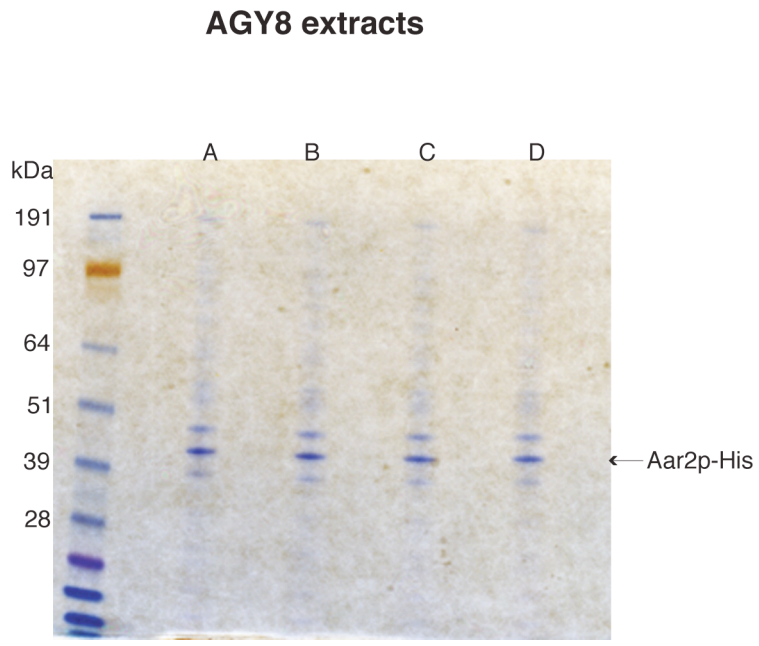

Figure 3.3. AGY8 extracts analysed by mass-spectrometry. Four yeast extracts (A, B, C and D) from AGY8 growing in 2% galactose (w/v) plus 2% raffinose (w/v) were prepared as before and a pulldown with NiNTA beads was made. The four bands corresponding to Aar2p-His_6 were isolated from the gel, and each one was used for an in-gel digest with one of the following proteases: elastase, trypsin, proteinase K and thermolysin. The digested samples were sent to J. Rappsilber lab to be analysed by mass-spectrometry.

The band corresponding to Aar2p was cut out and four protease in-gel digests with elastase, trypsin, proteinase K or thermolysin were performed for 16 hours at 30ºC in NH_4HCO_3 pH 8 (Schlosser *et al*., 2005). The resulting digested peptides were analysed by mass-spectrometry by F. de Lima Alves in J. Rappsilber's lab (Wellcome Trust Centre for Cell Biology, Edinburgh). Figure 3.4 shows the Aar2p peptide coverage obtained with each protease digest and the candidate phosphorylated amino acids identified in each assay.

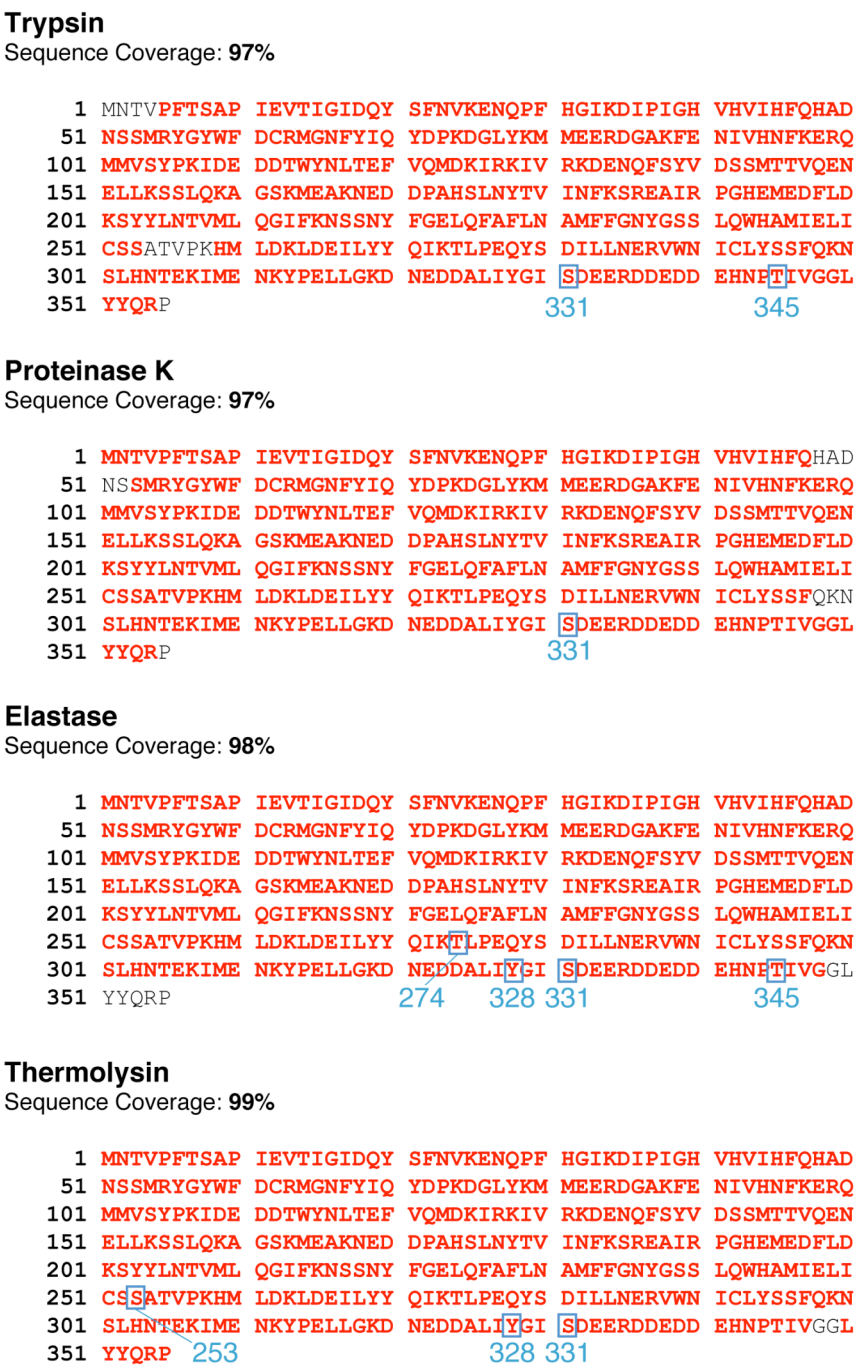

Figure 3.4. Mass-spectrometry results. Aar2p peptide sequence coverage and phosphorylated peptides identified with each protease digest. The aminoacids in red represent the peptide coverage obtained with the indicated digestion while the ones in grey represent the ones not covered. The candidate phosphorylated aminoacids are indicated with a blue square. Trypsin digest had a sequence coverage of 97% and identified S331 and T345. proteinase K digest with also 97% of sequence coverage and S331 identified. 98% of sequence coverage was obtained with elastase digest which recognized T274, Y328, S331 and T345 as phosphorylated sites. With thermolysin digest 99% of Aar2p sequence was covered and S253, Y328 and S331 were identified as phosphorylated.

Complete sequence coverage was obtained with the combination of enzymes used: trypsin 97%, proteinase K 97%, elastase 98% and thermolysin 99%. However, not all of the digests identified the same phosphorylated aminoacids. Trypsin digestion revealed S331 and T345; proteinase K digestion identified S331; elastase digestion uncovered the highest number of phosphorylated sites, T274, Y328, S331 and T345; and finally S253, Y328 and S331 were revealed after thermolysin digest. Overall, five phosphorylated sites were identified in Aar2p: S253, T274, Y328, S331 and T345.

These results are in agreement with my α-Phospho-serine and α-Phospho-tyrosine western blots that show the presence of phospho-serines and tyrosines in Aar2p. The α-Phospho-threonine western indicates that there are no phosphorylated threonines, whereas the mass-spectrometry analysis identifies two, T274 and T345. This discrepancy can be due to a low sensitivity of the α-Phospho-threonine antibody compared to the mass-spectrometry analysis. Another plausible explanation is that mass spectrometry, not being quantitative in the conditions used, detected a very minor fraction of Aar2p not detectable by western blot analysis.

3.5 Aar2p sequence alignment

To determine if any of the phosphorylated amino acids identified is conserved across eukaryotes, I did a multiple sequence alignment of Aar2p orthologs in different species. Amino acid sequences of Aar2p were retrieved from Genbank for *Saccharomyces cerevisiae* and other species including *Homo sapiens*. The sequences were then aligned in Jalview 2.5 (Waterhouse *et al.*, 2009) using the MUSCLE alignment algorithm (Edgar, 2004) (Figure 3.5). The five phosphorylated aminoacids identified by mass-spectrometry in *S. cerevisiae* are highlighted in Figure 3.5 with a red asterisk. S253 is conserved in almost all of the species, including in humans, with the exception of *Arabidopsis thaliana*, *Caenorhabditis elegans*, and *Xenopus laevis*. On the other hand, none of the remaining phosphorylated sites is conserved across the species compared. These results suggest that only phosphorylation of S253 might be significant for a function of Aar2p that is conserved across eukaryotes.

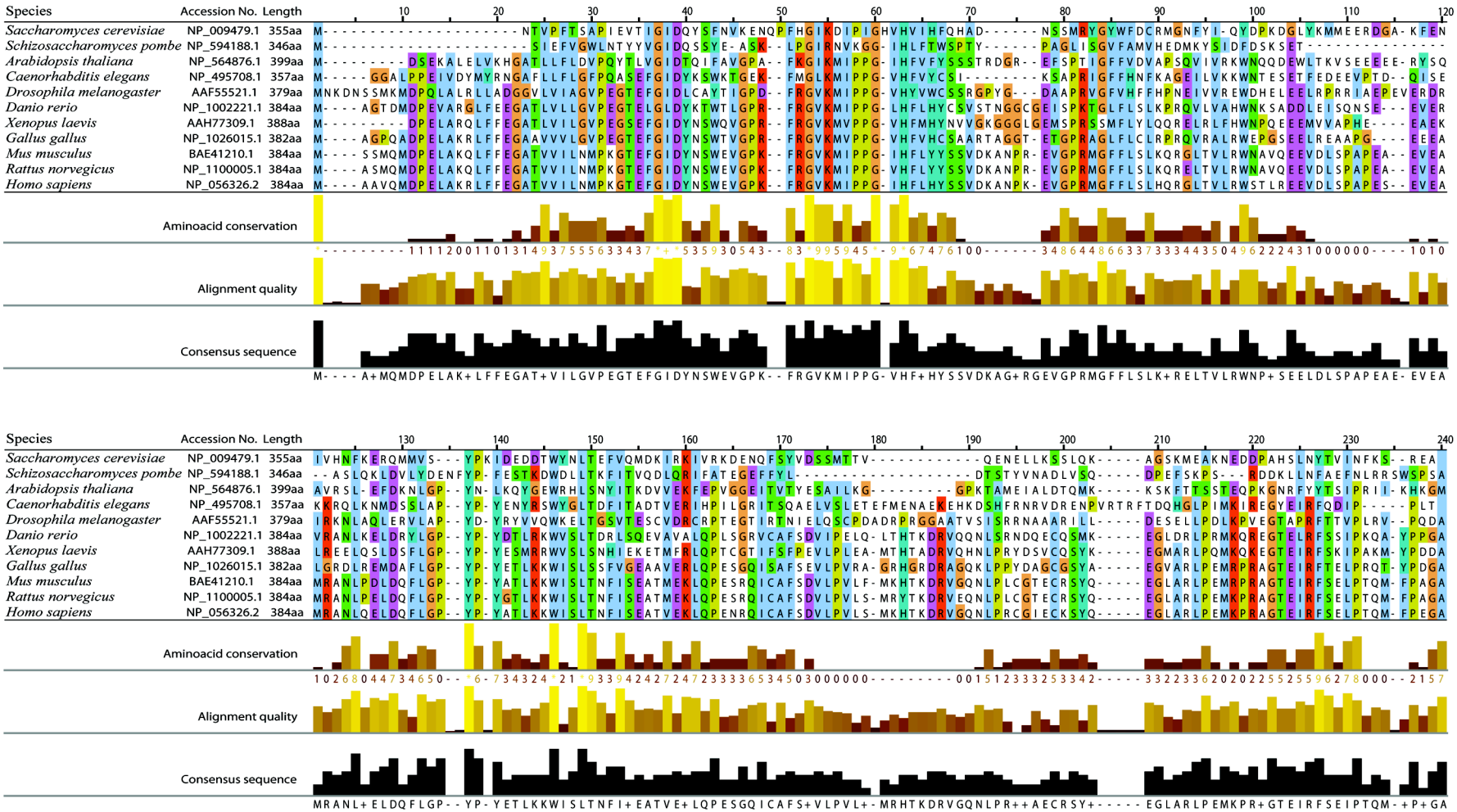

Figure 3.5. Multiple sequence alignment of Aar2p homologs in different species. (Figure continues on next page. See legend on page 50)

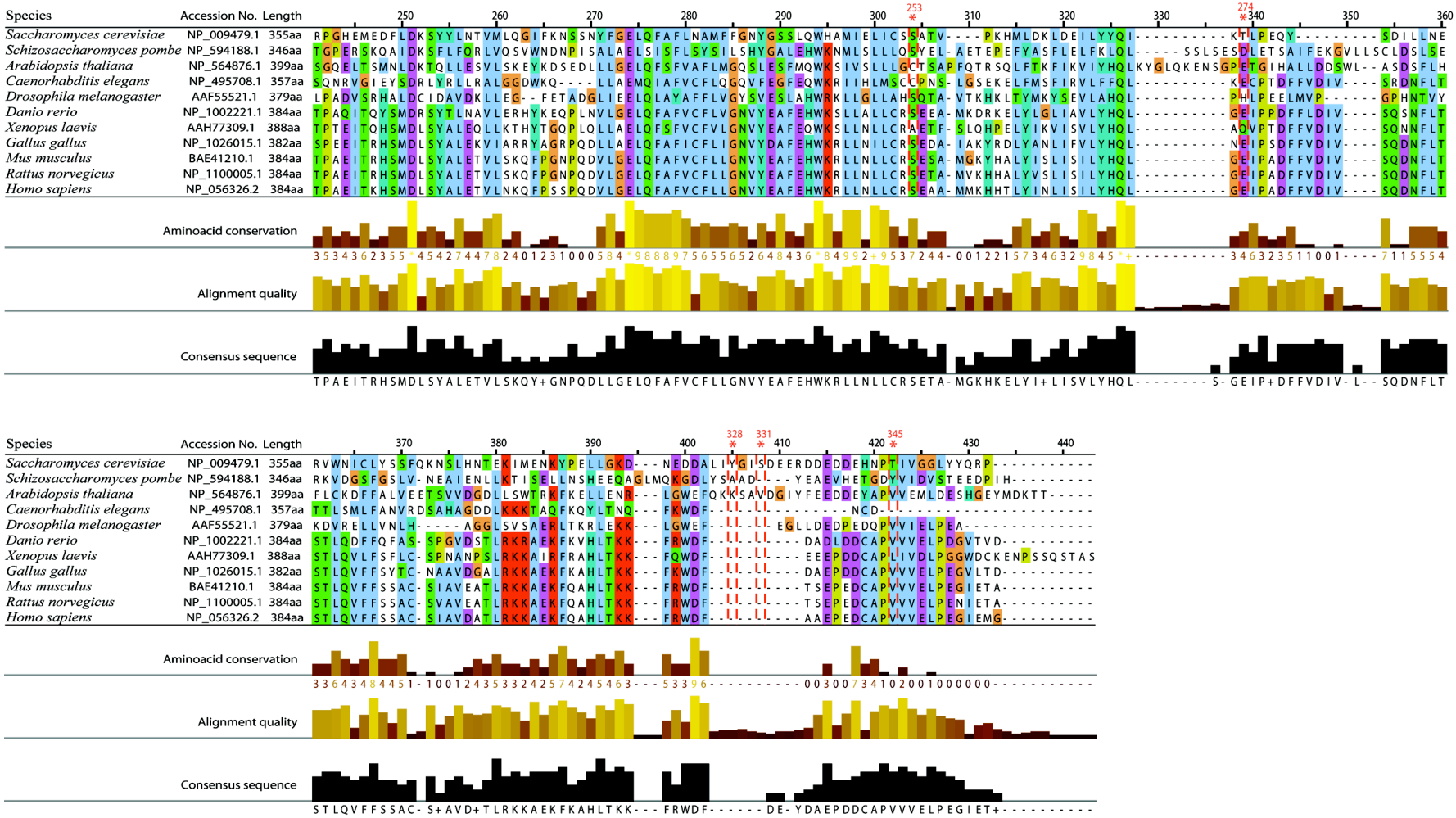

Figure 3.5. Multiple sequence alignment of Aar2p homologs in different species. (Continued. See legend on page 50)

Figure 3.5. Multiple sequence alignment of Aar2p homologs in different species. Aminoacid sequences of Aar2p were retrieved from Genbank for representative fungal, plant and animal taxa. Sequences were aligned in Jalview 2.5 (Waterhouse *et al.*, 2009) using MUSCLE alignment algorithm (Edgar, 2004) as this method tends to be more accurate than ClustalW when dealing with a diverse set of sequences. Each aminoacid is assigned a colour if it meets a conservation threshold. Colours represent a combination of this threshold with residue group type-specific criteria.
The five phosphorylated aminoacids identified by mass-spectrometry in *S. cerevisiae* are highlighted here with a red asterisk. S253 shows the highest aminoacid conservation among the phosphorylated sites, suggesting its hypothetical signaling function might be conserved across taxa. T345 is conserved in other budding yeasts (not shown).

3.6 Discussion

Using a set of complementary techniques I confirm that Aar2p is phosphorylated *in vivo* in *Saccharomyces cerevisiae* and identify five phosphorylated aminoacids: S253, T274, Y328, S331 and T345. Supporting these data, a phosphoproteome study identified Aar2p S331 to be phosphorylated in *S.cerevisiae* after DNA-damage induction by genotoxic stress with methyl methanesulfonate (Albuquerque *et al*, 2008). This is an allusion to a new putative role for Aar2p besides its involvement in pre-mRNA splicing. It is possible that Aar2p is required for a stress-related response and phosphorylation of S331 might play a role in this mechanism. Since S331 is not conserved in any other species this could be a feature exclusive to *S. cerevisiae*.

Comparison of Aar2p orthologues suggests that S253 is conserved across several eukaryotes, including in humans, suggesting its function could be conserved throughout evolution. Hence it is possible that the phosphorylation state of S253 controls Aar2p activity and/or regulates its interaction with other proteins.

This study suggests that a phosphorylation/dephosphorylation event can have a role in U5 snRNP maturation, likely triggering Aar2p release from the precursor form of U5-snRNP. Subsequently, this would allow Brr2p to bind Prp8p, completing the maturation process. Due to its conservation, S253 is the most likely Aar2p phosphorylated amino acid to play a role in U5 snRNP maturation.

Further work is required to clarify which kinase is responsible for Aar2p phosphorylation and to disclose the functional importance of each of the five phosphorylated aminoacids.

CHAPTER 4 – Aar2p/Prp8p interaction

4.1. Introduction

Several clues exist for a physical interaction between Aar2p and components of the intermediate U5 snRNP, particularly with Prp8p (Gottschalk *et al*., 2001; Gavin *et al.,* 2002; Gavin *et al*., 2006; Boon *et al*, 2006; Collins *et al*., 2007; Boon *et al*, 2007). It was observed that Prp8p fragmentation at $Prp8p_{2173}$ interferes with Prp8p association with Aar2p. Also, the amount of Aar2p associated with $Prp8p_{771-2413}$ was increased compared to the full-length Prp8p (Boon *et al*, 2006). Although it is generally believed that Aar2p interacts with C-terminal Prp8p (Boon *et al*., 2006; Boon *et al*, 2007), a direct interaction was never demonstrated and the exact region of interaction required is not known for either Prp8p or Aar2p.

Kutach (unpublished data – personal communication) purified yeast $Prp8p_{1806-2413}$, which he termed Prp8p-CTF, and identified one co-purifying protein - Aar2p. He obtained a Prp8p/Aar2p/Brr2p complex from a mixture of Aar2p, Brr2p and Prp8p-CTF *in vitro.* From his observations, binding of Brr2p to Prp8p-CTF does not inhibit the subsequent interaction of Aar2p with Prp8p-CTF, however, pre-binding an excess of Aar2p to CTF inhibits subsequent binding of Brr2p. He suggests that Aar2p binds to CTF-N and clamps down the CTF-C, impairing Brr2 binding to this region.

In this chapter I look into Aar2p interaction with Prp8p. I show here that Aar2p does not contribute to Prp8p and Snu114p nuclear import and that $Aar2p_{1-170}$ interacts with $Prp8p_{1649-2413}$ in Y2H and in pull-down assays. In addition I discover that the Aar2p mutation S253E strongly disrupts the Aar2p/Prp8p interaction. Finally I discard any potential role of Prr2p and Gcn2 kinases might have in the regulation of Aar2p/Prp8p interaction.

4.2. Localisation experiments

It is known that Prp8p's NLS has a role in Prp8p nuclear import (Boon *et al*., 2007). It is possible however that Aar2p can be an additional cofactor in this process, helping the nuclear import of Prp8p and other components of the Aar2p-U5 particle, such as Snu114p. Using the AGY8 strain as a base I created two new strains: one

expressing *PRP8-GFP* - strain VCY1; and another expressing *SNU114-GFP* - strain VCY2. When growing the cells in decreasing galactose concentrations the corresponding decrease in *AAR2-his6* expression is evident (Figure 4.1).

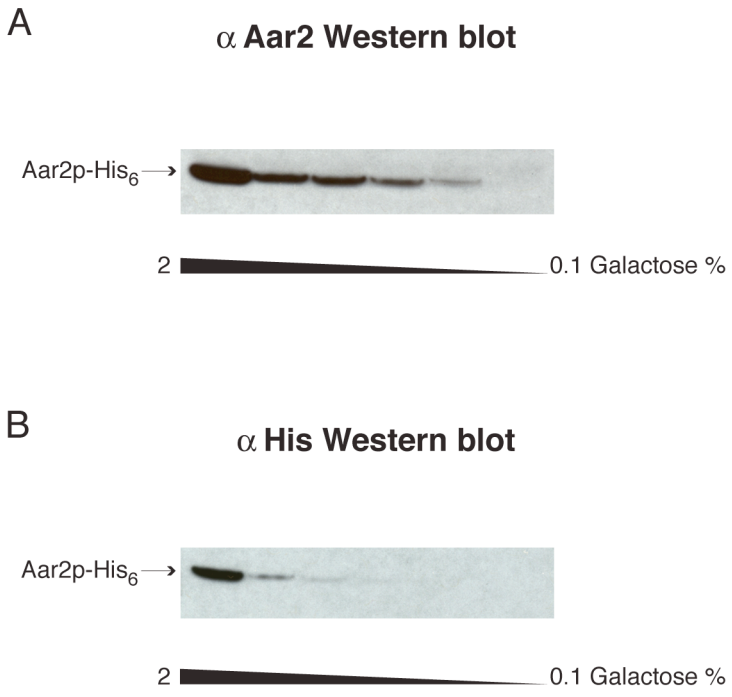

Figure 4.1. Aar2p-His$_6$ production decreases with decrease in galactose concentration in the AGY8 strain. A) AGY8 cells were grown in 2%, 0.5%, 0.4%, 0.3%, 0.2% and 0.1%, galactose (w/v) plus 2%, 3.5%, 3.6%, 3.7%, 3.8% and 3.9% raffinose (w/v) respectively. Cell extracts were run in a denaturing gel, blotted and probed with αAar2p antibody. **B**) The same extracts as in A) run in a different gel and blotted with αHis antibody.

Hence, switching off *AAR2* expression by growing the cells on glucose, allows the role of Aar2p in Prp8p and Snu114p import into the nucleus to be examined. Strains AGY8, VCY1 and VCY2 were grown in 2% galactose and 2% glucose in parallel and Prp8p-GFP and Snu114p-GFP localisation in live cells was investigated by fluorescence microscopy. In Figure 4.2 is clear that both Snu114p and Prp8p are predominantly nuclear either with *AAR2* overexpression or repression. Thus, Aar2p is not required for Snu114p and Prp8p nuclear import.

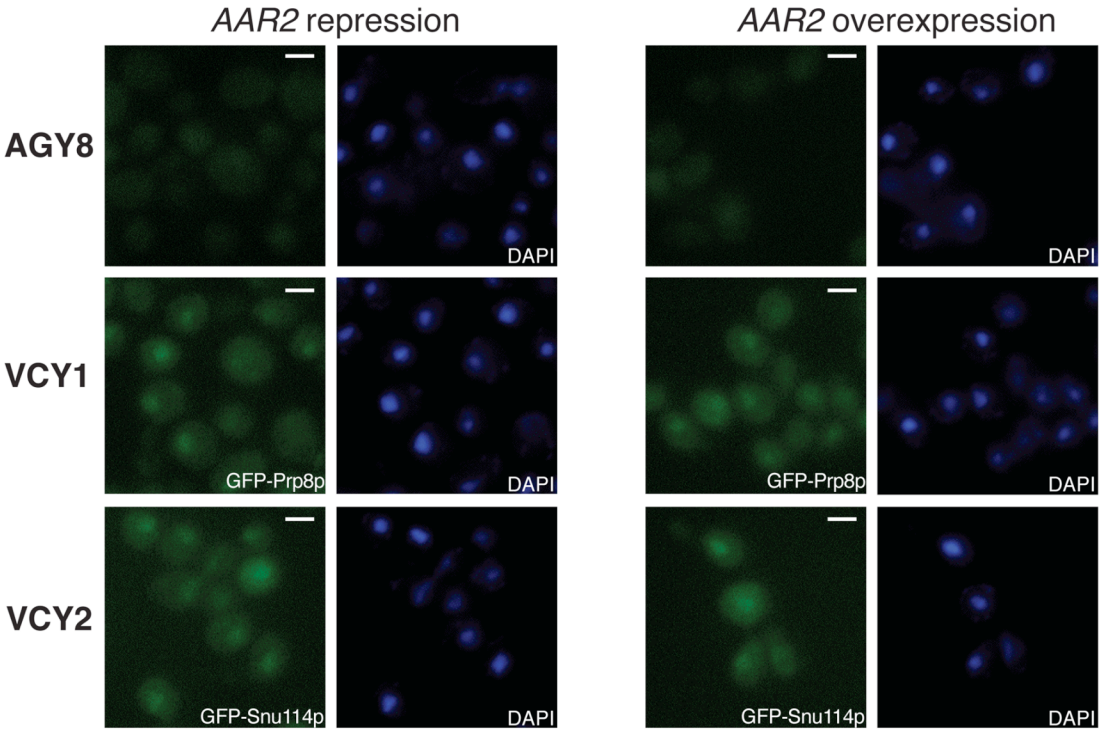

Figure 4.2. Aar2p does not affect GFP-Prp8p and GFP-Snu114p localisation. Strains AGY8, VCY1 and VCY2 were grown on 2% glucose (*AAR2* repression) and on 2% galactose (*AAR2* overexpression) and observed by fluorescence microscopy. The cells were mounted on glass slides with DAPI to stain the nuclear DNA. The non-tagged control strain (AGY8) shows some auto-fluorescence. It is clear that the nuclear localisation of GFP-Prp8p and GFP-Snu114p in the VCY1 and VCY2 strains is unaffected regardless of the *AAR2* expression level. Both VCY1 and VCY2 strains show more fluorescence in the cytoplasm than the AGY8 strain, possibly due to higher levels of GFP-Prp8p and GFP-Snu114p in the cytoplasm. Scale bar corresponds to 10 μm.

4.3. Yeast two-hybrid assays

A yeast two-hybrid (Y2H) assay was set up to investigate the Aar2p/Prp8p interaction in detail. Full-length Aar2p, Aar2p$_{1-170}$ and Aar2p$_{150-355}$ were used as bait fusions (with a LexA tag) and Prp8p$_{1649-2413}$ (E1), Prp8p$_{2010-2413}$ (E3) and Prp8p$_{2010-2413}$-prp8-52 (Y2037H, I2051T-located in domain IV; E3H) as prey fusions (with an HA tag) (Figure 4.3).

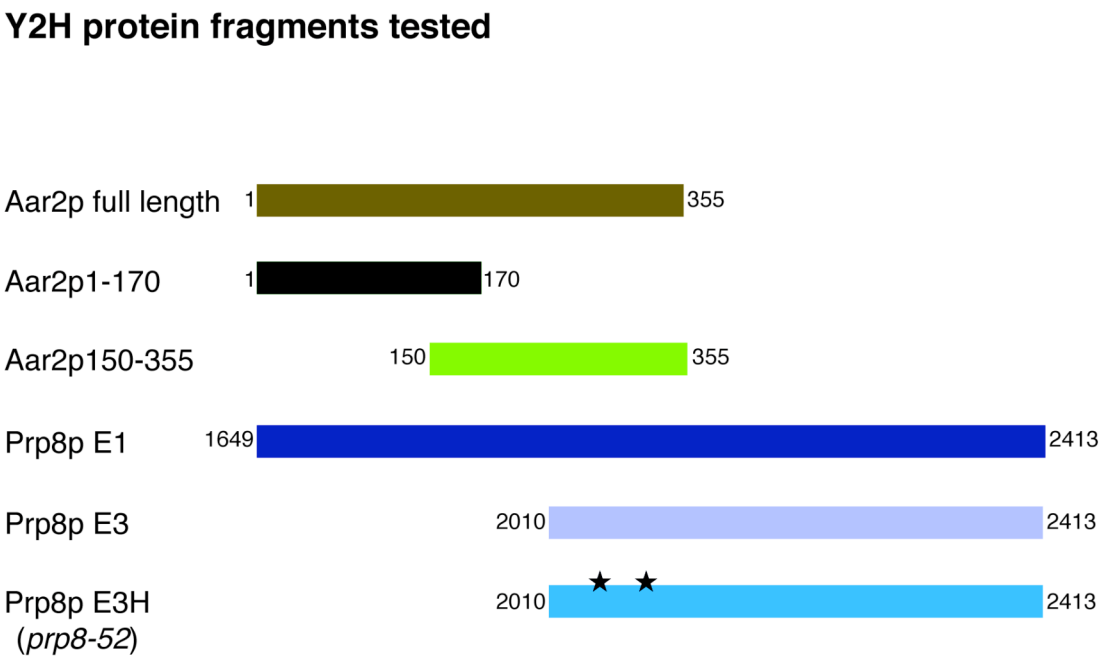

Figure 4.3. Schematic representation of the protein fragments used for Y2H assays. In this work, all full length and partial Aar2p fragments were cloned into the pBTM116-1 vector to be used as baits. The Prp8p fragments were previously cloned (van Nues *et al*., 2001) into the pACTII-stop vector as prey fusions. The E3H fragment differs from E3 in two point mutations (indicated by ★), Y2037H and I2051T, the same as in the *prp8p-52* mutant. Please note that the figure is not to scale.

Prp8p$_{2010-2413}$-prp8-52 was previously reported (van Nues & Beggs, 2001) as having an increased binding affinity to Brr2p when compared to Prp8p$_{2010-2413}$ in a yeast two-hybrid assay. The interactions were tested at 18, 25, 30 and 33°C with 1, 5, 10, 25 and 50 mM of 3AT (Figure 4.4). Full-length Aar2p shows auto-activation activity, since the strain that contains Aar2p as bait plus pActII empty vector grows in -LWH and in -LWH supplemented with 3AT. This fact limits the conclusions that can be drawn from the assays where full-length Aar2p was used as bait. Nevertheless two remarkable conclusions can be made from this experiment. The first is a cold-sensitive (cs) growth phenotype when the Aar2p full-length bait is combined with the E3H fragment (Prp8p$_{2010-2413}$-prp8-52) as a prey. The second is the fact that Aar2p$_{1-170}$ interacts with E1 (Prp8p$_{1649-2413}$), E3 (Prp8p$_{2010-2413}$) and E3H (Prp8p$_{2010-2413}$-prp8-52). Although this interaction does not seem very strong (the

cells cannot survive at high 3AT concentrations), it is possible to conclude that Aar2p$_{1-170}$ interacts with C-terminal Prp8p.

The next step was to mutate the Aar2p phosphorylation sites described in Chapter 3, and search for an effect on Aar2p/Prp8p interaction. Accordingly, the full-length Aar2p bait was subjected to site-directed mutagenesis (SDM) in order to individually mutate S253, T274, Y328, S331 and T345 to Alanine (A) or Glutamic acid (E). This mimics the effect of non-phosphorylated (Alanine) and phosphorylated (Glutamic acid) aminoacid residues in the Aar2p/Prp8p interaction in the Y2H system.

In this Y2H spotting assay all the phosphomutants auto-activate, growing in -LWH plates when in combination with empty pActII vector, just like the *wt* Aar2p bait fusion (data not shown). Yet several important observations can be made. Some of the phosphomutants show cs growth phenotypes when in combination with the E3 and E3H Prp8p fusions (similar to *wt* Aar2p), while others rescue the growth phenotype (Figure 4.5). The low temperature exacerbates the defect in the majority of the mutants with exception of T274A, Y328A, T345A and T345E. Mutations S253A, T274E, Y328E, S331A and S331E behave like *wt* when in combination with E3 and E3H fragments. When growth defects are observed, they are stronger if the mutations are combined with the E3H than with the E3. On the other hand, high temperatures aggravate the growth defect on the T274E, Y328E, S331A and S331E mutants. Five mutants rescue the *wt* growth phenotype at 18, 25 and 33°C: S253E (very weakly), T274A, Y328A, T345A and T345E.

Figure 4.4. Aar2p$_{1-170}$ interacts with Prp8p fragments E1, E3 and E3H. Y2H spotting assay shows cells growing at 18, 25 and 33˚C. Cells were plated on -LW, -LWH and -LWH supplemented with different 3AT concentrations (1, 5, 10 25 and 50 mM). It is not possible to conclude about the interaction of full length Aar2p with the Prp8p fragments since the negative control (Aar2p full length + pActII empty vector) auto-activates and grows in non-permissive conditions. Aar2p$_{150-355}$ does not interact with any of the Prp8p fragments tested and Aar2p$_{1-170}$ interacts with all of them.

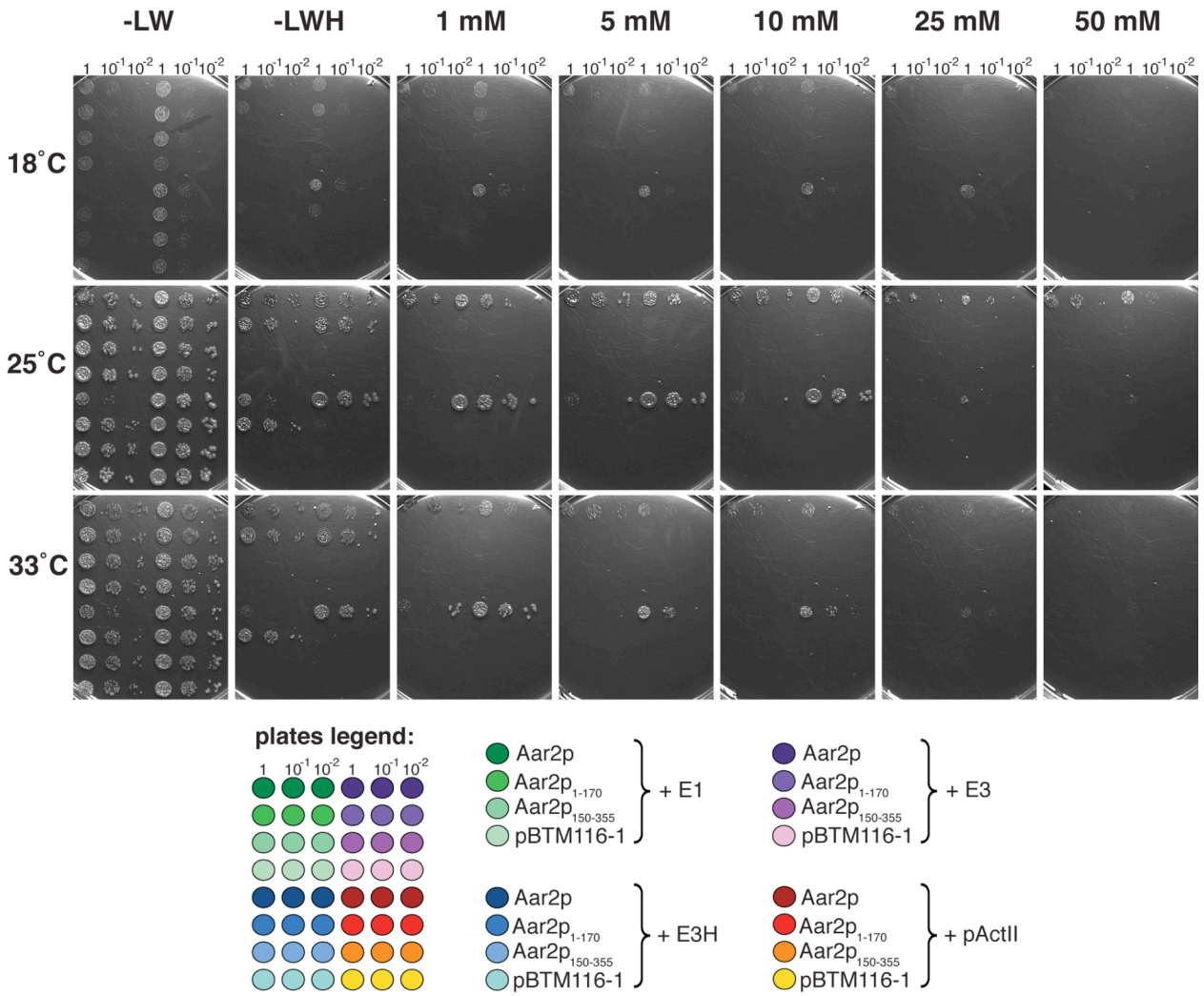

Figure 4.4. Aar2p$_{1-170}$ interacts with Prp8p fragments E1, E3 and E3H. (See legend on page 55)

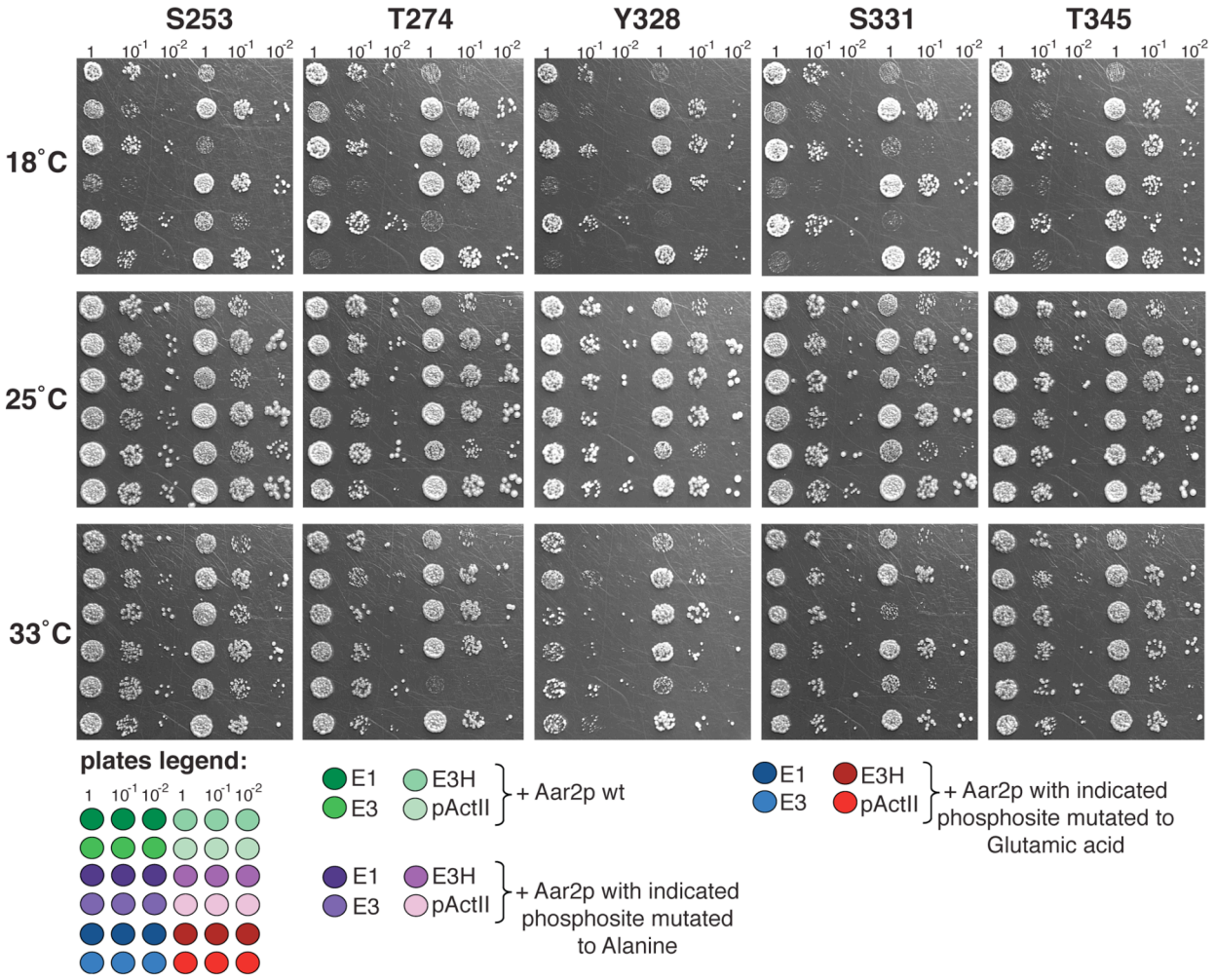

Figure 4.5. Aar2p phospho mutations confer growth defects when in combination with E3 and E3H Prp8p fragments. (See legend on page 58)

Figure 4.5. Aar2p phospho mutations confer growth defects when in combination with E3 and E3H Prp8p fragments. Cells were plated on -LW and grown at different temperatures. No growth defects were observed when combining the mutations with E1 or empty pActII vector. Auto-activation of pActII is also observed in -LWH plates (not shown). Some of the phospho mutations cause stronger growth defects than seen with the *wt* whereas others rescue the growth defect. See Table 4.1 for details of the phospho mutants and corresponding phenotypes.

4.4. Aar2p/Prp8p Co-Immunoprecipitation

Due to the observed auto-activation of Aar2p and its phosphomutants, an alternative way to test for Aar2p/Prp8p interaction is to perform immunoprecipitations of the Aar2p-LexA wild type and mutant fusion proteins and compare the amount of Prp8p-HA E1 fragment co-precipitated (Figure 4.6). After confirming that all the Aar2p fusion proteins had similar expression levels (Figure 4.6A) the immunoprecipitations were carried out in all the strains with mouse αLexA antibody coupled to protein G Dynabeads. This was followed by a rabbit αHA + rabbit αPrp8p Western blot to probe for the Prp8p-HA E1 fragment and the endogenous Prp8p simultaneously (Figure 4.6B). These results show that mutating Aar2p S253 to Glutamic acid disrupts Aar2p/Prp8p interaction both with Prp8 E1 fragment and with endogenous Prp8p. None of the other mutations affects the amount of Prp8p pulled down by Aar2p.

Bearing in mind the immunoprecipitation results (Figure 4.6) together with the fact that all the phosphomutants, *wt* Aar2p and the Prp8p fragments are being overproduced, a rather straightforward explanation can be found for the growth phenotypes. The overproduced proteins will imbalance the cellular Aar2p/Prp8p/Brr2p equilibrium since E3 and E3H fragments have high affinity for Brr2p, being able to deviate it from the interaction with endogenous Prp8p. In addition, the overexpressed *wt* Aar2p and Aar2p-S253A will bind to endogenous Prp8p, exacerbating the effect caused by the E3 and E3H overexpression in the cell. On the other side Aar2p-S253E is not able to bind Prp8p efficiently, relieving the stress caused by its overexpression. As a consequence, Aar2p-S253E can partially rescue the growth phenotype observed with *wt* and S253A.

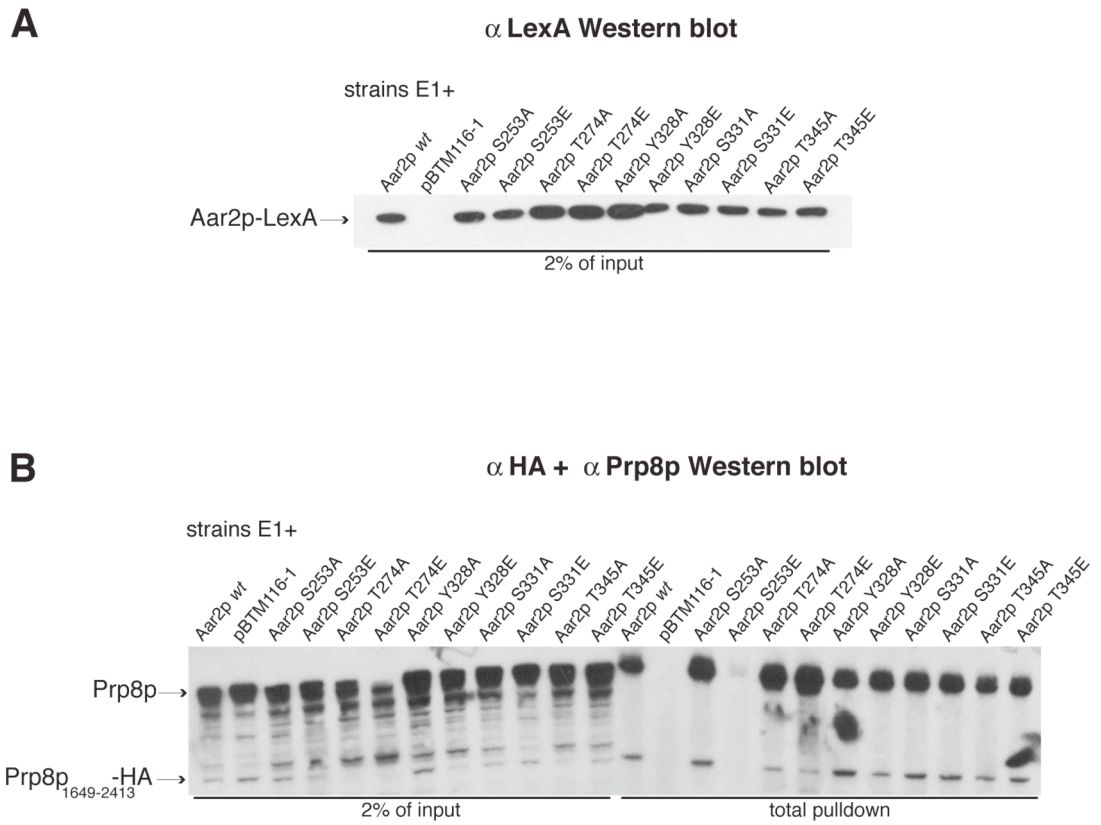

Figure 4.6. Aar2p S253E mutation disrupts Aar2p/Prp8p interaction. Cell extracts were prepared and immunoprecipitation with protein G dynabeads bound to mouse αLexA was performed. **A)** 2% of the input was run in a gel and the Western blot was probed with rabbit α LexA. This shows that Aar2p-LexA expression level is the same in *wt* Aar2p and in all the phospho mutants. **B**). 2% of the input and the pulldown totals were run in a gel and the Western blot was probed with rabbit αHA and rabbit αPrp8p simultaneously.

To test this argument a series of Prp8p-HA immunoprecipitations were performed, followed by a Western blot with rabbit αLexA + rabbit αBrr2p. If the above explanation is correct more Brr2p is expected to be pulled down by the E3 and E3H Prp8p fragments than by E1. Also, when Aar2p S253 is mutated to a Glutamic acid (consequently less Aar2p bound to Prp8p and Prp8p-HA) the amount of Brr2p pulled down by Prp8p-HA should increase. However that is not observed in Figure 4.7. There is no increase on Brr2p level pulled down neither by E3 or E3H nor with the Aar2p S253E mutation. In fact there is no detectable amount of pulled down Brr2p, it is only visible on the input lanes. However, this experiment shows that only the E1 and not E3 or E3H Prp8p fragments pull down Aar2p.

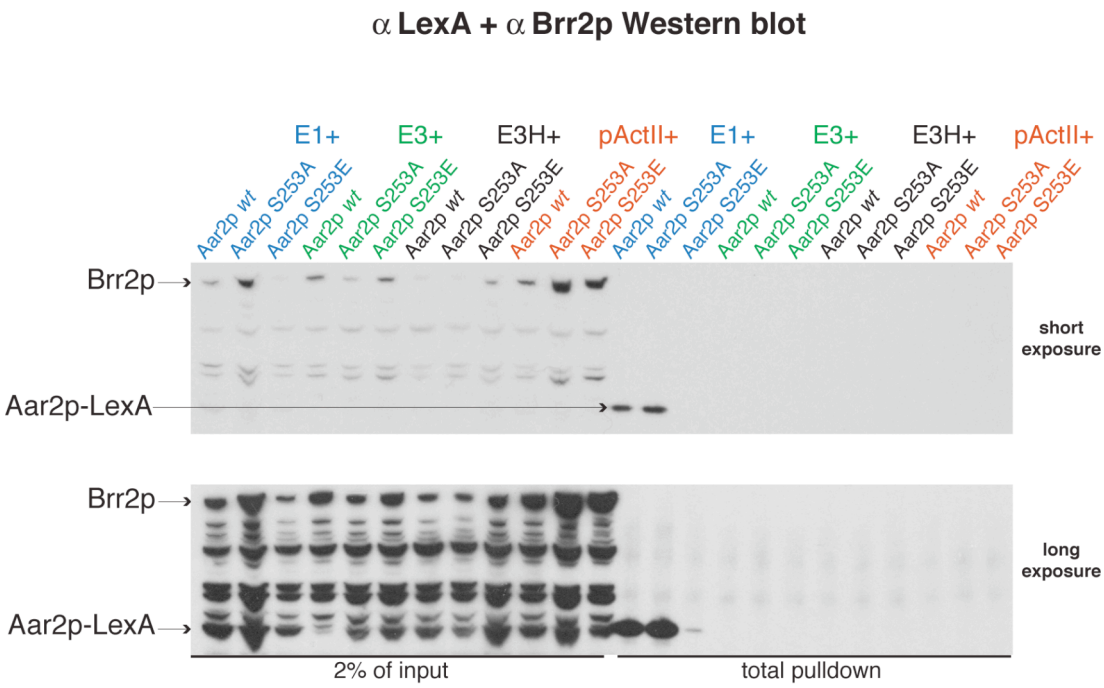

Figure 4.7. Aar2p interacts with E1 Prp8p fragment, but not with E3 and E3H. Cell extracts were prepared and the Prp8p fragments were immunoprecipitated with protein G dynabeads bound to mouse αHA. 2% of the input was run in a gel and the Western blot was probed with rabbit αLexA and rabbit αBrr2p simultaneously. E1 is the only Prp8p fragment that pulls down Aar2p-LexA and Aar2p-S253A-LexA. None of Prp8p fragments pulls down Brr2p, contrary to the expected.

4.5. Aar2p/Prp8p interaction regulation – two putative kinases

After showing that the Aar2p S253 phospho-mimic mutation inhibits the Aar2p/Prp8p interaction, two candidate kinases were revealed as putative interaction regulators: Prr2p and Gcn2p. Aar2p, Lsm12p and Prp40p were previously recognized as *in vitro* substrates for Prr2p kinase (Ptacek *et al.*, 2005), and Gcn2p was identified as a physical interactor of Aar2p, Brr2p, Prp4p, Prp6p, Prp8p, Prp31p, Snu66p and Snu114p by a genome-wide screen (Gavin *et al.*, 2002; Gavin *et al.*, 2006).

I got the *prr2Δ* and *gcn2Δ* yeast strains from the EUROSCARF deletion collection and compared the level of Prp8p pulled down by Aar2p in these two strains and in wild type. I first optimized the immunoprecipitation and Western blot conditions since neither Aar2p nor Prp8p was tagged in these strains. Hence rabbit

αAar2p serum had to be used for the immunoprecipitation and rabbit αPrp8p serum was used for the Western blot.

Figure 4.8 exhibits Aar2p immunoprecipitation from BY4741, BY4741-ΔPRR2 and BY4741-ΔGCN2 yeast cell extracts followed by αPrp8p Western blot. The LI-COR Odyssey imaging system was used in order to quantify the amount Prp8p pulled down in each gel lane. As the values demonstrate in the table (Figure 4.8), the amount of Prp8p pulled down is very similar in all strains, leading to the conclusion that neither Prr2p nor Gcn2p regulate the Aar2p/Prp8p interaction.

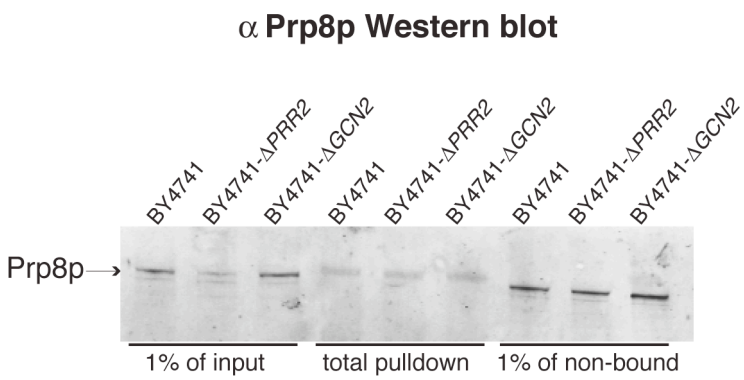

	intensity counts per lane				
strain	input	pulldown	non-bound	**pulldown/input**	**pulldown/non-bound**
BY4741	0.9	0.42	1.56	**0.47**	**0.27**
BY4741-Δ*PRR2*	0.44	0.41	1.55	**0.93**	**0.26**
BY4741-Δ*GCN2*	0.99	0.55	2.54	**0.56**	**0.22**
BY4741	0.62	0.28	1.54	**0.45**	**0.18**
BY4741-Δ*PRR2*	0.09	0.17	0.95	**1.89**	**0.18**
BY4741-Δ*GCN2*	0.16	0.14	1.22	**0.88**	**0.11**
BY4741	0.87	1.06	0.7	**1.22**	**1.51**
BY4741-Δ*PRR2*	1.04	0.8	1.06	**0.77**	**0.75**

Figure 4.8. Neither Prr2p nor Gcn2p kinases regulates the Aar2p/Prp8p interaction. Aar2p immunoprecipitations were carried out on *wt* (BY4741) and Δ kinase strains (BY4741-Δ*PRR2* and BY4741-Δ*GCN2*) followed by a Western blot probed with αPrp8p antibody. In order to quantify the amount of Prp8p pulled down in each lane with the LI-COR Odyssey system, a fluorescent αrabbit secondary antibody was used. The table lists the fluorescence intensity registered for each Western blot lane and the ratios pulldown/input and pulldown/non-bound for each of the strains. The white part of the table shows the results of the experiment illustrated in the figure. The yellow part of the table shows the values obtained with a biological replicate of this experiment. The BY4741-Δ*PRR2* ratio pulldown/input suggests that the absence of Prr2p might favour the Aar2p/Prp8p interaction, however the ratio pulldown/non-bound in both experiments shows that Prr2p absence is irrelevant for Aar2p/Prp8p interaction. The green part of the table shows the values for an experiment done with the BY4741 and BY4741-Δ*PRR2* strains only. From the last

experiment Δ*PRR2* seems to have the opposite effect from the previous two experiments. Thus from this data it is not possible to conclude that Prr2p is a regulator of the Prp8p/Aar2p interaction.

Looking at the ratio pulldown/input from the BY4741-Δ*PRR2* strain in the first two experiments it gives a suggestion that Prr2p has a weak effect on the Aar2/Prp8p interaction. On the other hand, the ratio pulldown/non-bound does not indicate any difference from BY4741. If we look at the values of the third experiment, Δ*PRR2* shows the opposite effect on the Prp8p/Aar2p interaction. The slight discrepancy in the results can be due to common experimental variability, such as pippeting and Western transfer efficiency. This, added to the fact that the Aar2p/Prp8p binding efficiency is very low, leading to relatively large fluctuations in the calculated ratios, makes it difficult to acknowledge if there is really an Aar2p/Prp8p binding effect in the BY4741-Δ*PRR2* strain. A large number of experiments would be necessary to test the statistical relevance of a putative effect of Prr2p on the Aar2p/Prp8p interaction.

4.6. Discussion

Novel and interesting results are presented in this chapter. It is revealed that Aar2p interacts with $Prp8p_{1649\text{-}2413}$ (Figure 4.7) and also that Aar2p S253E mutation abolishes the Aar2p/Prp8p interaction (Figure 4.6).

From the information gathered here it is possible to divide Aar2p in two functional halves. The N-terminal half is the Prp8p interacting domain and the C-terminal half regulates the interaction through Aar2p phosphorylation state. The results suggest that Prp8p interacts with Aar2p in its non-phosphorylated form and once S253 is phosphorylated the interaction is reduced or abolished. This fits the proposed U5 snRNP maturation model (Boon *et al*., 2007) in which after the U5 precursor complex enters the nucleus, Aar2p is replaced with Brr2p on the Prp8p C-terminus interacting region. The same authors suggest that Aar2p and Brr2p compete for the interaction with Prp8p, and that Aar2p might function as a chaperone preventing Brr2p from binding to Prp8p earlier than required for splicing to occur. My data help to sustain this model since S253 phosphorylation seems to be a mechanism by which the Aar2p/Prp8p interaction is disrupted, allowing Brr2p to

bind the Prp8p C-terminus. Also, I discard a possible role that Aar2p might have on nuclear import of Prp8p and Snu114p (Figure 4.2), reinforcing the idea that Aar2p can be in fact a Prp8p chaperone for the Brr2p interaction.

Puzzling results were obtained with the phosphomutants spotting assays (Figure 4.5). A series of growth defects were observed when *wt* Aar2p and some phosphomutations were combined with E3 and E3H Prp8p fragments, while other phosphomutations rescued the phenotype obtained with *wt* Aar2p. If the Prp8p/Aar2p/Brr2p mutually exclusive model is correct (Boon *et al*., 2007; Kutach, unpublished data), the growth phenotypes can be explained by a competition between endogenous Prp8p and the Prp8p-HA fragments to bind endogenous Brr2p. Since the E3 and E3H Prp8p fragments have high affinity for Brr2p (in particular E3H), they will sequester it from its interaction with endogenous Prp8p. This imbalance is exacerbated by the overexpression of Aar2p-LexA that in turn binds to endogenous Prp8p. All of this disturbs the cellular equilibrium between precursor (Aar2p/Prp8p-containing) and mature (Brr2p/Prp8p-containing) U5 snRNP forms, most likely affecting vital splicing levels and leading to growth defects.

The S253A mutation causes a cs growth phenotype very similar to *wt* both at 18˚C and 25˚C while S253E partially rescues it. Such effect was foreseeable since Aar2p-S253A binds to Prp8p with the same efficiency as the *wt* while Aar2p-S253E does not (Figure 4.6). According to the experiment illustrated in Figure 4.6 all the other phosphomutants bind to Prp8p similarly to *wt* Aar2p, so growth phenotypes are expected when combining any of these mutant proteins with E3 or E3H in the cells. It is therefore surprising to observe that T274A, Y328A, T345A and T345E can rescue the *wt*+E3H phenotype at all temperatures. On the other hand T274A, T274E, Y328A and Y328E show stronger growth defects than *wt* when combined with E3 at 18˚C. Also interesting are the S331A/S331E mutations +E3 and +E3H at 18˚C causing growth defects stronger than the *wt.* Finally, S331+E3H at 33˚C results in a growth defect more serious than with *wt* Aar2p. Either T274, Y328, S331 and T345 phosphomutations indirectly affect the Aar2p/Prp8p/Brr2p equilibrium perturbing pre-mRNA splicing, or they distress other cellular processes that have a cumulative effect with E3 and E3H over expression. S331 was previously described as being phosphorylated as a result of DNA damage (Albuquerque *et al*, 2008). Therefore, the

effect observed with S331A/S331E might be due to disruption of the cell stress response.

Brr2p was shown previously to bind E1, E3 and E3H Prp8p fragments by Y2H assay (van Nues & Beggs, 2001), however when I did the Prp8p-HA immunoprecipitations (Figure 4.7) I do not detect Brr2p being pulled down by any of the Prp8p-HA fragments. A similar situation happened with Aar2p. From the first Y2H assay (Figure 4.4) I observed that Aar2p$_{1\text{-}170}$-LexA interacts with all the Prp8p-HA fragments E1, E3 and E3H. Although from the Prp8p-HA immunoprecipitations (Figure 4.7), only E1 pulled down full-length Aar2p-LexA. This can be due to either the interactions not being stable in the conditions used for the immunoprecipitations or the Prp8p-HA fragments pulldown such a low level of Brr2p and Aar2p-LexA that the proteins cannot be detected by the Western blot.

Known candidate kinases for regulation of Aar2p/Prp8 interaction through S253 phosphorylation are Prr2p and Gcn2p, since Prr2p was found to phosphorylate Aar2p *in vitro* (Ptacek *et al*., 2005) and Gcn2p was isolated in a complex with Aar2p and other U5 snRNP and tri-snRNP proteins (Gavin *et al*., 2006). However, the role of Prr2p and Gcn2p kinases in controlling Aar2p/Prp8p interaction was not supported by immunoprecipitation assays (Figure 4.8).

Prr2p - Pheromone Response Regulator 2 (Burchett *et al*., 2001) - is a serine/threonine kinase that inhibits pheromone induced signaling downstream of MAPK, probably at the level of Ste12p transcription factor (Zhu *et al*., 2000; Burchett *et al*., 2001). Although Aar2p was found to be an *in vitro* substrate for Prr2p (Ptacek *et al*., 2005) that does not necessarily mean that Prr2p will phosphorylate Aar2p *in vivo*. Even if it does, it might not phosphorylate S253 and therefore will not play any role regulating Aar2p/Prp8p interaction, as my results suggest. Prr2p can possibly phosphorylate one or more of the other Aar2p phospho-sites described in this work and play a role regulating a hypothetical Aar2p interaction with another protein.

Gcn2 - General Control Nonderepressible 2 (Lucchini *et al*., 1984) - is a kinase that in response to starvation phosphorylates the alpha-subunit of translation initiation factor eIF2 (Hinnebusch & Fink, 1983; Thireos *et al*., 1984; Hinnebusch & Natarajan, 2002) and is activated by uncharged tRNAs and the Gcn1p-Gcn20p

complex (Garcia-Blanco *et al*., 2000; Kubota *et al*., 2001). Gcn2p also has a role in DNA damage checkpoint control (Menacho-Marquez *et al*., 2007). Aar2p was isolated in a complex with other proteins (Brr2p, Prp4p, Prp6p, Prp8p, Prp31p, Snu114p, Snu66p, Rpl27b, Ssa2, Tef2, Ura2 and Utp21), being identified as physical interactors of Gcn2p (Gavin *et al*., 2006). With the exception of Aar2p, all the splicing factors in this complex are components of the U4/U6.U5 tri-snRNP (Brr2p, Prp4p, Prp6p, Prp8p, Prp31p, Snu114p and Snu66p) and Brr2p, Prp8p and Snu114p are also found in the mature U5 snRNP. Adding this information to my results leads to the conclusion that Gcn2p does not phosphorylate Aar2p S253 and that Aar2p might not even be a Gcn2p substrate. The kinase may actually act on other tri-snRNP proteins isolated in the complex with Aar2p.

Several questions were answered by the work described in this chapter and the data obtained raise others. These results lead me to question what will be the effect of introducing the Aar2p phosphomutations into the genome of a yeast strain and if there will be implications on Aar2p association with U5 snRNP.

CHAPTER 5 – Aar2p and the U5 snRNP

5.1. Introduction

The results presented so far in this thesis indicate that residue S253 in Aar2p may be a landmark for the Aar2p/Prp8p interaction (Chapter 4 - Section 4.4). The phosphorylation of this serine possibly regulates an important step for U5 snRNP maturation - the substitution of Aar2p by Brr2p on C-terminal Prp8p.

To understand more about the involvement of Aar2p in U5 snRNP maturation, I inserted mutations at the five described phosphosites (Chapter 3 - Section 3.4) into the genome of a yeast strain. In this chapter I study their effect on cell growth and on Aar2p interaction with U5 snRNP components.

I observe that the phosphomutations do not cause growth phenotypes when inserted into the genome of BY4742 cells but confer cold sensitivity at 14˚C when introduced into the genome of W303 cells. Also, contrary to what was expected, mutations S253A and S253E do not affect Aar2p interaction with endogenous Prp8p, or Aar2p association with U5 snRNA.

5.2. Introducing phosphomutations into genomic *AAR2*

In order to introduce the mutations into the genome, I transferred the C-terminal half of Aar2p bearing each mutation from the mutated pBTM116-1-Aar2 plasmids into the pGID3 plasmid (Decourty *et al*., 2008). This plasmid allows inserting the mutations into genomic *AAR2* together with a prMFα2Nat^R cassette (NAT selection), by PCR amplification and homologous recombination. A *wt*-NAT control was constructed alongside the phosphomutants. Because the promoter of the prMFα2Nat^R cassette is only active in *MAT*α cells, BY4742α and W303α were used as recipient strains in these experiments.

The mutations were first inserted into the genome of yeast strain BY4742 without any visible growth defect at the temperatures tested (Figure 5.1). Subsequently the phosphomutations were introduced into the W303 strain and an interesting result was observed. W303 is cold sensitive at 14˚C, however the simple introduction of the prMFα2Nat^R-*AAR2* cassette without any mutation - W303-NAT - rescues the cold-sensitive phenotype at 14˚C (Figure 5.2). The same effect was

observed with most of the phosphomutations except S253A, T274E and S331A. Cells in which the latter mutations were introduced behave like *wt* W303 cells, showing cold sensitivity at 14˚C (Figure 5.2). These results are somewhat surprising since it was expected that at least the S253E mutation would cause a relative growth defect due to the disruption of Aar2p/Prp8p interaction.

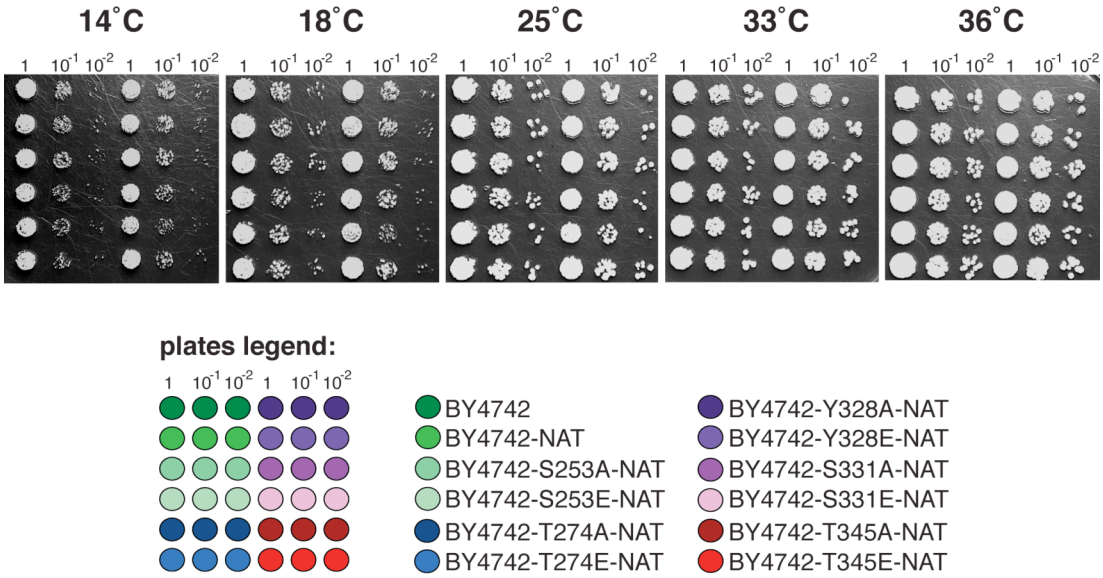

Figure 5.1. Aar2p phosphomutations do not confer a growth phenotype when inserted into the genome of BY4742. Phosphomutant strains were plated on YPDA alongside BY4742 and BY4742-NAT controls and grown at 14, 18, 25, 33 and 36˚C. No growth phenotypes were detected with the introduction of the phosphomutations into the genome, all the strains are healthy at the temperatures tested.

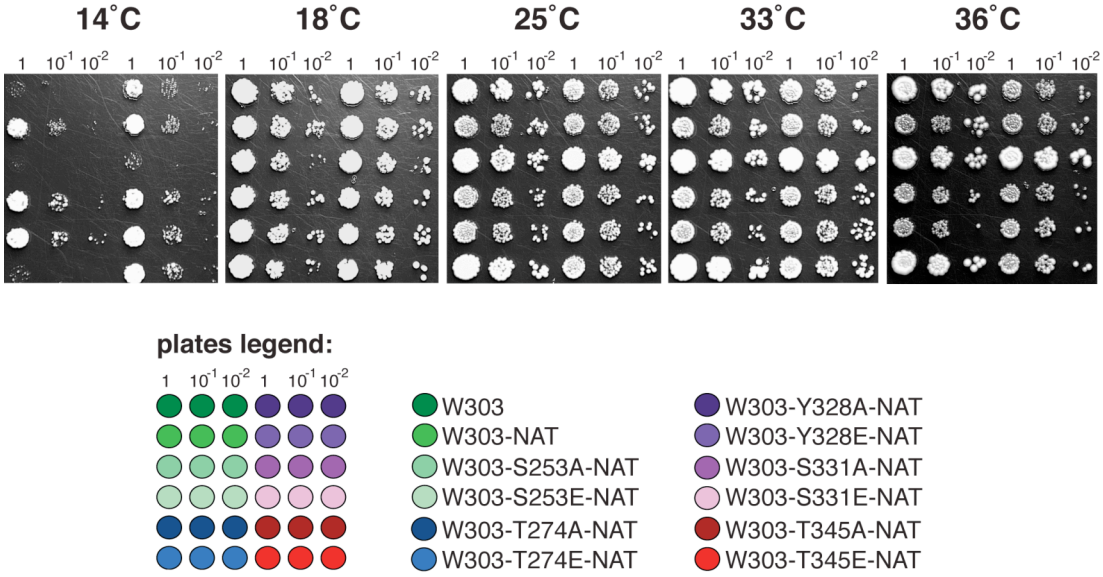

Figure 5.2. S253A, T274E and S331A confer cold-sensitivity when inserted into the genome of W303. Phosphomutant strains were plated on YPDA alongside W303 and W303-NAT controls and grown at 14, 18, 25, 33 and 36˚C. Some growth defects were observed at 14˚C. As can be seen by the W303-NAT growing at 14˚C, the prMFα2Nat^R cassette insertion into the genome rescues the W303 cold sensitivity by itself. This effect is detected in almost all the phosphomutants with the exception of W303-S253A-NAT, W303-T274E-NAT and W303-S331A-NAT, which reveal themselves as cold sensitive similarly to the W303 strain.

5.3. The effect of phosphomutants on U5 snRNP association

Despite the lack of significant phenotypes with the growth experiments, I studied the effect of mutations S253A/E on Aar2p association with U5 snRNP components, specifically Prp8p and U5 snRNA.

I started looking at the level of Prp8p pulled-down by immunoprecipitated Aar2p in the strains W303, W303-NAT, W303-S253A-NAT, and W303-S253E-NAT (Figure 5.3). The Prp8p Western blot was quantified using the LI-COR Odyssey system and the ratios pulldown/input and pulldown/non-bound were calculated for all the strains (Figure 5.3, table). Contrary to what was observed with the Y2H S253A/E strains (Chapter 4, Figures 4.6 and 4.7), here the Aar2p-S253E mutant pulls down Prp8p at the same level as does the *wt* Aar2p (Figure 5.3, table). The prMFα2Nat^R cassette insertion appears to cause a reduction in the amount of Prp8p pulled down by Aar2p, when comparing the W303-NAT and W303 strains. Nonetheless, comparison of W303-S253A-NAT and

W303-S253E-NAT with their counterpart W303-NAT control does not indicate any difference on the amount of pulled down Prp8p.

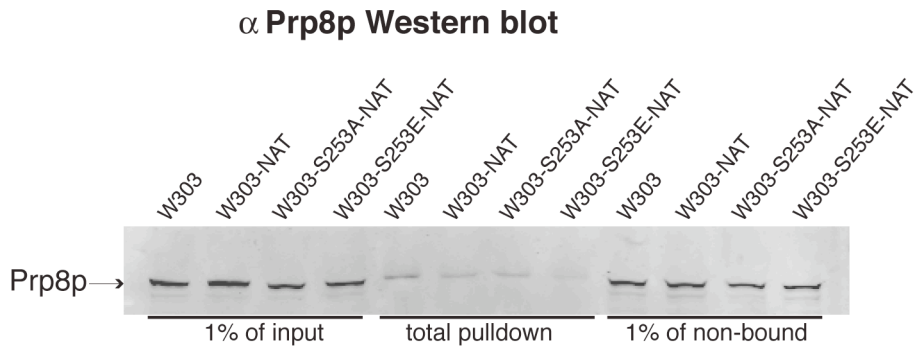

	intensity counts per lane				
strain	input	pulldown	non-bound	**pulldown/input**	**pulldown/non-bound**
W303	7.81	2.04	6.38	**0.26**	**0.32**
W303-NAT	9.27	1.13	6.89	**0.12**	**0.16**
W303-S253A-NAT	6.12	0.98	5.26	**0.16**	**0.19**
W303-S253E-NAT	5.51	0.7	5.85	**0.13**	**0.12**

Figure 5.3. Mutation S253E does not disrupt Aar2p/Prp8p interaction *in vivo*. Aar2p was immunoprecipitated from W303, W303-NAT, W303-S253A-NAT, and W303-S253E-NAT cell extracts. The Western blot was probed with αPrp8p primary antibody and fluorescent α rabbit secondary antibody for quantification with the LI-COR Odyssey system. The table shows the fluorescence intensity recorded for each lane as well as the ratios pulldown/input and pulldown/non-bound. There is an apparent reduction of pulldown/input and pulldown/non-bound ratios on the W303-NAT in contrast to W303. In spite of this no significant difference is detected in the ratios of W303-S253A-NAT, and W303-S253E-NAT comparatively to the W303-NAT control.

The next logical experiment was to determine the amount of U5 snRNA precipitated by the Aar2p-S253A and Aar2p-S253E mutant proteins. Consequently, Aar2p was immunoprecipitated and the level of pulled down U5 snRNA detected by Northern blot was quantified with the PhosphorImager (Figure 5.4). It is evident from the ratio pulldown/input that the level of precipitated U5 snRNA (both U5L and U5S forms) is the same in the four strains tested. These observations together with the results from the previous experiment indicate that Aar2p, Aar2p-S253A and Aar2p-S253E associate with the U5 snRNP at the same extent.

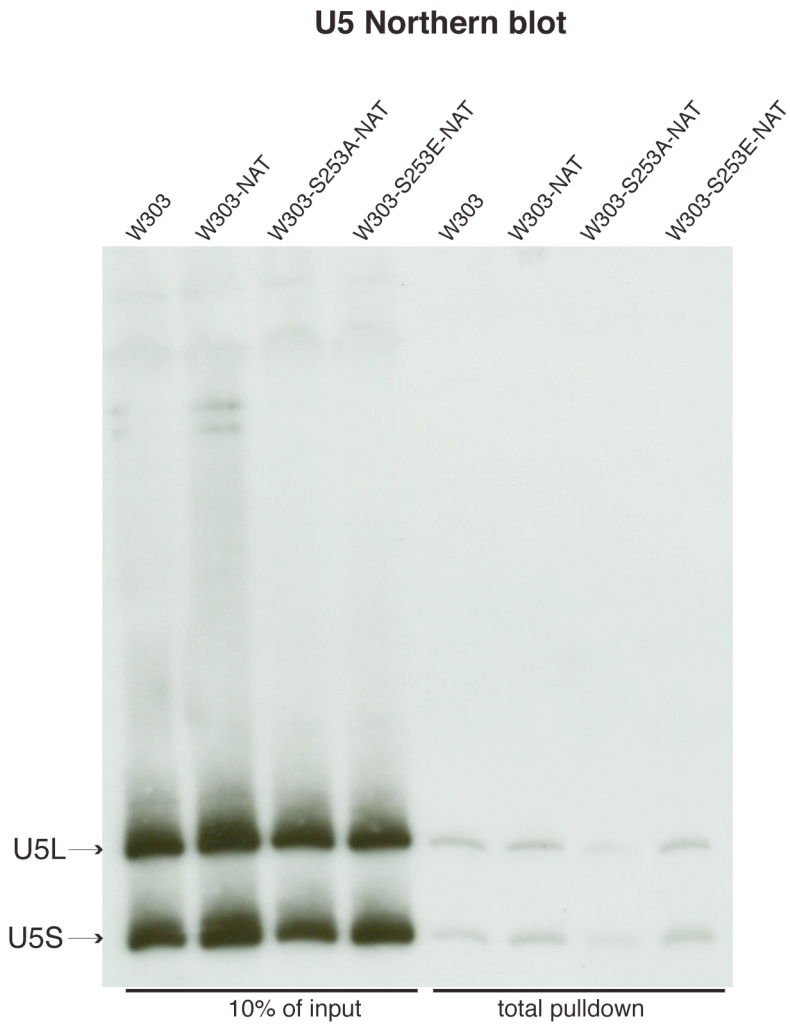

		PhosphorImager counts		
	strain	input	pulldown	**pulldown/input**
U5L	W303	14777.93	773.15	**0.05**
	W303-NAT	19875.58	740.94	**0.04**
	W303-S253A-NAT	13081.98	344.54	**0.03**
	W303-S253E-NAT	14402.10	592.68	**0.04**
U5S	W303	12748.64	706.76	**0.06**
	W303-NAT	19661.22	825.55	**0.04**
	W303-S253A-NAT	10794.58	408.90	**0.04**
	W303-S253E-NAT	14128.97	695.27	**0.05**

Figure 5.4. Mutation S253E does not affect Aar2p association with U5 snRNA *in vivo*. Aar2p was immunoprecipitated as in the previous experiment and RNA was extracted from input samples and pulldowns. A Northern blot was performed with a U5 snRNA probe and the results quantified in the PhosphorImager are shown in the table. There is no difference in the ratio pulldown/input amongst the strains for either U5L or U5S, indicating that the mutations S253A and S253E do not have any effect on Aar2p interaction with U5 snRNA.

5.4. Discussion

The results obtained in this chapter are highly discordant from those found in Chapter 4, perhaps raising the doubt if S253 has a role in Aar2p/Prp8p interaction regulation *in vivo* or not. It was expected that at least S253E would cause a growth phenotype since it severely disrupted Aar2p/Prp8p interaction in the Y2H system (Chapter 4, Figures 4.6 and 4.7). However, S253E neither caused a growth phenotype (Figure 5.2), nor did it disturb Aar2p interaction with Prp8p *in vivo* (Figure 5.3) or its association with U5 snRNA (Figure 5.4).

The combination of several factors can contribute to the discrepancy between Chapter 4 and Chapter 5 results. One of them is the strategy used to insert the mutations into the genome. A prMFα2Nat^R cassette (Decourty *et al*., 2008) was inserted immediately after the *AAR2* STOP codon by homologous recombination in order to replace the last 380bp of genomic *AAR2* ORF with the same DNA sequence containing the desired phosphomutation. According to a tiling array analysis by Granovskaia (Granovskaia *et al*., 2010), *AAR2* and *SSA3* (the gene located immediately 3' of *AAR2*) appear to be a single transcription unit. In this case, the prMFα2Nat^R cassette insertion may be disrupting *SSA3* expression which could mask any effect caused by the phosphomutations. Ssa3p is part of the heat shock protein 70 family, being implicated in protein folding and response to stress (Werner-Washburne *et al*., 1987). This protein is an ATPase localized to the cytoplasm (Hartl & Hayer-Hartl, 2002) and has a function in SRP-dependent cotranslational protein-membrane targeting and translocation (Becker *et al*., 1996). On the other hand *SSA3* gene deletion is viable with no visible phenotype (Giaever *et al*., 2002, Breslow *et al.*, 2008) and this gene is induced at high temperatures or after diauxic shift (Werner-Washburne *et al*., 1987, Werner-Washburne *et al*., 1989) thus it is unlikely that it would interfere with Aar2p phosphomutant phenotypes, or that at least it would have a strong effect by itself.

Another distressing factor seems to be the prMFα2Nat^R cassette itself. It was observed in this chapter that the simple prMFα2Nat^R cassette insertion alters W303 normal cell growth (Figure 5.2). Also, it seems to reduce Aar2p interaction with Prp8p (Figure 5.3, note in the table that the ratios pulldown/input and pulldown/non-bound are reduced from W303 to W303-NAT strains), which can

mask the effect that S253E mutation would have in this interaction.

Finally, the fact that Y2H strains are *MAT*a while the strains in which the mutations were inserted into the genome are *MAT*α can be another reason for concern. Aar2p was originally described as being required for splicing of *MATa1* (a gene only expressed in *MAT*a cells) but not of *ACT1* (Nakazawa *et al*, 1991). The same authors did not detect *AAR2* transcript in the logarithmic growth phase. They suggested that its expression level would be very low in the absence of appropriate mating pheromone induction, since they found one copy of pheromone-responsive element 5' of *AAR2*. Consequently we could be facing a mating-type specific effect with the S253E mutation.

In order to reduce the problems described above and to be able to reach a definite conclusion regarding the role of Aar2p phosphosites in U5 snRNP maturation, the mutant strains will have to be constructed by plasmid shuffle. Probably the best strategy will be to start from a heterozygous diploid *AAR2* deletion strain from the EUROSCARF deletion collection (BY4743; *Mat* a/α; *his3Δ1/his3Δ*; *leu2Δ0/leu2Δ0*; *lys2Δ0/LYS2*; *MET15/met15Δ0*; *ura3Δ0/ura3Δ0*; YBL074c::kanMX4/YBL074c). Thus two plasmid shuffle strains can be constructed in parallel, one *MAT*a and another *MAT*α, with plasmids containing *AAR2* endogenous promoter followed by *AAR2* and *SSA3* coding regions. This will clarify if the effects previously observed are mating type dependant or not, minimize interference with *SSA3* transcription and eliminate the effect of prMFα2Nat^R cassette insertion.

CHAPTER 6 – Looking for Aar2p interactors: Y2H screens

6.1. Introduction

Besides Aar2p requirement for *MATa1* splicing (Nakazawa *et al.*, 1991), and its interaction with the U5 snRNP (Gottschalk *et al*., 2001; Boon *et al*., 2007), not much is known about this protein. To learn more about Aar2p, I planned a Y2H screen looking for new Aar2p interactors.

As I have previously shown in Chapter 4, the full-length Aar2p has auto-activation activity, which makes it ineffective for a Y2H screen. Hence, here I use the two Aar2p halves (already used for the Y2H assays in Chapter 4), Aar2p$_{1\text{-}170}$ and Aar2p$_{150\text{-}355}$ as baits for two separate Y2H screens. For each of these screens a genomic *S. cerevisiae* prey library is used (kindly provided by J. C. Rain, Hybrigenics, Paris). The resulting prey interactions are classified as A1, A2, A3, A4 and B, following Fromont-Racine *et al*. (1997; see Table 6.2). The out of frame clones are regarded as significant since they can be expressed by frameshifting (Fromont-Racine *et al*., 1997).

Both screens indicate that Aar2p N-terminal half interacts with Aar2p C-terminal half. Although no splicing factors are found in the prey clones, candidate new Aar2p interactors are unveiled. These results suggest links between Aar2p and intracellular transport, chromosome biology and DNA-damage repair.

6.2. Aar2p$_{1\text{-}170}$-bait screen

Table 6.1 summarizes the general information for this screen. All the preys obtained are alphabetically compiled in Table 6.2 together with the corresponding class of interaction (see Table 6.2 on page 81). From the total 108 preys, 23 are A1 class interactors, three are A2, 43 are A4 and 39 are B class interactors. No A3 class interactions are found.

The principal hit of this screen (A1 interaction with 10 different clones isolated) is Aar2p itself, mostly C-terminal Aar2p. From the information on Table 6.2, Aar2p$_{170\text{-}276}$ can be defined as a minimal region of interaction for the bait Aar2p$_{1\text{-}170}$. Other Aar2p$_{1\text{-}170}$-bait A1 class interactors include Arc1p, Cab1p, Ecm32p, Fir1p, Fms1p, Mon1p, Nis1p, Rad4p, Rad16p, Rcy1p, Sam4p, San1p,

Sap1p, Sdc25p, Sno3p, Sse1p, Swi1p, Tdp1p, Yta6p, Yta7p, YDR026C and YMR209C.

As A2 class interactors I find Rpl25p, Tdh2p and Tim9p.

Also noteworthy are the Aar2p$_{1-170}$ B class interactions with ARS902, an autonomously replicating sequence; TEL15R, telomere on the right arm of chromosome XV; and TEL12R-YP2, the most centromere-proximal region of two telomeric Y' elements on the right arm of chromosome XII. Surprisingly I do not find any splicing factors in the prey list.

Table 6.1 – General information for Aar2p$_{1-170}$ screen.

Total number of interactions	$1.7x10^8$
Mating efficiency	50.40%
Total number of prey colonies	248
Number of different preys obtained	108

6.3. Aar2p$_{150-355}$-bait screen

As shown in Table 6.3, from the $2.5x10^8$ total interactions tested I only recover 34 prey colonies. Table 6.4 lists in alphabetical order the four different prey proteins identified and their class of interaction with the Aar2p$_{150-355}$-bait (see Table 6.4 on page 92). Two preys are A1 class interactors and the other two are A4. No A2, A3 or B class interactions are observed.

The N-terminal half of Aar2p is the prime hit for this screen (13 different clones are obtained, A1 class interaction), Aar2p$_{1-127}$ being defined as the minimal region of interaction for the Aar2p$_{150-355}$-bait. All the Aar2p prey-clones start several base pairs into 5' UTR of *AAR2* and have several STOP codons before the initiation codon of the gene.

Rps8Ap is also an A1 interactor and Swi1p and YBL073W are A4 class interactors. Similarly to the Aar2p$_{1-170}$ screen, I do not find any splicing factors amongst the prey clones.

Table 6.3 – General information for Aar2p$_{150-355}$ screen.

Total number of interactions	2.5x10^8
Mating efficiency	56.18%
Total number of prey colonies	34
Number of different preys obtained	4

6.4. Discussion

6.4.1. Comparing Aar2p$_{1-170}$-bait and Aar2p$_{150-355}$-bait screens

There is a large discrepancy regarding the amount of prey clones obtained in the two screens I preformed. The Aar2p$_{1-170}$-bait screen produced a total of 108 different preys and the Aar2p$_{150-355}$-bait screen generated four preys only. We can speculate that Aar2p$_{150-355}$ is not a prime contact region and it possibly regulates Aar2p interaction with other proteins. Since Aar2p$_{150-355}$ encloses the five phosphosites, Aar2p conformational state could be changed via phospho- and dephosphorylation events making it more or less accessible to interact with other proteins.

Rather exciting is that the most frequent hit for both screens is the complementary half of Aar2p (Aar2p$_{170-276}$ and Aar2p$_{1-127}$ are the minimal regions of interaction for Aar2p$_{1-170}$ and Aar2p$_{150-355}$ baits, respectively). This is a strong indicator that the two Aar2p halves interact with each other and suggests that Aar2p is a protein with a closed conformation. My results are in perfect agreement with very recent findings from the Wahl lab (Markus Wahl, Berlin – personal communication). This lab was able to crystallize Aar2p and observed that it is indeed

formed by two distinct domains very tightly associated with each other.

A common prey for both screens is Swi1p. In the Aar2p$_{1-170}$-bait screen it is an A1 class interactor and in the Aar2p$_{150-355}$ it is an A4. Swi1p is a component of the SWI/SNF chromatin remodeling complex (Peterson *et al*., 1994; Smith *et al*., 2003) that controls transcription of several genes by remodeling chromosomes (Peterson & Herskowitz, 1992).

Peculiarly, I do not find any splicing factor as prey in either of the two screens. Not even Prp8p that I showed to interact with Aar2p in Chapter 4 of this thesis. One possibility is that this interaction is not observed here because full-length Aar2p is required for interaction with Prp8p. Substantiating this hypothesis Wahl has recently crystallized Aar2p associated with the Prp8-RNaseH domain and observed Prp8p contact sites on both N- and C-terminal Aar2p (Wahl, 2010 – personal communication).

The high number of different prey proteins found in the Aar2p$_{1-170}$-bait screen suggests that this half is highly interactive with other proteins, or alternatively but less likely, that it is a sticky fragment. Despite that, I observe significant interactions with proteins from several categories: ubiquitin-binding proteins, chaperones, membrane and vacuolar proteins, a nuclear pore complex component, proteins localized to sites of polarized growth, chromatin-binding/remodeling proteins, a telomere binding protein, a DNA helicase and proteins involved in DNA-damage repair. Amongst the prey list there are also telomeric regions of three chromosomes.

6.4.2. Aar2p and trafficking

Recent Aar2p structural results reveal that it is composed of an N-terminal domain with a structure related to pore-forming toxins, and a C-terminal domain extremely similar to a VHS domain (Wahl, 2010, personal communication). The VHS domains are characteristic of proteins involved in clathrin-mediated endocytosis and vesicular trafficking (Lohi & Lehto, 1998). Also, these domains are thought to have a membrane-targeting/cargo recognition role and very frequently contain one or two ubiquitin-interacting motifs (reviewed in Lohi *et al*., 2002).

Remarkably, I find as preys for Aar2p$_{1-170}$-bait two ubiquitin-binding proteins, Cue2p and San1p. Cue2p has unknown function but contains two CUE ubiquitin-

binding domains that might assist intramolecular mono-ubiquitination and coupling to ER degradation (Biederer *et al.*, 1997; Shih *et al.*, 2003). San1p is an Ubiquitin-protein ligase, implicated in the degradation of abnormal nuclear proteins by the proteasome (Dasgupta *et al.*, 2004; Gardner *et al.*, 2005). Also in conformity I find Aar2p$_{1\text{-}170}$-bait interacting with membrane and vacuolar proteins: Mon1p is required for fusion of autophagosomes and cvt-vesicles with the vacuole (Meiling-Wesse *et al.*, 2002); and Kin1p is a serine/threonine kinase localized in the plasma membrane, which contributes to exocytosis regulation (Elbert *et al.*, 2005). In accordance as well are the interactions of Aar2p$_{1\text{-}170}$-bait with proteins directed to sites of polarized growth: Nis1p is localized at the bud neck where it interacts with septins (Iwase & Toh-e, 2001); Pkc1p is a serine/threonine kinase located in the mother-daughter bud neck and other sites of polarized growth and is fundamental for cell wall remodeling during growth (Levin *et al.*, 1994; Watanabe *et al.*, 1994; Andrews & Stark, 2000); Rcy1 is an F-box protein implicated in recycling plasma membrane proteins internalized by endocytosis (Wiederkehr *et al.*, 2000; Galan, *et al.*, 2001); YFR016C is a protein with unknown function; and finally Yta6p is a presumed ATPase of the CDC48/PAS1/SEC18 (AAA) family, localized only to the cortex of mother cells (Schnall *et al.*, 1994; Swaffield & Purugganan, 1997; Beach & Bloom, 2001).

Another interesting prey obtained with the Aar2p$_{1\text{-}170}$-bait is Nup116p. This protein is a nuclear pore complex component and is located to both sides of the pore. It contains a GLFG motif that interacts with Mex67p (mRNA export factor) and with the karyopherin Kap95p (Rout *et al.*, 2000; Strawn *et al.*, 2001; Lutzmann *et al.*, 2005). Additionally, it was shown by Boon (2005) that Kap95p is required for nuclear import of Snu114p, U2, U5 and U6 snRNAs. Since Wahl observes Prp8p RNaseH β-hairpin binding in the groove between the two VHS helices, he suggests that Aar2p imports Prp8p into the nucleus via the same cargo-recognition tactic as other VHS domain proteins (Wahl, 2010 - personal communication).

In conclusion, the evidence presented above suggests that Aar2p can be a transport factor for U5 snRNP-components, such as Prp8p; especially that it can be involved in their nuclear import.

6.4.3. Aar2p and the chromosomes

Other interesting preys interacting with the Aar2p$_{1-170}$-bait are chromatin-binding proteins. I have: Swi1p (described above); Rlf2p is part of the major subunit of Chromatin Assembly Complex 1 (CAF-1) assembling histones on recently replicated DNA (Glowczewski *et al.*, 2004) and involved in the maintenance of silent chromatin (Adams & Kamakaka, 1999); and Yta7p, which regulates histone gene expression after binding to chromatin (Gradolatto *et al.*, 2008; Fillingham *et al.*, 2009).

Furthermore, I find Aar2p$_{1-170}$-bait associating with a potential telomere-binding Arc1p protein (Frantz & Gilbert, 1995) and to three telomeric regions. ARS902 is one of them; it is a presumed replication origin (ARS) on chromosome IX telomere (Wyrick *et al.,* 2001; Raveendranathan *et al.*, 2006; Xu *et al.*, 2006). ARSs are believed to facilitate DNA unwinding, thereby enhancing the replication initiation efficiency (Shirahige *et al.*, 1993). In agreement, an A1 class Aar2p$_{1-170}$ interactor is Ecm32p, a DNA-dependent ATPase/DNA helicase part of the Dna2p- and Nam7p-like family of helicases (Biswas *et al.*, 1995; Bean & Matson, 1997). The other two telomeric regions on the prey list are TEL12R-YP2 and TEL15R. TEL12R-YP2 is the most centromere-proximal of two telomeric Y' elements on the right arm of chromosome XII and includes an ARS consensus sequence (Louis & Haber, 1992; Pryde *et al.*, 1997; Yamada *et al.*, 1998). TEL15R is the chromosome XV right arm telomere with typical telomeric structure enclosing an X element core sequence, X element combinatorial repeats, a long Y' element, and a very short terminal stretch of telomeric repeats (Louis *et al.*, 1994; Louis, 1995). Interestingly and in complement of these results, when searching for genes that affect telomere length using a collection of strains that carry hypomorphic alleles (DAmP collection) Ungar and colleagues observed that *AAR2*-DAmP induces telomeres longer than those found in *wt* (Ungar *et al.*, 2009).

Integrating all this information I suggest that Aar2p can have an effect in chromosome architecture being involved in chromatin remodeling on sites of active replication.

6.4.4. Aar2p and DNA-damage repair

The Aar2p$_{1-170}$-bait captured numerous preys involved in DNA damage repair, many of them related to UV-induced DNA damage. They are Dna2p, Mus81p, Ogg1p, Rad4p, Rad16p, Rad53p, Rad54p and Tdp1p. I will discuss each of these preys in more detail.

Dna2p is a DNA replication factor with single-stranded DNA-dependent ATPase, ATP-dependent nuclease, and helicase activities (Bae *et al.*, 1998) and is also involved in Okazaki fragment processing (Bae & Seo, 2000).

Mus81p is an Mms4p-Mus81p endonuclease subunit that cleaves branched DNA (Bastin-Shanower *et al.*, 2003); it is implicated in replication fork stability during meiotic recombination (Oh *et al.*, 2008) and has a role in the response to UV and methylation-induced DNA damage (Interthal & Heyer, 2000).

Ogg1p, acts on mitochondrial DNA oxidative damage repair (Nash *et al.*, 1996; Singh *et al.*, 2001) and mediates UVA resistance (Kozmin *et al.*, 2005).

Rad4p is a homolog of human XPC protein (Foury, 1997), it is a subunit of Nuclear Excision Repair Factor 2 (NEF2) (de Laat *et al.* 1999; Prakash & Prakash, 2000) and together with Rad23p recognizes and binds UV damaged DNA. Rad4p is ubiquitinated and degraded by the 26S proteasome, in a process controlled by Rad23p (Lommel *et al.* 2002; Gillette *et al.*, 2006).

Rad16p together with Rad7p form Nucleotide Excision Repair Factor 4 (NEF4) complex (Gillette *et al.*, 2006). NEF 2 and NEF4 bind synergistically to UV damaged DNA in an ATP-dependent manner during nucleotide excision repair (Guzder, *et al.* 1999; Prakash & Prakash, 2000).

Rad53p is a kinase that in reaction to DNA damage induces cell-cycle arrest. It associates with hyperphosphorylated Rad9p and is activated in trans (Schwartz *et al.,* 2002; Toh & Lowndes, 2003). Rad53p interacts as well with ARS1 (autonomously replicating sequence) and causes initiation of DNA replication (Dohrmann & Sclafani, 2006).

Rad54p is a member of the SWI/SNF family (Eisen *et al.*, 1995). Throughout vegetative growth and meiosis this protein is implicated in DNA double-strand breaks repair. Rad54p is a DNA-dependent ATPase that alters the topology of

double-stranded DNA and promotes strand exchange (Clever *et al.*, 1997; Petukhova *et al.*, 1999).

Finishing this long list of DNA damage related preys there is Tdp1p. This protein repairs DNA lesions caused by topoisomerases I and II (Pouliot *et al.*, 1999; Nitiss *et al.*, 2006; He *et al.*, 2007).

The report of Aar2p S331 being phosphorylated after DNA-damage induction by genotoxic stress (Albuquerque *et al.*, 2008) is in agreement with the results above and suggests a function for Aar2p in DNA-damage repair. In addition, Ben-Aroya *et al.* (2010) reported a strong chromosome instability phenotype caused by a random *ts AAR2* mutant in a study that proves a link between proteasome degradation and double strand break (DSB) repair. The authors demonstrate for the first time a DSB repair protein (Mms22p) being ubiquitinated and targeted to the proteasome (Ben-Aroya *et al.*, 2010). It is then possible that after DNA damage induction (UV in particular) S331 is phosphorylated, targeting Aar2p to sites of double strand breaks. There, via its VHS domain Aar2p would recognize ubiquitinated DSB proteins, bind them and escort them to the proteasome for degradation.

6.4.5. Conclusion

The results I present in this chapter support three potential new functions for Aar2p. One of them, the U5 snRNP-components transport, corroborates the proposed model for U5 snRNP maturation (Boon *et al*., 2007), adding a new role for Aar2p in it. The other two, the putative roles for Aar2p in chromatin remodeling and DNA damage repair, corroborate and complement previous and recent unpublished findings (*e.g*. Albuquerque *et al.*, 2008, Ben-Aroya *et al.*, 2010, Wahl, 2010 - personal communication). Altogether, these results open new perspectives for the study of this interesting protein.

Table 6.2 –Results from the Y2H screen preformed with Aar2p$_{1-170}$ as bait. Prey interactions were classified as A1, A2, A3, A4 and B, according to Fromont-Racine *et al.*, 1997. A1 are the most significant interactions in which more than one overlapping fusion is found. A2, A3 and A4 are only found as a single fusion, even if the same fusion is found several times. A2 are fusions starting close to the initiation codon of an ORF. A3 are fusions containing coding inserts of more than 1000 bases. A4 are all the other fusion types. B fusions are non-biological peptides, like antisense or intergenic regions. No A3 class interactions are found in this screen.

Prey	Class of interaction	Insert (bp)	Chromosome coordinates	Aminoacids	No. of isolates	Remarks
AAR2	A1	894	ChrII 87282-86389	170-355 (end)	1	In frame
		954	ChrII 87678-86725	37-355	1	In frame
		894	ChrII 87538-86645	84-355	1	Out of frame -1
		511	Chr II 87439-86929	117-286	1	In frame
		495	Chr II 87453-86959	113-276	1	In frame
		860	Chr II 87678-86819	39-313	1	In frame
		495	Chr II 87453-86959	113-276	2	Out of frame +1
		993	Chr II 87679-86687	39-355	1	Out of frame +1
		889	Chr II 87666-86778	42-330	2	Out of frame +1
		561	Chr II 87660-87099	94-279	1	Out of frame -1
ACS1	A4	969	Chr I 44895-43927	44-365	1	In frame
APA1	A4	897	Chr III 38106-37210	232-321 (end)	1	Out of frame +1
ARC1	A1	702	Chr VII 307831-308532	132-362	1	In frame
		720	Chr VII 307739-308458	103-339	1	Out of frame -1
		639	Chr VII 307833-308471	133-344	1	In frame

ARO1	A4	520	Chr IV 708553-709072	1358-1530	1	In frame
ATG26	A4	507	Chr XII 532464-531958	645-810	1	Out of frame -1
CAB1	A1	354	Chr IV 1498265-1498618	14-131	2	In frame
		388	Chr IV 1498265-1498652	15-141	1	Out of frame -1
CUE2	A4	378	Chr XI 272419-272796	300-425	1	In frame
DNA2	A4	493	Chr VII 425793-425301	1130-1293	1	In frame
DYN1	A4	153	Chr XI 541032-540880	2181-2228	2	In frame
ECM1	A4	918	Chr III 45911-44994	333-637	2	Out of frame -1
ECM32	A1	510	Chr V 543970-544480	763-932	1	Out of frame +1
		553	Chr V 543943-544495	754-937	1	Out of frame -1
ERR2	A4	370	Chr XVI 10397-10766	36-143	1	In frame
FAS2	A4	546	Chr XVI 110428-110974	593-774	2	In frame
FIR1	A1	858	Chr V 216810-217668	584-876 (end)	1	Out of frame +1
		836	Chr V 216815-217650	589-876	1	In frame
		436	Chr V 217207-217642	716-859	1	In frame
		869	Chr V 216815-217683	586-868	1	In frame
FMS1	A1	336	Chr XIII 316332-316667	320-430	2	In frame
		337	Chr XIII 316332-316667	320-430	1	Out of frame +1
HAL5	A4	893	Chr X 108943-108051	172-469	2	In frame

KIN1	A4	362	Chr IV 694796-695157	36-151	2	In frame
MHP1	A4	892	Chr X 362243-363134	336-630	1	In frame
MLS1	A4	864	Chr XIV 406366-407211	3-290	1	In frame
MON1	A1	589	Chr VII 276706-276118	12-195	1	In frame
		567	Chr VII 276701-276135	8-195	2	In frame
MSA1	A4	743	Chr XV 449802-450544	127-369	1	Out of frame -1
MUS81	A4	764	Chr IV 1247626-1248389	518-632 (end)	1	Out of frame -1
NAR1	A4	784	Chr XIV 199099-198316	313-491	1	Out of frame +1
NIS1	A1	489	Chr XIV 480527-481015	255-407 (end)	1	Out of frame +1
		890	Chr XIV 480776-481665	337-407	1	Out of frame +1
NMA111	A4	675	Chr XIV 397326-398000	882-997	1	Out of frame -1
NUP116	A4	884	Chr XIII 365517-364634	337-687	1	In frame
OGG1	A4	328	Chr XIII 152346-152673	160-252	5	In frame
PIM1	A4	491	Chr II 181017-180527	89-250	1	In frame
PKC1	A4	901	Chr II 16736-15836	321-621	1	In frame
PPE1	A4	440	Chr VIII 249579-249140	23-168	1	In frame
RAD4	A1	200	Chr V 502055-501856	279-344	1	In frame
		201	Chr V 502056-501856	279-344	1	Out of frame +1
RAD16	A1	687	Chr II 467424-468110	62-289	3	In frame

		741	Chr II 467338-468078	33-279	1	Out of frame -1
		574	Chr II 467404-467977	57-296	1	Out of frame -1
RAD53	A4	832	Chr XVI 262916-262085	428-692	1	In frame
RAD54	A4	523	Chr VII 194651-194129	539-760	2	In frame
RCY1	A1	476	Chr X 51151-50676	668-825	1	In frame
		393	Chr X 51068-50676	696-825	1	Out of frame -1
		446	Chr X 51115-50670	680-825	1	Out of frame +1
RLF2	A4	494	Chr XVI 595084-595577	87-385	1	Out of frame -1
RPL25	A2	899	Chr XV 79965-80863	1-171	1	In frame, but there are 4 STOP codons before *RPL25* ATG
RPO31	A4	290	ChrXV 541860-541571	763-858	1	In frame
SAM4	A1	667	Chr XVI 25503-26170	140-325 (end)	1	In frame
		776	Chr XVI 25431-26206	116-325	1	Out of frame +1
			Chr XVI 25545-26078	154-325	1	Out of frame +1
SAN1	A1	542	Chr IV 743872-743331	2-181	1	In frame
		410	Chr IV 743804-743395	24-159	1	Out of frame +1
SAP1	A1	890	Chr V 245066-244177	481-757	1	Out of frame -1
		735	Chr V 245104-244370	468-724	1	Out of frame -1
SDC25	A1	751	Chr XII 115531-116281	879-1048 (end)	1	In frame
		755	Chr XII 115527-116281	896-1048	1	Out of frame -1

SNO3	A1	902	Chr VI 11053-10152	1-223	1	In frame
		912	Chr VI 11053-10141	1-333 (end)	1	In frame
SPT8	A4	469	Chr XII 251771-251303	438-593	1	Out of frame +1
SSE1	A1	199	Chr XVI 351916-351718	120-185	1	In frame
		412	Chr XVI 352126-351718	50-185	1	Out of frame -1
STP4	A4	840	Chr IV 367744-366905	158-434	1	In frame
SWI1	A1	575	Chr XVI 522645-523249	546-746	1	In frame
		611	Chr XVI 522639-523249	546-746	1	In frame
		745	Chr XVI 521283-522027	92-339	1	Out of frame -1
TDH1	A4	545	Chr X 338267-338811	65-182	1	Out of frame +1
TDH2	A2	567	Chr X 454693-454127	1-182	5	In frame
TDP1	A1	950	Chr II 670193-669244	35-355	1	In frame
		967	Chr II 670239-669743	19-183	1	Out of frame -1
TED1	A4	360	Chr IX 279402-279761	327-443	1	In frame
THI21	A4	814	Chr XVI 54715-53902	148-415	1	In frame
TIM9	A2	519	ChrV 116970-117488	1-88 (end)	1	In frame
TRA1	A4	836	Chr VIII 308978-309813	2073-2349	1	Out of frame +1
TRM1	A4	448	Chr IV 692735-692288	176-324	1	In frame

VID27	A4	283	Chr XIV 247974-248256	173-262	2	In frame
VTC2	A4	514	Chr VI 133143-133656	440-617	1	In frame
YOR1	A4	526	Chr VII 1054327-1054852	500-672	1	In frame
YTA6	A1	439	Chr XVI 416974-417412	406-533	6	In frame
		438	Chr XVI 416975-417412	406-533	1	In frame
YTA7	A1	872	Chr VII 1031280-1032152	1303-1379 (end)	1	Out of frame -1
		838	Chr VII 1031293-1032131	1315-1379	1	In frame
		910	Chr VII 1031280-1032190	1303-1379	2	Out of frame -1
YAL037W	A4	241	Chr I 74040-74280	8-87	1	In frame
YCL074W	A4	150	Chr III 3369-3519	206-227	1	In frame
YCR013C	A4	176	Chr III 138680-138505	124-181	1	In frame
YCR015C	A4	814	Chr III 141823-141010	118-317 (end)	1	In frame
YDR026C	A1	422	Chr IV 493251-492829	340-475	2	Out of frame +1
		834	Chr IV 493243-492409	342-570 (end)	1	Out of frame -1
		855	Chr IV 493243-492388	342-570	1	Out of frame -1
YFR016C	A4	828	Chr VI 177863-177034	958-1234 (end)	1	Out of frame -1
YGL109W	A4	723	Chr VII 303678-304400	55-107 (end)	1	Out of frame +1
YMR209C	A1	873	Chr XIII 686693-685821	197-457 (end)	2	In frame

		874	Chr XIII 686693-685820	197-457	2	In frame
		895	Chr XIII 686698-685804	198-457	1	Out of frame +1
		772	Chr XIII 686693-685922	198-457	1	In frame
TEL12R-YP2	B	327	Chr XII 1071337-1071663	-	1	Y' element
TEL15R	B	325	Chr XV 1090965-1091289	-	1	Telomere
		320	Chr XV 1090965-1091284	-	2	
ARS902	B	466	Chr IX 8399-8864	-	1	Autonomously replicating sequence
RDN5-1	B	170	Chr XII 459631-459800	-	1	rRNA
RDN18-1	B	108	Chr XII 456915-457022	-	1	rRNA
RDN18-2	B	108	Chr XII 466052-466159	-	1	rRNA
5' UTR YIR014W	B	245	Chr IX 380854-381099	-	1	
Antisense *AAC3*	B	647	ChrII 416982-416336	-	1	-
Antisense *BAT2*	B	504	Chr X 705811-705308	-	2	-
		741	Chr X 705806-705066	-	1	-
		542	Chr X 705812-705271	-	1	-
Antisense *BAT2-HMS2*	B	850	Chr X 705806-704957	-	2	Antisense sequence that spans from C-terminal *HMS2* to N-terminal *BAT2*
		623	Chr X 705806-705184	-	2	

		854	Chr X 705812-704959	-	1	
		805	Chr X 705806-705002	-	1	
		833	Chr X 705806-704974	-	1	
		735	Chr X 705812-705078	-	1	
		741	Chr X 705806-705066	-	1	
		705	Chr X 705812-705108	-	1	
		695	Chr X 705812-705118	-	1	
		641	Chr X 705812-705172	-	1	
		653	Chr X 705812-705160	-	1	
		806	Chr X 705806-705001	-	1	
		725	Chr X 705812-705088	-	1	
		714	Chr X 705812-705099	-	1	
Antisense *CDC60*	B	271	Chr XVI 248808-248538	-	1	
Antisense *DAP2*	B	706	Chr VIII 166097-166802	-	1	Antisense sequence that spans *DAP2*
		424	Chr VIII 166112-166535	-	1	
Antisense *EAF3*	B	655	Chr XVI 609573-610227	-	1	Antisense sequence that spans from N-terminal *EAF2*
Antisense *EMI2*	B	870	Chr IV 1475612-1476481	-	1	Antisense sequence that spans N-terminal half *EMI2*
Antisense *GAL4*	B	101	Chr XVI 79714-79814	-	2	

		102	Chr XVI 79714-79815	-	3
Antisense *HAP1*	B	612	Chr XII 648171-647486	-	1
		612	Chr XII 648164-647553	-	1
		672	Chr XII 648178-647507	-	1
Antisense *HEK2*	B	754	Chr II 161656-160903	-	1
		728	Chr II 161656-160928	-	1
		684	Chr II 161656-160973	-	1
			ChrII 161656-160973	-	1
Antisense *HIR3*	B	896	Chr X 694161-695056	-	1
Antisense *IMD2*	B	560	Chr VIII 554685-554126	-	1
Antisense *KIC1*	B	189	Chr VIII 317199-3107011	-	1
Antisense *PAU1*	B	466	Chr X 8382-8847	-	1
Antisense *PDR11*	B	204	Chr IX 331316-331519	-	1
		210	Chr IX 331316-331525	-	13
		214	Chr IX 331316-331529	-	1
		891	Chr IX 331315-332205	-	2
		196	Chr IX 331330-331525	-	1
		192	Chr IX 331316-331507	-	1
		192	Chr IX 331336-331524	-	1

		189	Chr IX 331317-331525	-	1
		846	Chr IX 331315-332160	-	1
		364	Chr IX 331295-331658	-	1
		702	Chr IX 331331-332032	-	4
		920	Chr IX 331325-332245	-	1
		917	Chr IX 331325-332241	-	1
		200	Chr IX 331325-331524	-	1
Antisense *PDR12*	B	96	Chr XVI 445796-445891	-	5
Antisense *PRP40*	B	250	Chr XI 419509- 419260	-	1
		308	Chr XI 419494-419187	-	2
		782	Chr XI 419542-418761	-	1
Antisense *RDN18*	B	108	Chr XIII 466052-466159	-	1
Antisense *RDN37-2*	B	108	Chr XII 466052-466159	-	1
Antisense *RPL35B*	B	248	Chr IV 218336-218089	-	1
Antisense *RPL41B*	B	573	Chr IV 221256-221828	-	1
Antisense *SNF3*	B	513	Chr IV 114077-113565	-	1
Antisense *SSN3*	B	667	Chr XVI 472728-473394	-	1
Antisense *STP1*	B	344	Chr IV 1387186-1386843	-	1
Antisense *STP1-MRPL28*	B	781	Chr IV 1387192-1386412	-	1

Antisense *UTR2*	B	461	Chr V 78368-78828	-	1
		444	Chr V 78811-78368	-	1
Antisense YDR026C	B	856	Chr IV 492460-493315	-	1
Antisense *YVH1*	B	477	Chr IX 405421-405897	-	2
Intergenic region 1	B	142	Chr XIII 619582-619723	-	2
Intergenic region 2	B	328	Chr XI 644081-644408	-	1
Intergenic region 3	B	670	Chr IV 543886-544555	-	1
Intergenic region 4	B	473	Chr IV 476408-475936	-	2
		226	Chr IV 476161-475936	-	1

Table 6.4 –Results from the Y2H screen preformed with Aar2p$_{150-355}$ as bait. Prey interactions were classified as A1, A2, A3, A4 and B, according to Fromont-Racine *et al.*, 1997. A1 are the most significant interactions in which more than one overlapping fusion is found. A2, A3 and A4 are only found as a single fusion, even if the same fusion is found several times. A2 are fusions starting close to the initiation codon of an ORF. A3 are fusions containing coding inserts of more than 1000 bases. A4 are all the other fusion types. B fusions are non-biological peptides, like antisense or intergenic regions. No A2, A3 nor B class interactions are found in this screen.

Prey	Class of interaction	Insert (bp)	Chromosome coordinates	Aminoacids	No. of isolates	Remarks
*AAR2**	A1	817	Chr II 88094-87278	1-168	1	Out of frame -1, but there are 4 STOP codons before *AAR2* ATG
		824	Chr II 88094-87271	1-172	2	Out of frame -1, but there are 4 STOP codons before *AAR2* ATG
		800	Chr II 88088-87289	1-166	6	Out of frame -1, but there are 4 STOP codons before *AAR2* ATG
		809	Chr II 88094-87286	1-167	2	Out of frame -1, but there are 4 STOP codons before *AAR2* ATG
		865	Chr II 88169-87305	1-160	1	Out of frame +1, but there are 4 STOP codons before *AAR2* ATG

	812	Chr II 88094-87283	1-168	6	In frame, but there are 7 STOP codons before wAAR2 ATG
	812	Chr II 88094-87283	1-168	6	In frame, but there are 7 STOP codons before *AAR2* ATG
	872	Chr II 88190-87319	1-156	1	Out of frame -1, but there are 4 STOP codons before *AAR2* ATG
	802	Chr II 88090-87289	1-166	1	In frame, but there are 7 STOP codons before *AAR2* ATG
	797	Chr II 88088-87291	1-166	1	Out of frame -1, but there are 4 STOP codons before *AAR2* ATG
	810	Chr II 88094-87284	1-168	1	Out of frame -1, but there are 4 STOP codons before *AAR2* ATG
	745	Chr II 88169-87424	1-121	1	Out of frame +1, but there are 4 STOP codons before AAR2 ATG
	940	Chr II 88109-87170	1-206	1	Out of frame -1, but there are 4 STOP codons before AAR2 ATG

RPS8A	A1	681	Chr II 88924-88244	67-end	1	Out of frame +1
		792	Chr II 88924-88133	67-end	1	Out of frame +1
		788	Chr II 88924-88137	67-end	1	Out of frame +1
		847	Chr II 88924-88078	67-end	1	Out of frame +1
		791	Chr II 88924-88134	67-end	1	Out of frame +1
SWI1	A4	892	Chr XVI 522693-523584	562-858	1	In frame
YBL073W	A4	385	Chr II 87475-87859	-	1	Out of frame -1

CHAPTER 7 - Final discussion and future work

7.1 Aar2p in U5 snRNP biogenesis

Aar2p was originally described as being essential for *MATa1* pre-mRNA splicing, one of the few two-intron genes in budding yeast, but not required for *ACT1* splicing (Nakazawa *et al*., 1991). Later this protein was isolated together with U5 snRNA and some components of the U5 snRNP. However it was never found as part of the U4/U6.U5 tri-snRNP and therefore is not considered to be an active participant in the splicing reaction (Gottschalk *et al*., 2001). Aar2p is necessary for splicing *in vivo* but not *in vitro.* Its depletion causes a reduction in the tri-snRNP levels and interferes with later rounds of splicing, indicating a possible role for Aar2p in snRNP recycling (Gottschalk *et al*., 2001). Aar2p was suggested to be involved in U5 snRNP biogenesis (Gottschalk *et al*., 2001; Boon *et al*., 2007). The Aar2p-U5 snRNP complex is viewed as an intermediate particle in U5 snRNP biogenesis and is thought to assemble in the cytoplasm (Boon *et al.*, 2007). Nevertheless, not much is known about Aar2p's exact role and mechanism of action in either snRNP recycling or U5 snRNP biogenesis.

I show in Chapter 3 of this study that Aar2p is phosphorylated in five aminoacid residues: S253, T274, Y328, S331 and T345; among them, S253 is very conserved between budding yeast and several higher eukaryotes.

From the results presented in Chapter 4, S253 comes across as an important element in regulation of the Aar2p/Prp8p interaction, which is disrupted *in vivo* by the phosphomimetic mutant S253E. At the same time, I rule out the Prr2p and Gcn2p kinases in regulating the Aar2p/Prp8p interaction. Results from Chapters 4 and 5 illustrate that this interaction is weak and only a small fraction of the total Prp8p is associated with Aar2p *in vivo*. Additionally I detect a low level of U5 snRNA associated with Aar2p, implying that the Aar2p-U5 snRNP precursor form is not very abundant in the cell.

Lastly, in Chapter 6 I find new Aar2p interactors. These suggest novel roles for Aar2p in protein transport, chromosome biology and DNA damage repair. I also observe Aar2p N-terminal fragment interacting with the Aar2p C-terminal, which suggests that the protein has a closed conformation.

My data support and complement the U5 snRNP maturation model proposed by Boon *et al*. (2007). Immunoprecipitation results suggest that S253 phosphorylation can be the mechanism for Aar2p replacement by Brr2p on C-terminus Prp8p, allowing U5 snRNP maturation to proceed. Aar2p can function then as a chaperone for the Brr2p/Prp8p interaction, preventing Brr2p from binding Prp8p before it is required and accelerating the splicing process inadvertently. My results corroborate also this model's assumption that the Aar2p/Prp8p and Brr2p/Prp8p complexes are in equilibrium. I observe growth defects when this equilibrium is disrupted by a simultaneous overproduction of Aar2p and E3 or E3H Prp8p fragments in the cell.

Regarding a potential role for Aar2p on Prp8p nuclear import Chapters 4 and 6 show potentially discordant data. In Chapter 4, I discard a role for Aar2p in the nuclear import of both Prp8p and Snu114p on the basis of *AAR2* overexpression and repression, under control of the *GAL1* promoter. I observe the same localisation pattern for GFP-Prp8p and GFP-Snu114p in both conditions. It is suggested that Aar2p level in the cell is normally very low (Nakazawa *et al.*, 1991). In addition, it is possible that the *GAL1* promoter is leaky, allowing Aar2p expression to levels similar to the normal situation during growth in glucose. In this case Prp8p and Snu114p localisation will not be affected by *AAR2* repression, since Aar2p level will be sufficient to maintain its function at normal levels. Most likely the Prp8p NLS has a major role in its nuclear import (Boon *et al*., 2007); Aar2p could be part of the process but with an accessory carrier function. If this is the case, the lack of alteration in Prp8p and Snu114p localisation with Aar2p overproduction and depletion is explained.

In Chapter 6 I show Aar2p interacting in a Y2H assay with Nup116p, a nuclear pore protein that interacts with Kap95p (Rout *et al.*, 2000; Strawn *et al.*, 2001; Lutzmann *et al.*, 2005). Boon (2005) showed that Kap95p is required for the nuclear import of Snu114p and U5 snRNA. The same author describes the Prp8p NLS as being responsible for Prp8p, Snu114p and U5 snRNA nuclear import but not interfering with Aar2p localisation (Boon *et al*., 2007). ΔNLS-Prp8p cells show defects on tri-snRNP formation and consequently on pre-mRNA splicing (Boon *et al*., 2007). However, splicing is not completely abolished and the cells survive,

suggesting that an additional mechanism for Prp8p import must be in place. Aar2p, which is normally localised in both nucleus and cytoplasm, accumulates in the nucleus after *PRP8* overexpression. Upon Prp8p depletion Aar2p shows a normal localisation pattern, indicating that Aar2p localisation is somehow linked to Prp8p (Boon *et al*., 2007). Furthermore, based on his structural data Wahl suggests that Aar2p binds Prp8p and may mediate its nuclear import (M. Wahl, personal communication). In resume, the evidence points to a role for Aar2p in Prp8p transport.

Aar2p C-terminal is found to interact with Prp8p and is composed of a VHS domain, typical of proteins involved in vesicular transport (M. Wahl, personal communication). VHS domains very frequently have associated ubiquitin interacting motifs (Lohi *et al*., 2002). This evidence agrees with Prp8p Jab1/MPN domain binding ubiquitin, and the isolation of Prp8p-ubiquitin with the tri-snRNP (Bellare *et al*., 2006, 2008).

Disruption of ubiquitin recognition in splicing extracts *in vitro* causes the spliceosome to stall at complex B. This effect is caused by a reduction in the tri-snRNP level due to an increase in the rate of U4/U6 unwinding catalysed by Brr2p. Therefore ubiquitin recognition seems to control tri-snRNP disassembly through Prp8p-ubiquitin repressing Brr2p unwinding activity (Bellare *et al*., 2008). The same authors do not rule out that ubiquitin recognition may also have a role promoting tri-snRNP formation (Bellare *et al*., 2008) and U5 snRNP maturation directly affects tri-snRNP formation. Additionally, in Chapter 6 I find two ubiquitin interacting proteins as Aar2p preys, reinforcing the idea that Aar2p recognizes and binds ubiquitinated proteins. This suggests that Aar2p can bind Prp8p-ubiquitin and facilitate its nuclear import. Thus, ubiquitination could be an additional mechanism regulating U5 snRNP maturation.

Summarizing the data above, I introduce new elements to the U5 snRNP maturation model (Figure 7.1). Aar2p would recognize Prp8p-ubiquitin in the cytoplasm and bind it through its VHS cargo-recognition domain. The Aar2p/Prp8p/Snu114p/U5 snRNP precursor complex is then imported to the nucleus in a Kap95-dependent manner due to cooperation between the Prp8p NLS and Aar2p. Once in the nucleus, a kinase X would phosphorylate S253, disrupting the

Aar2p/Prp8p interaction. Brr2p can then bind C-terminal Prp8p and complete the U5 snRNP maturation process.

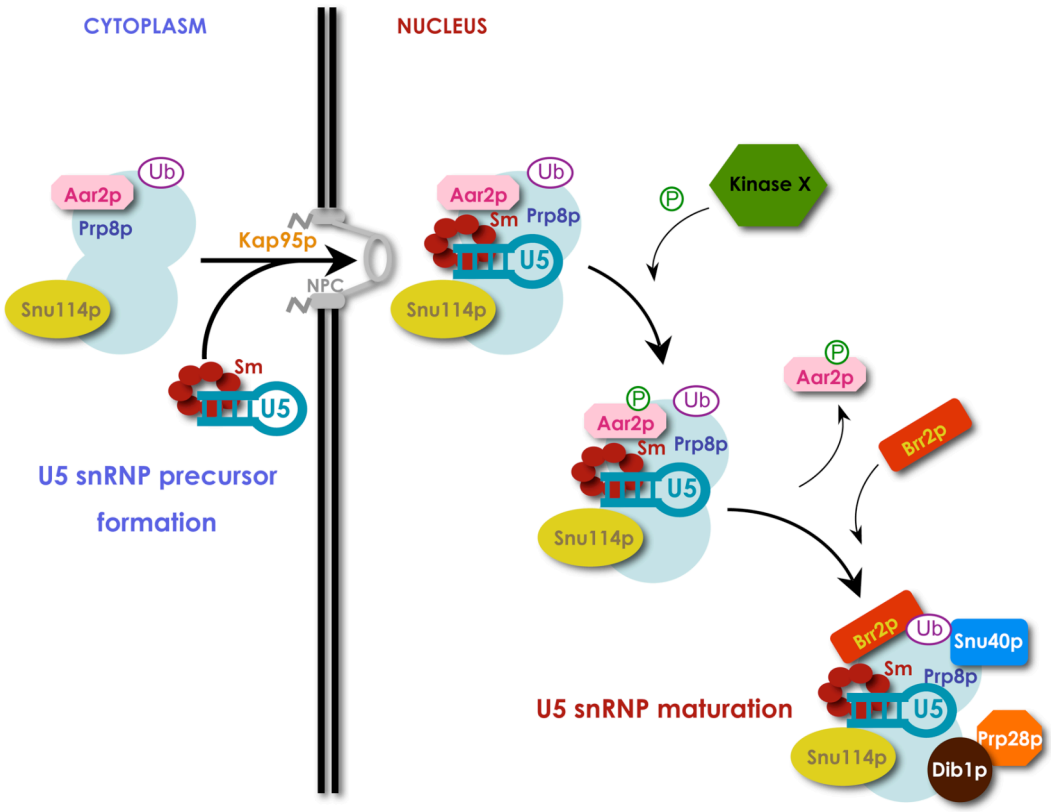

Figure 7.1. Updated view of the U5 snRNP maturation model. New elements are added to the U5 snRNP maturation model proposed by Boon *et al*. (2007). Special emphasis is given to Aar2p S253 phosphorylation, which can be the trigger for disruption of the Aar2p/Prp8p interaction. Prp8p-ubiquitin is also added to this model, as a possible mechanism for Aar2p recognition and binding to Prp8p in the cytoplasm.

7.2 New roles for Aar2p

From the Y2H screen results I present in Chapter 6, potential new roles for Aar2p can be suggested. In particular, roles in DNA damage repair and chromatin remodeling.

Using Aar2p$_{1\text{-}170}$ as bait for the Y2H screen I obtain a vast number of prey proteins. Amongst them I find ubiquitin-binding proteins, proteins involved in DNA-damage repair (a great part of them associated with UV-induced DNA damage) and one DNA helicase. In agreement, Aar2p S331 is phosphorylated upon

DNA damage (Albuquerque *et al.*, 2008) reinforcing the hypothesis of a link between Aar2p and DNA damage repair. This suggests a functional separation of the Aar2p phosphosites. S253 would be involved in U5 snRNP biogenesis and S331 in DNA damage repair. Also here the Aar2p VHS domain could take part, mediating cargo binding and transport by ubiquitin recognition. Aar2p could be a link between double strand break repair and proteasome degradation as proposed for other proteins (Ben-Aroya *et al.,* 2010). DNA damage can target Aar2p to sites of double strand breaks, probably through S331 phosphorylation. There, Aar2p can bind DSB proteins and mediate its transport to the proteasome. Sustaining this idea, a *ts aar2* mutant was observed to promote chromosome instability (Ben-Aroya *et al.,* 2010). This mutant could have an effect on DNA damage repair and therefore cause the chromosome instability.

In the prey list I find also telomeric regions of three chromosomes, together with chromatin-binding/remodeling proteins and one telomere-binding protein. DAmP alleles of splicing factors have been found to affect telomere length in budding yeast. Mutations in *PRP4*, *PRP22*, *PRP31*, *PRP38*, *PRP43* and *NTR2* caused short telomeres (Ungar *et al*., 2009). Prp4p, Prp31p and Prp38p are components of the tri-snRNP (Stevens & Abelson, 1999); Prp22p and Prp43p are DEAH-box RNA-dependent ATPase/ATP-dependent RNA helicases. Prp22p is responsible for mRNA release from the spliceosome (Schneider *et al*., 2002). Prp38p together with Ntr2p mediates intron-lariat complex release and spliceosome disassembly (Martin *et al*., 2002; Tsai *et al*., 2005).

On the other hand, DAmP alleles of *AAR2* and *SAD1* cause long telomeres (Ungar *et al*., 2009). Sad1p is a conserved protein required for U4 assembly into the U4/U6 dimer (Lygerou *et al*., 1999).

Proteins required for the later steps of the splicing reaction or even spliceosome disassembly seem to be involved in telomere elongation. On the other hand, the proteins required for the earliest steps of spliceosome assembly (with indirect effects on tri-snRNP formation) appear to shorten the telomeres. These opposing effects on telomere length are rather interesting. It seems that the equilibrium between spliceosome assembly/disassembly contributes in some way to telomere size maintenance.

The chromosome ends are protected by the telomeres from being recognized as DNA breaks and from getting shorter as a consequence of DNA replication (Blackburn, 2005). Therefore, Aar2p association with telomeres, an autonomously replicating sequence, a telomere-binding protein and chromatin binding/remodeling proteins can be related to its putative involvement in DNA damage repair. Aar2p can be targeted to sites of active replication by a mechanism similar to that proposed for DNA damage repair. Once at the replication sites, it can mediate rearrangements in chromosome architecture on replication sites. Alternatively, Aar2p could be directed to the DNA by default and its mode of action would vary according to the scenario presented, either a double strand break or active replication.

In conclusion, this study contributes to the current knowledge about Aar2p role on U5 snRNP biogenesis and unveils new study potential for this protein.

7.3 Future work

This thesis raises new questions to be answered regarding Aar2p function in both U5 snRNP biogenesis and DNA damage repair. In the following sections new directions are proposed for the study of Aar2p in these two processes.

7.3.1 Aar2p role in U5 snRNP maturation

One fundamental experiment to be done, and already suggested in Chapter 5, is to study the effect of the phosphomutants in two plasmid shuffle strains, one *MAT*a and another *MAT*α. This may clarify whether the different effects observed in Chapters 4 and 5 are mating type-specific or not.

It would be interesting to combine the Aar2p phosphomutants with ΔNLS-Prp8p. If Aar2p really is an accessory transport factor for Prp8p, one or more of the phosphomutants might block Prp8p nuclear import completely and lead to lethality. At the same time the individual phosphomutants effect on Prp8p and Aar2p localisation can be assessed by fluorescence microscopy. Different combinations of phosphomutations can also be tested in this process.

Additionally the role of ubiquitination in U5 snRNP biogenesis can be verified. This can be done by immunoprecipitation to test whether Aar2p really recognizes

and binds Prp8p-ubiquitin to mediate its nuclear import; and also testing if ubiquitin recognition disruption affects Prp8p localisation.

Prp8p rp mutants accumulate Aar2p/Prp8p/U5 snRNP in the nucleus and have reduced levels of Brr2p/Prp8p/U5 snRNP leading to splicing defects (Boon *et al*., 2007). This happens probably due to a stabilization of the Aar2p/Prp8p interaction, inhibiting Brr2p binding to Prp8p. Consequently, the Aar2p-S253E mutation may reverse this effect. A way to test this is to combine the Prp8p rp mutants with Aar2p-S253A/E and study the effect on cell growth and pre-mRNA splicing. Aar2p S253A should exacerbate the rp phenotype and S253E should rescue it. At the same time the levels of Aarp2/Prp8p and Brr2p/Prp8p can be checked by glycerol gradient fractionation followed by Prp8p immunoprecipitation. Aar2p-S253A should cause an increase in Aarp2/Prp8p and a decrease in Brr2p/Prp8p levels. The reverse effect is expected with Aar2p-253E.

A relevant and yet unidentified player in the updated U5 snRNP biogenesis model is kinase X (Figure 7.1). It is important to find the identity of this kinase, which seems to have a role in regulation of the Aar2p/Prp8p interaction. Although kinase/substrate interactions are usually very transient, this can be approached by Aar2p immunoprecipitation from yeast extracts followed by mass spectrometry. The kinases found amongst the interactors can be tested for Aar2p/Prp8p interaction regulation.

7.3.2 Aar2p, chromosomes and DNA damage repair

Investigating a role for Aar2p in DNA damage repair and chromosome biology should start by confirming the major interactions described in this study. The robustness of the prey interactions with $Aar2p_{1\text{-}170}$ can be tested in the presence of increasing 3AT concentrations. At the same time Y2H assays can be set up where the prey clones can be used as bait, and $Aar2p_{1\text{-}170}$ as prey to confirm the reciprocity of the interaction.

The confirmed interactions can be tested *in vivo* by immunoprecipitation performed in cells subjected to DNA damage, primarily to UV-induced DNA damage. The relative importance of each Aar2p phosphosite in this process can be accessed studying the effect its effect under the same DNA damage conditions.

APPENDIX - Mass-spectrometry data

A) Technique description

F. de Lima Alves in J. Rappsilber lab identified the candidate phosphosites for Aar2p. That was done using an LTQ-Orbitrap mass spectrometer (ThermoElectron) coupled on line to an Agilent 1100 binary nanopump and an HTC PAL autosampler (CTC Analytics). To prepare an analytical column with a self-assembled particle frit (25), C18 material (ReproSil-Pur C18-AQ 3 μm, Dr. Maisch, GmbH) was packed into a spray emitter (75 μm inner diameter, 8 μm opening, 70 mm length; New Objectives) using an air pressure pump (Proxeon Biosystems). Mobile phase A consisted of water, 5% acetonitrile, and 0.5% acetic acid. Mobile phase B consisted of acetonitrile and 0.5% acetic acid. The gradient used for each sample was 2 h. Peptides were loaded onto the column at a flow rate of 0.7 μL/min and eluted at a flow rate of 0.3 μL/min. For a 2 h gradient run, elution used a gradient from 0% B to 20% B over 75 min and then from 20% B to 80% B over 13 min. Fourier transform mass spectrometry spectra were recorded at 30,000 resolution, and the six most intense peaks of the MS scan were selected in the ion trap for fragmentation (normal scan; wideband activation; filling, 7.5×10^5 ions for MS scan and 1.5×10^4 ions for MS/MS; maximum fill time, 150 ms; dynamic exclusion for 60 s). Raw files were processed using DTA Super Charge (v.1.19), Mascot (v.2.2.0) and MS Quant (v.1.4.3a74) software.

Searches were conducted using Mascot (version 2.2.0) against a SwissProt database containing *Saccharomyces Cerevisiae* sequence (6556 sequences). The following search parameters were used: mass tolerance for precursor ions, 6 ppm; mass tolerance for fragment ions, 0.6 Da; enzyme specificity, fully tryptic (no cleavage N-terminally of proline); allowed number of missed cleavages, 2; fixed modification, carbamidomethylation on cysteine; variable modification, oxidation on methionine, Phospho(ST) and Phospho(Y).

B) Spectra

Below are included representative spectra for each of the identified phosphosites. The underlined aminoacid in the peptides indicates the phosphosite identified.

S253

This phosphopeptide was the least abundant of the 5 sites, being identified in one peptide with the thermolysin digest. Peptide represented in the spectrum with a score of 3: S<u>S</u>ATVP. In red are indicated the relevant phosphopeaks.

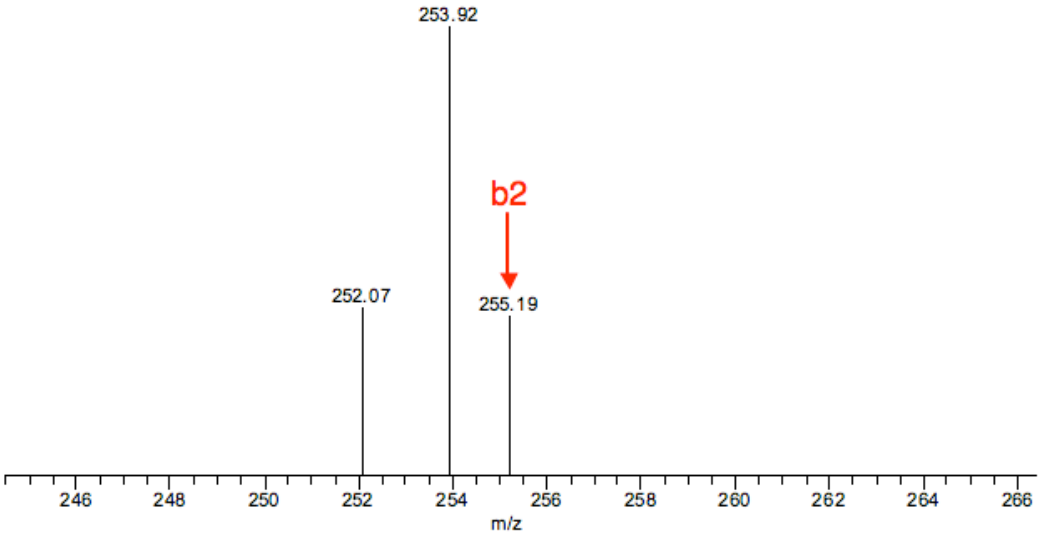

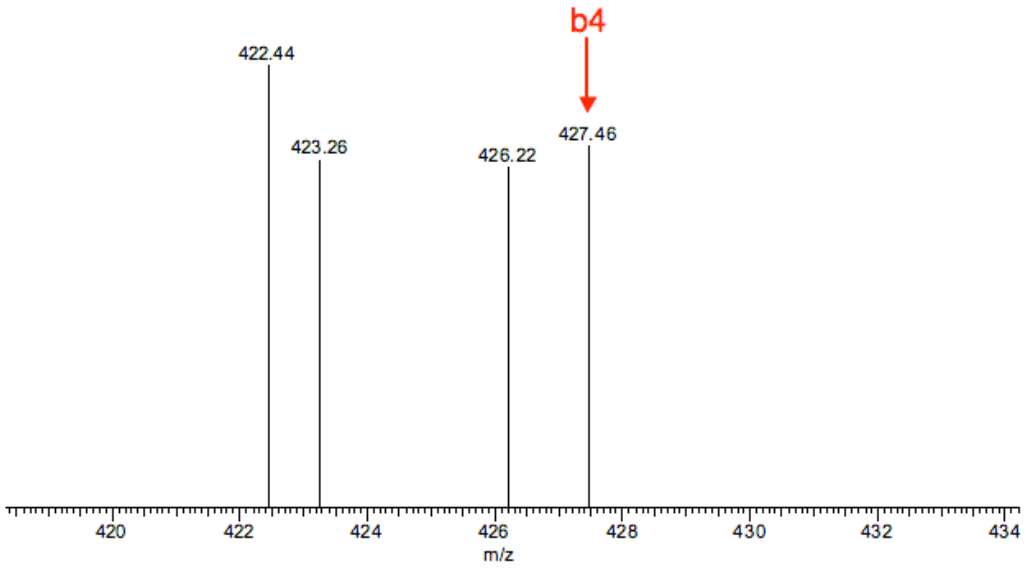

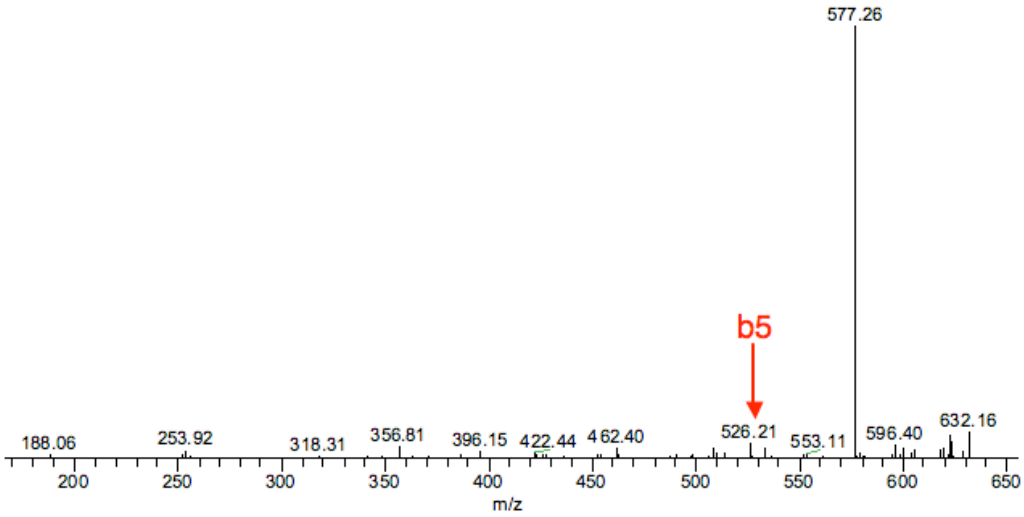

T274

This phosphosite was identified in one peptide with the elastase digest. Peptide in the spectrum with a score of 12: LICSSATVPKHMLDKLDEILYYQIKTL.

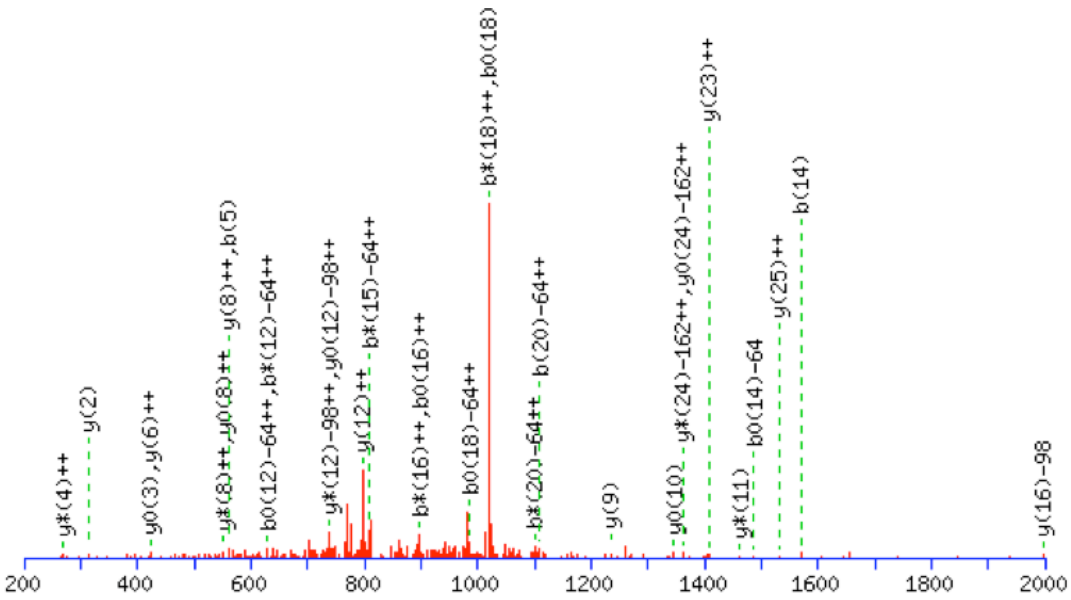

Y328

This phosphosite was identified in 8 peptides with the elastase digest and in three peptides with the thermolysin digest. Peptide in this spectrum with a score of 51: GKDNEDDALIYGISDEERDDEDDEHNPTIV.

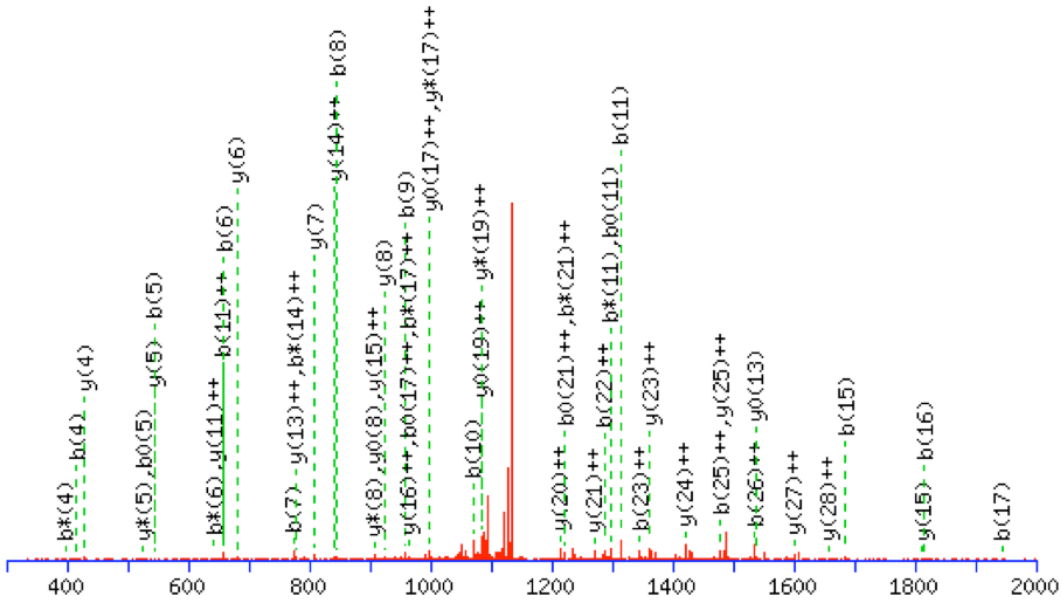

S331

This phosphosite was very abundant and identified in all the digests performed. It was detected in 7 peptides with trypsin, 21 peptides with proteinase K, 26 peptides with elastase and 54 peptides with thermolysin. Peptide in this spectrum with a score of 53: GISDEERDDEDDEHNPTIV.

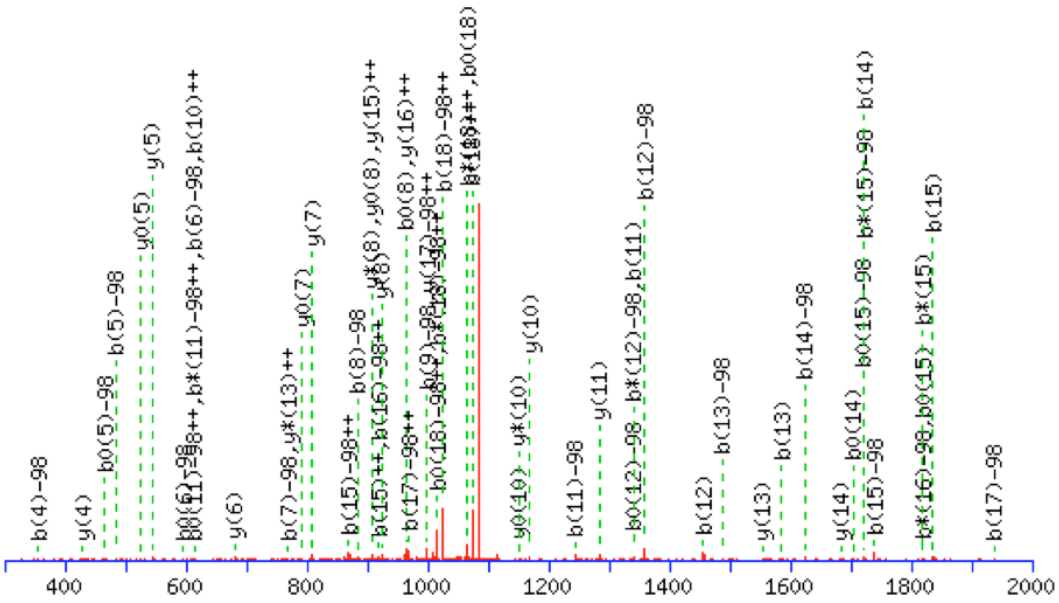

T345

This phosphosite was identified in one peptide with the trypsin digest and in another peptide with the elastase dygest. Peptide in this spectrum with a score of 5: TIVGGL.

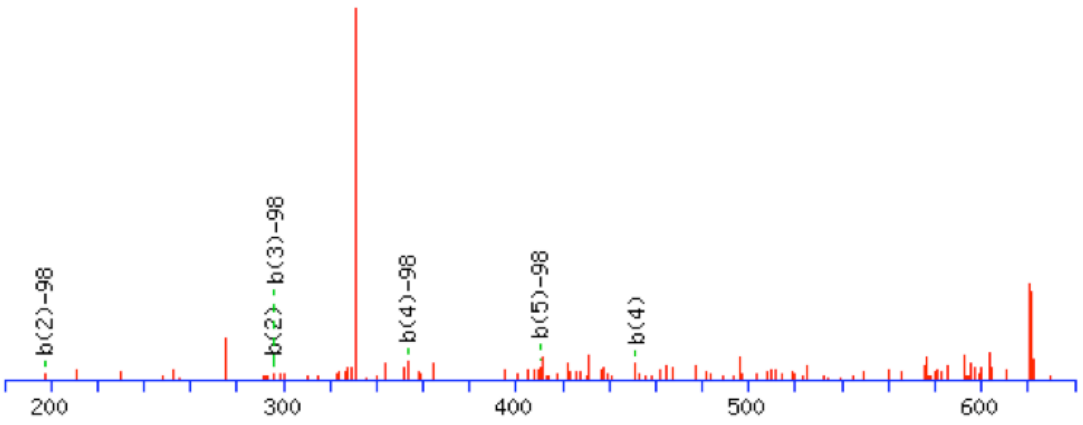

REFERENCES

Achsel, T., Ahrens, K., Brahms, H., Teigelkamp, S., and Lührmann, R. (1998) The human U5-220kD protein (hPrp8) forms a stable RNA-free complex with several U5-specific proteins, including an RNA unwindase, a homologue of ribosomal elongation factor EF-2, and a novel WD-40 protein. Mol Cell Biol 18, 6756-6766.

Adams, C. R., and Kamakaka, R. T. (1999) Chromatin assembly: biochemical identities and genetic redundancy. Curr Opin Genet Dev 9, 185-190.

Albuquerque, C. P., Smolka, M.B., Payne, S. H., Bafna, V., Eng, J., and Zhou, H. A. (2008) multidimensional chromatography technology fot in-depth phosphoproteome analysis. Mol Cell Proteomics 7, 1389-1396.

Anderson, G. J., Bach, M., Luhrmann, and R., Beggs, J. D. (1989) Conservation between yeast and man of a protein associated with U5 small ribonucleoprotein. Nature 342, 819-821.

Andrews, P. D., and Stark, M. J. (2000) Dynamic, Rho1p-dependent localization of Pkc1p to sites of polarized growth. J Cell Sci 113, 2685-2693.

Arenas, J. E., and Abelson, J. N. (1997) Prp43: An RNA helicase-like factor involved in spliceosome disassembly. Proc Natl Acad Sci USA 94, 11798-11802.

Bae, S. H., and Seo, Y. S. (2000) Characterization of the enzymatic properties of the yeast dna2 Helicase/endonuclease suggests a new model for Okazaki fragment processing. J Biol Chem 275, 38022-38031.

Bae, S. H., Choi, E., Lee, K. H., Park, J. S., Lee, S. H., and Seo, Y. S. (1998) Dna2 of *Saccharomyces cerevisiae* possesses a single-stranded DNA-specific endonuclease activity that is able to act on double-stranded DNA in the presence of ATP. J Biol Chem 273, 26880-26890.

Bartels, C., Klatt, C., Lührman, R., and Fabrizio, P. (2002) The ribosomal translocase homologue Snu114p in involved in unwinding U4//U6 RNA during activation of the spliceosome. EMBO Rep 3, 875-880.

Bartels, C., Urlaub, H., Lührman, R., and Fabrizio, P. (2003) Mutagenesis suggests several roles of Snu114p in pre-mRNA splicing. J Biol Chem 278, 28324-28334.

Bastin-Shanower, S. A., Fricke, W. M., Mullen, J. R., and Brill, S. J. (2003) The mechanism of Mus81-Mms4 cleavage site selection distinguishes it from the homologous endonuclease Rad1-Rad10. Mol Cell Biol 23, 3487-3496.

Beach, D. L., and Bloom, K. (2001) ASH1 mRNA localization in three acts. Mol Biol Cell 12, 2567-2577.

Bean, D. W., and Matson, S. W. (1997) Identification of the gene encoding scHelI, a DNA helicase from *Saccharomyces cerevisiae*. Yeast 13, 1465-1475.

Becker, J., Walter, W., Yan, W., and Craig, E. A. (1996) Functional interaction of cytosolic hsp70 and a DnaJ-related protein, Ydj1p, in protein translocation in vivo. Mol Cell Biol 16, 4378-4386.

Beggs, J. D. (2001). Pre-mRNA Splicing. In Encyclopedia of Genetics (Brenner, S. & Miller, J. H., eds), pp. 1536. London, Elsevier Science Inc.

Beggs, J. D. (2005) Lsm proteins and RNA processing. Biochem Soc Trans 33, 433-438.

Bellare, P., Kutach, A. K., Rines, A. K., Guthrie, C., and Sontheimer, E. J. (2006) Ubiquitin binding by a variant Jab1/MPN domain in the essential pre-mRNA splicing factor Prp8p. RNA 12, 292-302.

Bellare, P., Small, E. C., Huang, X., Wohlschlegel, J. A., Staley, J. P., and Sontheimer, E. J. (2008) A role for ubiquitin in the spliceosome assembly pathway. Nat Struct Mol Biol 15, 444-451.

Ben-Aroya, S., Agmon, N., Yuen, K., Kwok, T., McManus, K., Kupiec, M., and Hieter, P. (2010) Proteasome nuclear activity affects chromosome stability by controlling the turnover of mms22, a protein important for DNA repair. PLoS Genet 6, e1000852.

Berget, S. M., Moore, C., and Sharp, P. A. (1977) Spliced segments at the 5' terminus of adenovirus 2 late mRNA. Proc Natl Acad Sci USA 74, 3171-3175.

Biederer, T., Volkwein, C., and Sommer, T. (1997) Role of Cue1p in ubiquitination and degradation at the ER surface. Science 278, 1806-1809.

Biswas, E. E., Chen, P. H., Leszyk, J., and Biswas, S. B. (1995) Biochemical and genetic characterization of a replication protein A dependent DNA helicase from the yeast, *Saccharomyces cerevisiae*. Biochem Biophys Res Commun 206, 850-856.

Blackburn, E. H. (2005) Telomeres and telomerase: their mechanisms of action and the effects of altering their functions. FEBS Lett 579, 859-862.

Boon, K. L. (2005) "Analysis of Yeast Prp8 Protein and its role in U5 snRNP Assembly". Thesis presented for the degree of Doctor of Philosophy, University of Edinburgh, December 2005.

Boon, K. L., Grainger, R. J., Ehsani, P., Barrass, J. D., Auchynnikava, T., Inglehearn, C. F., and Beggs J. D. (2007) prp8 mutations that cause human retinitis pigmentosa lead to a U5 snRNP maturation defect in yeast. Nat Struct Mol Biol 14, 1077-1083.

Boon, K. L., Norman, C. M., Grainger, R. J., Newman, A. J., and Beggs J. D. (2006) Prp8 Dissection Reveals Domain Structure and Protein Interaction Sites. RNA 12, 198-205.

Brenner, T. J., and Guthrie C. (2005) Genetic Analysis Reveals a Role for the C Terminus of the Saccharomyces cerevisiae GTPase Snu114 During Spliceosome Activation. Genetics 170, 1063-1080.

Brenner, T. J., and Guthrie C. (2006) Assembly of Snu114 into U5 snRNP requires Prp8 and a functional GTPase domain. RNA 12, 862-871.

Brown J. D., and Beggs J. D. (1992) Roles of PRP8 protein in the assembly of splicing complexes. EMBO J 11, 3721-3729.

Burchett, S. A., Scott, A., Errede, B., and Dohlman, H. G. (2001) Identification of novel pheromone-response regulators through systematic overexpression of 120 protein kinases in yeast. J Biol Chem 276, 26472-26478.

Chan, S. P., Kao, D. I., Tsai, W. Y., and Cheng S. C. (2003) The Prp19p-associated complex in spliceosome activation. Science 302, 279-282.

Chanfreau, G., Elela, S. A., Ares, M., Jr., and Guthrie, C. (1997) Alternative 3'-end processing of U5 snRNA by Rnase III. Genes Dev 11, 2741-2751.

Chow, L. T., Gelinas, R. E., Broker, T. R., and Roberts, R. J. (1977) An amazing sequence arrangement at the 5' ends of adenovirus 2 messenger RNA. Cell 12, 1-8.

Clever, B., Interthal, H., Schmuckli-Maurer, J., King, J., Sigrist, M., and Heyer, W. D. (1997) Recombinational repair in yeast: functional interactions between Rad51 and Rad54 proteins. EMBO J 16, 2535-2544.

Cohen, P. (2000) The regulation of protein function by multisite phosphorylation – a 25 year update. Trends Biochem Sci 25, 596-601.

Collins SR, Kemmeren P, Zhao XC, Greenblatt JF, Spencer F, Holstege FC, Weissman JS, Krogan NJ (2007) Toward a Comprehensive Atlas of the Physical Interactome of Saccharomyces cerevisiae. Mol Cell Proteomics 6(3):439-50

Dasgupta, A., Ramsey, K. L., Smith, J. S., and Auble, D. T. (2004) Sir Antagonist 1 (San1) is a ubiquitin ligase. J Biol Chem 279, 26830-26838.

de Laat, W. L., Jaspers, N. G., and Hoeijmakers, J. H. (1999) Molecular mechanism of nucleotide excision repair. Genes Dev 13, 768-785.

Decourty, L., Saveanu, C., Zemam, K., Hantraye, F., Frachon, E., Rousselle, J. C., Fromont-Racine, M., and Jacquier, A. (2008) Linking functionally related genes by sensitive and quantitative characterization of genetic interaction profiles. Proc Natl Acad Sci USA 105, 5821-5826.

Dix, I., Russell C. S., and Beggs J. D. (2001) Introns. Encyclopedia of genetics (Ed. E.C.R. Reeve) Fitzroy Dearborn, London, 712-720.

Dix, I., Russell, C. S., O'Keefe, R. T., Newman, A. J., and Beggs J. D. (1998) Protein-RNA interactions in the U5 snRNP of *Saccharomyces cerevisiae*. RNA 4, 1675-1686.

Dohrmann, P. R., and Sclafani, R. A. (2006) Novel role for checkpoint Rad53 protein kinase in the initiation of chromosomal DNA replication in *Saccharomyces cerevisiae*. Genetics 174, 87-99.

Edgar, R. C. (2004) MUSCLE: a multiple sequence alignment method with reduced time and space complexity. BMC Bioinformatics 5, 113.

Eisen, J. A., Sweder, K. S., and Hanawalt, P. C. (1995) Evolution of the SNF2 family of proteins: subfamilies with distinct sequences and functions. Nucleic Acids Res 23, 2715-2723.

Elbert, M., Rossi, G., and Brennwald, P. (2005) The yeast par-1 homologs kin1 and kin2 show genetic and physical interactions with components of the exocytic machinery. Mol Biol Cell 16, 532-549.

Enomoto, S., McCune-Zierath, P. D., Gerami-Nejad, M., Sanders, M. A., and Berman, J. (1997) RLF2, a subunit of yeast chromatin assembly factor-I, is required for telomeric chromatin function in vivo. Genes Dev 11, 358-370.

Fabrizio, P., Dannenberg, J., Dube, P., Kastner, B., Stark, H., Urlaub, H., and Lührmann, R. (2009) The evolutionarily conserved core design of the catalytic activation step of the yeast spliceosome. Mol Cell 36, 593-608.

Fabrizio, P., Laggerbauer, B., Lauber, J., Lane, W. S., and Luhrmann, R. (1997) An evolutionarily conserved U5 snRNP-specific protein is a GTP-binding factor closely related to the ribosomal translocase EF-2. EMBO J 16, 4092-4106.

Fillingham, J., Kainth, P., Lambert, J. P., van Bakel, H., Tsui, K., Peña-Castillo, L., Nislow, C., Figeys, D., Hughes, T. R., Greenblatt, J., and Andrews, B. J. (2009) Two-color cell array screen reveals interdependent roles for histone chaperones

and a chromatin boundary regulator in histone gene repression. Mol Cell 35, 340-351.

Fischer, U., Darzynkiewicz, E., Tahara, S. M., Dathan, N. A., Lührmann, R., and Mattaj, I. W. (1991) Diversity in the signals required for nuclear accumulation of U snRNPs and variety in the pathways of nuclear transport. J Cell Biol 113, 705-714.

Fischer, U., Liu, Q., and Dreyfuss, G. (1997) The SMN-SIP1 complex has an essential role in spliceosomal snRNP biogenesis. Cell 90, 1023-1029.

Fornerod, M., Ohno, M., Yoshida, M., and Mattaj, I. W. (1997) CRM1 is an export receptor for leucine-rich nuclear export signals. Cell 90, 1051-1060.

Foury, F. (1997) Human genetic diseases: a cross-talk between man and yeast. Gene 195(1):1-10.

Frantz, J. D., and Gilbert, W. (1995) A novel yeast gene product, G4p1, with a specific affinity for quadruplex nucleic acids. J Biol Chem 270, 20692-20697.

Frazer, L. N., Lovell, S. C., O'Keefe, R. T. (2009) Analysis of synthetic lethality reveals genetic interactions between the GTPase Snu114p and snRNAs in the catalytic core of the *Saccharomyces cerevisiae* spliceosome. Genetics 183, 497-515.

Frazer, L. N., Nancollis, V., and O'Keefe, R. T. (2008) The role of Snu114p during pre-mRNA splicing. Biochem Soc Trans 36, 551-553.

Frilander, M. J., and Steitz, J. A. (2001) Dynamic exchanges of RNA interactions leading to catalytic core formation in the U12-dependent spliceosome. Mol Cell 7, 217-226.

Fromont-Racine, M., Rain, J. C., and Legrain, P. (1997) Toward a functional analysis of the yeast genome through exhaustive two-hybrid screens. Nat Genet 16, 277-282.

Fromont-Racine, M., Rain, J. C., and Legrain, P. (2002) Building protein-protein networks by two-hybrid mating strategy. Methods Enzymol 350, 513-524.

Galan, J. M., Wiederkehr, A., Seol, J. H., Haguenauer-Tsapis, R., Deshaies, R. J., Riezman, H., and Peter , M. (2001) Skp1p and the F-box protein Rcy1p form a non-SCF complex involved in recycling of the SNARE Snc1p in yeast. Mol Cell Biol 21, 3105-3117.

Garcia-Barrio, M., Dong, J., Ufano, S., and Hinnebusch, A. G. (2000) Association of GCN1-GCN20 regulatory complex with the N-terminus of eIF2alpha kinase GCN2 is required for GCN2 activation. EMBO J 19, 1887-1899.

Gardner, R. G., Nelson, Z. W., and Gottschling, D. E. (2005) Degradation-mediated protein quality control in the nucleus. Cell 120, 803-815.

Gavin, A. C., Aloy, P., Grandi, P., Krause, R., Boesche, M., Marzioch, M., Rau, C., Jensen, L. J., Bastuck, S., Dümpelfeld, B., Edelmann, A., Heurtier, M. A., Hoffman, V., Hoefert, C., Klein, K., Hudak, M., Michon, A. M., Schelder, M., Schirle, M., Remor, M., Rudi, T., Hooper, S., Bauer, A., Bouwmeester, T., Casari, G., Drewes, G., Neubauer, G., Rick, J. M., Kuster, B., Bork, P., Russell, R. B., and Superti-Furga, G. (2006) Proteome survey reveals modularity of the yeast cell machinery. Nature 440, 631-636.

Gavin, A. C., Bosche, M., Krause, R., Grandi, P., Marzioch, M., Bauer, A., Schultz, J., Rick, J. M., Michon, A. M., Cruciat, C. M., Remor, M., Hofert, C., Schelder, M., Brajenovic, M., Ruffner, H., Merino, A., Klein, K., Hudak, M., Dickson, D., Rudi, T., Gnau, V., Bauch, A., Bastuck, S., Huhse, B., Leutwein, C., Heurtier, M. A., Copley, R. R., Edelmann, A., Querfurth, E., Rybin, V., Drewes, G., Raida, M., Bouwmeester, T., Bork, P., Seraphin, B., Kuster, B., Neubauer, G., and Superti-Furga, G. (2002) Functional organization of the yeast proteome by systematic analysis of protein complexes. Nature 415, 141-147

Gietz, R. D., and Schiestl, R. H. (1991) Applications of high efficiency lithium acetate transformation of intact yeast cells using single-stranded nucleic acids as carrier. Yeast 7, 253-263.

Gillette, T. G., Yu, S., Zhou, Z., Waters, R., Johnston, S. A., and Reed, S. H. (2006) Distinct functions of the ubiquitin-proteasome pathway influence nucleotide excision repair. EMBO J 25, 2529-2538.

Glowczewski, L., Waterborg, J. H., and Berman, J. G. (2004) Yeast chromatin assembly complex 1 protein excludes nonacetylatable forms of histone H4 from chromatin and the nucleus. Mol Cell Biol 24, 10180-10192.

Gornemann, J., Kotovic, K. M., Hujer, K., and Neugebauer, K. M. (2005) Cotranscriptional spliceosome assembly assembly occurs in a stepwise fashion and requires the cap binding complex. Mol Cell 19, 53-63.

Gottschalk, A., Kastner, B., Luhrmann, R., and Fabrizio, P. (2001) The yeast U5 snRNP coisolated with the U1 snRNP has an unexpected protein composition and includes the splicing factor Aar2p. RNA 7, 1554-1565.

Grabowski, P. J., and Sharp, P. A. (1986) Affinity chromatography of splicing complexes: U2, U5, and U4+U6 small nuclear ribonucleoprotein particles in the spliceosome. Science 233, 1294-1299.

Gradolatto, A., Rogers, R. S., Lavender, H., Taverna, S. D., Allis, C. D., Aitchison, J. D., and Tackett, A. J. (2008) *Saccharomyces cerevisiae* Yta7 Regulates Histone Gene Expression. Genetics 179, 291-304.

Grainger, R. J., and Beggs J. D. (2005) Prp8 protein: at the heart of the spliceosome. RNA 11, 533-557.

Granovskaia, M. V., Jensen, L. J, Ritchie, M. E., Toedling, J., Ning, Y., Bork, P., Huber, W., and Steinmetz, L. M. (2010) High-resolution transcription atlas of the mitotic cell cycle in budding yeast. Genome Biology 11, R24.

Green, M. R. (1986) Pre-mRNA splicing. Annu Rev Genet 20, 671-708.

Guzder S. N., Sung P., Prakash L., Prakash S. (1999) Synergistic interaction between yeast nucleotide excision repair factors NEF2 and NEF4 in the binding of ultraviolet-damaged DNA. J Biol Chem 274(34):24257-62.

Hahn D, Beggs JD. Brr2p RNA helicase with a split personality: insights into structure and function. Biochem Soc Trans. 2010 Aug;38(4):1105-9.

Hamm, J., and Mattaj, I. W. (1990) Monomethylated cap structures facilitate RNA export from the nucleus. Cell 63, 109-118.

Hartl, F. U., and Hayer-Hartl, M. (2002) Molecular chaperones in the cytosol: from nascent chain to folded protein. Science 295, 1852-1858.

Hazbun, T. R., Malmström, L., Anderson, S., Graczyk, B. J., Fox, B., Riffle, M., Sundin, B. A., Aranda, J. D., McDonald, W. H., Chiu, C. H., Snydsman, B. E., Bradley, P., Muller, E. G., Fields, S., Baker, D., Yates, Jr. 3rd, and Davis, T. N. (2003) Assigning function to yeast proteins by integration of technologies. Mol Cell 12, 1353-1365.

He, X., van Waardenburg, R. C., Babaoglu, K., Price, A. C., Nitiss, K. C., Nitiss, J. L., Bjornsti, M. A., and White, S. W. (2007) Mutation of a Conserved Active Site Residue Converts Tyrosyl-DNA Phosphodiesterase I into a DNA Topoisomerase I-dependent Poison. J Mol Biol 372, 1070-1081.

Hetzer, M., and Mattaj, I. W. (2000) An ATP-dependent, Ran-independent Mechanism for Nuclear Import of the U1A and U2B" Spliceosome Proteins. J Cell Biol 148, 293-304.

Hinnebusch, A. G., and Fink, G. R. (1983) Positive regulation in the general amino acid control of *Saccharomyces cerevisiae*. Proc Natl Acad Sci USA 80, 5374-5378.

Hinnebusch, A. G., and Natarajan, K. (2002) Gcn4p, a master regulator of gene expression, is controlled at multiple levels by diverse signals of starvation and stress. Eukaryot Cell 1, 22-32.

Hinz, M., Moore, M. J., and Bindereif, A. (1996) Domain analysis of human U5 RNA. Cap trimethylation, protein binding, and spliceosome assembly. J Biol

Chem 271, 19001-19007.

Hogg, R., McGrail, J. C., and O'Keefe, R. T. (2010) The function of the NineTeen Complex (NTC) in regulating spliceosome conformations and fidelity during pre-mRNA splicing. Biochem Soc Trans 38, 1110-1115.

Huber, J., Cronshagen, U., Kadokura, M., Marshallsay, C., Wada, T., Sekine, M., and Luhrmann, R. (1998) Snurportin1, an m3G-cap-specific nuclear import receptor with a novel domain structure. EMBO J 17, 4114-4126.

Huh, W. K., Falvo, J. V., Gerke, L. C., Carroll, A. S., Howson, R. W., Weissman, J. S., and O'Shea, E. K. (2003) Global analysis of protein localization in budding yeast. Nature 425, 686-691.

Interthal, H., and Heyer, W. D. (2000) MUS81 encodes a novel helix-hairpin-helix protein involved in the response to UV- and methylation-induced DNA damage in *Saccharomyces cerevisiae*. Mol Gen Genet 263, 812-827.

Iwase, M., and Toh-e, A. (2001) Nis1 encoded by YNL078W: a new neck protein of *Saccharomyces cerevisiae*. Genes Genet Syst 76, 335-343.

Izaurralde, E., Kutay, U., von Kobbe, C., Mattaj, I. W., and Görlich, D. (1997) The asymmetric distribution of the constituents of the Ran system is essential for transport into and out of the nucleus. EMBO J 16, 6535-6547.

Izaurralde, E., Lewis, J., Gamberi, C., Jarmolowski, A., McGuigan, C., and Mattaj, I. W. (1995) A cap binding protein complex mediating U snRNA export. Nature 376, 709-712.

Jackson, S. P., Lossky, M., and Beggs, J. D. (1988) Cloning of the RNA8 gene of *Saccharomyces cerevisiae*, detection of the RNA8 protein, and demonstration that it is essential for nuclear pre-mRNA splicing. Mol Cell Biol 8, 1067-1075.

Jantsch, M. F., and Gall, J. G. (1992) Assembly and localization of the U1-specific snRNP C protein in the amphibian oocyte. J Cell Biol 119, 1037-1046.

Jurica, M. S., and Moore, M. J. (2003) Pre-mRNA splicing: awash in a sea of proteins. Mol Cell 12, 5-14.

Kanemaki, M., Sanchez-Diaz, A., Gambus, A., and Labib, K. (2003) Functional proteomic identification of DNA replication proteins by induced proteolysis in vivo. Nature 423, 720-724.

Kaufman, P. D., Kobayashi, R., and Stillman, B. (1997) Ultraviolet radiation sensitivity and reduction of telomeric silencing in *Saccharomyces cerevisiae* cells lacking chromatin assembly factor-I. Genes Dev 11, 345-357.

Kennan, A., Aherne, A., and Humphries, P. (2005) Light in retinitis pigmentosa.

Trends Genet 21, 103-110.

Keren, H., Lev-Maor, G., and Ast, G. (2010) Alternative splicing and evolution: diversification, exon definition and function. Nat Rev Genet 11, 345-355.

Kershaw, C. J., Barrass, J. D., Beggs, J. D., and O'Keefe, R. T. (2009) Mutations in the U5 snRNA result in altered splicing of subsets of pre-mRNAs and reduced stability of Prp8. RNA 15, 1292-1304.

Kim, D. H., and Rossi J. J. (1999) The first ATPase domain of the yeast 246-kDa protein is required for in vivo unwinding of the U4/U6 duplex. RNA 5, 959-971.

Kiss, T. (2004) Biogenesis of small nuclear RNPs. J Cell Sci 117, 5949-5951.

Konarska MM, Query CC. Insights into the mechanisms of splicing: more lessons from the ribosome. Genes Dev. 2005 Oct 1;19(19):2255-60.

Konarska, M. M. (2008) A purified catalytically competent spliceosome. Nat Struct Mol Biol 15, 222-224.

Kosmaoglou, M., Schwarz, N., Bett, J. S., and Cheetham, M. E. (2008) Molecular chaperones and photoreceptor function. Prog Retin Eye Res 27, 434-449

Kotovic, K. M., Lockshon, D., Boric, L., and Neugebauer, K. M. (2003) Cotranscriptional recruitment of the U1 snRNP to intron-containing genes in yeast. Mol Cell Biol 23, 5768-5779.

Kozmin, S., Slezak, G., Reynaud-Angelin, A., Elie, C., de Rycke, Y., Boiteux, S., and Sage, E. (2005) UVA radiation is highly mutagenic in cells that are unable to repair 7,8-dihydro-8-oxoguanine in *Saccharomyces cerevisiae*. Proc Natl Acad Sci USA 102, 13538-13543.

Kubota, H., Ota, K., Sakaki,Y., and Ito, T. (2001) Budding yeast GCN1 binds the GI domain to activate the eIF2alpha kinase GCN2. J Biol Chem 276, 17591-17596.

Kuhn, A. N., and Brow, D. A. (2000) Suppressors of a cold-sensitive mutation in yeast U4RNA define five domains in the splicing factor Prp8 that influence spliceosome activation. Genetics 155, 1667-1682.

Kuhn, A. N., Li, Z., and Brown, D. A. (1999) Splicing factor Prp8 governs U4/U6 RNA unwinding during activation of the spliceosome. Mol Cell 3, 65-75.

Lacadie, S. A., and Rosbash, M. (2005) Cotranscriptional spliceosome assembly dynamics and the role of U1 snRNA:5'ss base pairing in yeast. Mol Cell 19, 65-75.

Leff, S. E., Rosenfeld, M. G., and Evans, R. M. (1986). Complex transcriptional units: diversity in gene expression by alternative RNA processing. Annu Rev Biochem 55, 1091–117.

Lerner, M. R., and Steitz, J. A. (1979) Antibodies to small nuclear RNAs complexed with proteins are produced by patients with systemic lupus erythematosus. Proc Natl Acad Sci USA 76,5495-5499.

Lerner, M. R., Boyle, J. A., Mount, S.M., Wolin, S. L., and Steitz, J. A. (1980) Are snRNPs involved in splicing? Nature 283, 220-224.

Levin, D. E., Bowers, B., Chen, C. Y., Kamada, Y., and Watanabe, M. (1994) Dissecting the protein kinase C/MAP kinase signalling pathway of *Saccharomyces cerevisiae*. Cell Mol Biol Res 40, 229-239.

Li, N., Mei, H., MacDonald, I.M., Jiao, X. and Fielding Hejtmancik, J. (2009) Mutations in ASCC3L1 on chromosome 2q11.2 are associated with autosomal dominant retinitis pigmentosa in a Chinese Family. Invest. Ophthalmol. Visual Sci. 51, 1036–1043.

Li, X., Gerber, S. A., Rudner, A. D., Beausoleil, S. A., Haas, W., Villen, J., Elias, J. E., and Gygi,S.P. (2007) Large-scale phosphorylation analysis of alpha-factor-arrested *Saccharomyces cerevisiae*. J Proteome Res 6, 1190-1197.

Liu, L., Query, C. C., and Konarska, M. M. (2007) Opposing classes of prp8 alleles modulate the transition between the catalytic steps of premRNA splicing. Nat Struct Mol Biol 14, 519-526.

Lohi, O., and Lehto, V. P. (1998) VHS domain marks a group of proteins involved in endocytosis and vesicular trafficking. FEBS Lett 440, 255-257.

Lohi, O., Poussu, A., Mao, Y., Quiocho, F., and Lehto, V.P. (2002) VHS domain – a longshoreman of vesicle lines. FEBS Lett 513, 19-23.

Lommel, L., Ortolan, T., Chen, L., Madura, K., and Sweder, K. S. (2002) Proteolysis of a nucleotide excision repair protein by the 26 S proteasome. Curr Genet 42, 9-20.

Longtine, M. S., McKenzie 3rd, A., Demarini, D. J., Shah, N. G., Wach, A., Brachat, A., Philippsen, P., and Pringle, J. R. (1998) Additional modules for versatile and economical PCR-based gene deletion and modification in *Saccharomyces cerevisiae*. Yeast 14, 953-961.

Lossky, M., Anderson, G. J., Jackson, S. P., and Beggs, J. (1987) Identification of a yeast snRNP protein and detection of snRNP-snRNP interactions. Cell 51, 1019-1026.

Louis, E. J. (1995) The chromosome ends of *Saccharomyces cerevisiae*. Yeast 11, 1553-1573.

Louis, E. J., and Haber, J. E. (1992) The structure and evolution of subtelomeric Y' repeats in *Saccharomyces cerevisiae*. Genetics 131, 559-574.

Louis, E. J., Naumova, E. S., Lee, A., Naumov, G., and Haber, J. E. (1994) The chromosome end in yeast: its mosaic nature and influence on recombinational dynamics. Genetics 136, 789-802.

Lucchini, G., Hinnebusch, A. G., Chen, C., and Fink, G. R. (1984) Positive regulatory interactions of the HIS4 gene of *Saccharomyces cerevisiae*. Mol Cell Biol 4, 1326-1333.

Luo, H. R., Moreau, G. A., Levin, N., and Moore, M. J. (1999) The human Prp8 protein is a component of both U2- and U12-dependent spliceosomes. RNA 5, 893-908.

Lutzmann, M., Kunze, R., Stangl, K., Stelter, P., Tóth, K. F., Böttcher, B., and Hurt, E. (2005) Reconstitution of Nup157 and Nup145N into the Nup84 complex. J Biol Chem 280, 18442-18451.

Lygerou, Z., Christophides, G., and Séraphin, B. (1999) A novel genetic screen for snRNP assembly factors in yeast identifies a conserved protein, Sad1p, also required for pre-mRNA splicing. Mol Cell Biol 19, 2008-2020.

Maeder, C., Kutach, A.K. and Guthrie, C. (2009) ATP-dependent unwinding of U4/U6 snRNAs by the Brr2 helicase requires the C terminus of Prp8. Nat Struct Mol Biol 16, 42-48.

Makarov, E. M., Makarova, O. V., Urlaub, H., Gentzel, M., Will, C. L., Wilm, M., and Lührmann, R. (2002) Small nuclear ribonucleoprotein remodeling during catalytic activation of the spliceosome. Science 298, 2205-2208.

Martin, A., Schneider, S. and Schwer, B. (2002) Prp43 is an essential RNA-dependent ATPase required for release of lariat-intron from the spliceosome. J Biol Chem 277, 17743–17750.

Mathew, R., Hartmuth, K., Möhlmann, S., Urlaub, H., Ficner, R., and Lührmann, R. (2008) Phosphorylation of human PRP28 by SRPK2 is required for integration of the U4/U6-U5 tri-snRNP into the spliceosome. Nat Struct Mol Biol. 15, 435-443.

Mayas RM, Maita H, Semlow DR, Staley JP. (2010) Spliceosome discards intermediates via the DEAH box ATPase Prp43p. Proc Natl Acad Sci U S A. 1;107(22).

Mayes, A. E., Potashkin, J. A., Beggs, J. D. (2000). Splicing pre-mRNA introns. The yeast nucleus (ed Fantes, P., and Beggs, J.). Oxford University Press, Great Clarendon Street, Oxford OX2 6DP. Pg246-275.

Maytal-Kivity, V., Reis, N., Hofmann, K., and Glickman, M.H. (2002). MPN+, a putative catalytic motif found in a subset of MPN domain proteins from eukaryotes and prokaryotes, is critical for Rpn11 function. BMC Biochem. 3, 28.

McKie, A. B., McHale, J. C., Keen, T. J., Tarttelin, E. E., Goliath, R., van Lith-Verhoeven, J. J., Greenberg, J., Ramesar, R. S., Hoyng, C. B., Cremers, F. P., Mackey, D. A., Bhattacharya, S. S., Bird, A. C., Markham, A. F., and Inglehearn, C. F. (2001) Mutations in the pre-mRNA splicing factor gene PRPC8 in autosomal dominant retinitis pigmentosa (RP13.). Hum Mol Genet 10, 1555-1562.

Meiling-Wesse, K., Barth, H., Voss, C., Barmark, G., Murén, E., Ronne, H., and Thumm, M. (2002) Yeast Mon1p/Aut12p functions in vacuolar fusion of autophagosomes and cvt-vesicles. FEBS Lett 530, 174-180.

Menacho-Marquez, M., Perez-Valle, J., Ariño, J., Gadea, J., and Murguía, J. R. (2007) Gcn2p regulates a G1/S cell cycle checkpoint in response to DNA damage. Cell Cycle 6, 2302-2305.

Methods in yeast genetics, a Cold Spring Harbor laboratory course manual. (2000). Edited by Burke D., Dawson, D., Stearns, T. Cold Spring Harbor Laboratory Press, Cold Spring Harbor, New York, United States of America.

Misteli, T. (1999) RNA splicing: What has phosphorylation got to do with it? Curr Biol 9, R198-200.

Miura, F., Kawaguchi, N., Sese, J., Toyoda, A., Hattori, M., Morishita, S., and Ito, T. (2006) A large-scale full-length cDNA analysis to explore the budding yeast transcriptome. Proc Natl Acad Sci USA 103, 17846-17851.

Mordes, D., Luo, X., Kar, A., Kuo, D., Xu, L., Fushimi, K., Yu, G., Sternberg, P. Jr, and Wu, J. Y. (2006) Pre-mRNA splicing and retinitis pigmentosa. Mol Vis 12, 1259-1271.

Mount, S. M. (1982). A catalogue of splice junction sequences. Nucleic Acids Res 10, 459-472.

Nakazawa, N., Harashima, S., and Oshima, Y. (1991) AAR2 a gene for splicing pre-mRNA of the MATa1 cistron in cell type control of *Saccharomyces cerevisiae*. Mol Cell Biol 11, 5693-5700.

Nash, H. M., Bruner, S. D., Schärer, O. D., Kawate, T., Addona, T. A., Spooner, E., Lane, W. S., and Verdine, G. L. (1996) Cloning of a yeast 8-oxoguanine DNA

glycosylase reveals the existence of a base-excision DNA-repair protein superfamily. Curr Biol 6, 968-980.

Nekrasov, V. S., Smith, M. A., Peak-Chew, S., and Kilmartin, J. V. (2003) Interactions between centromere complexes in *Saccharomyces cerevisiae*. Mol Biol Cell 4931-4946.

Nesic, D., Tanackovic, G., and Kramer, A. (2004) A role for Cajal bodies in the final steps of U2 snRNP biogenesis. J Cell Sci 117, 4423-4433.

Newman, A. J., and Nagai, K. (2010) Structural studies of the spliceosome: blind men and an elephant. Curr Opin Struct Biol 20, 82-89.

Nitiss, K. C., Malik, M., He, X., White, S. W., and Nitiss, J. L. (2006) Tyrosyl-DNA phosphodiesterase (Tdp1) participates in the repair of Top2-mediated DNA damage. Proc Natl Acad Sci USA 103, 8953-8958.

Noble, S. M., and Guthrie, C. (1996) Identification of novel genes required for yeast pre-mRNA splicing by means of cold-sensitive mutations. Genetics 143, 67-80.

O'Keefe, R. T., and Newman, A. J. (1998) Functional analysis of the U5 snRNA loop 1 in the second catalytic step of yeast pre-mRNA splicing. EMBO J 17, 565-574.

O'Keefe, R. T., Norman, C., and Newman, A. J. (1996) The invariant U5 snRNA loop1 sequence is dispensable for the first catalytic step of pre-mRNA splicing in yeast. Cell 86, 679-689.

Oh, S. D., Lao, J. P., Taylor, A. F., Smith, G. R., and Hunter, N. (2008) RecQ helicase, Sgs1, and XPF family endonuclease, Mus81-Mms4, resolve aberrant joint molecules during meiotic recombination. Mol Cell 31, 324-336.

Ohno, M., Segref, A., Bachi, A., Wilm, M., and Mattaj, I. W. (2000) PHAX, a mediator of U snRNA nuclear export whose activity is regulated by phosphorylation. Cell 101, 187-198.

Palacios, I., Hetzer, M., Adam, S. A., and Mattaj I. W. (1997) Nuclear import of U snRNPs requires importin beta. EMBO J 16, 6783-6792.

Pandit, S., Lynn, B., and Rymond, B. C. (2006) Inhibition of a spliceosome turnover pathway suppresses splicing defects. Proc Natl Acad Sci USA 103, 13700-13705.

Patel, S. B., and Bellini, M. (2008) The assembly of a spliceosomal small nuclear ribonucleoprotein particle. Nucleic Acids Res 36, 6482-6493.

Patterson, B., and Guthrie, C. (1987) An essential yeast snRNA with a U5-like domain is required for splicing in vivo. Cell 49, 613-624.

Pena, V., Liu, S., Bujnicki, J. M., Lührmann, R., and Wahl, M. C. (2007) Structure of a multipartite protein-protein interaction domain in splicing factor prp8 and its link to retinitis pigmentosa. Mol Cell 25, 615-624.

Pena, V., Rozov, A., Fabrizio, P., Lührmann, R., and Wahl, M. C. (2008) Structure and function of an RNase H domain at the heart of the spliceosome. EMBO J 27, 2929-2940.

Peterson, C. L., and Herskowitz, I. (1992) Characterization of the yeast SWI1, SWI2, and SWI3 genes, which encode a global activator of transcription. Cell 68, 573-583.

Peterson, C. L., Dingwall, A., and Scott, M. P. (1994) Five SWI/SNF gene products are components of a large multisubunit complex required for transcriptional enhancement. Proc Natl Acad Sci USA 91, 2905-2908.

Petukhova, G., Van Komen, S., Vergano, S., Klein, H., and Sung, P. (1999) Yeast Rad54 promotes Rad51-dependent homologous DNA pairing via ATP hydrolysis-driven change in DNA double helix conformation. J Biol Chem 274, 29453-29462.

Pouliot, J. J., Yao, K. C., Robertson, C. A., and Nash, H. A. (1999) Yeast gene for a Tyr-DNA phosphodiesterase that repairs topoisomerase I complexes. Science 286, 552-555.

Prakash, S., and Prakash, L. (2000) Nucleotide excision repair in yeast. Mutat Res 451, 13-24.

Pryde, F. E., Gorham, H. C., and Louis, E. J. (1997) Chromosome ends: all the same under their caps. Curr Opin Genet Dev 7, 822-828.

Ptacek, J., Devgan, G., Michaud, G., Zhu, H., Zhu, X., Fasolo, J., Guo, H., Jona, G., Breitkreutz, A., Sopko, R., McCartney, R. R., Schmidt, M. C., Rachidi, N., Lee, S. J., Mah, A. S., Meng, L., Stark, M. J., Stern, D. F., De Virgilio, C., Tyers, M., Andrews, B., Gerstein, M., Schweitzer, B., Predki, P. F., and Snyder, M. (2005) Global analysis of protein phosphorylation in yeast. Nature 438, 679-684.

Raghunathan, P. L., and Guthrie C. (1998) RNA unwinding in U4/U6 snRNPs requires ATP hydrolysis and the DEIH-box splicing factor Brr2. Curr Biol 8, 847-855.

Raveendranathan, M., Chattopadhyay, S., Bolon, Y. T., Haworth, J., Clarke, D. J., and Bielinsky, A. K. (2006) Genome-wide replication profiles of S-phase checkpoint mutants reveal fragile sites in yeast. EMBO J 25, 3627-3639.

Romac, J. M. J., Graff, D. H., and Keene, J. D. (1994) The U1 small nuclear

ribonucleoprotein (snRNP) 70k protein is transported independently of U1 snRNP particles via a nuclear localization signal in the RNA-binding domain. Mol. Cell Biol 14, 4662-4670.

Roumanie, O., Weinachter, C., Larrieu, I., Crouzet, M., and Doignon, F. (2001) Functional characterization of the Bag7, Lrg1 and Rgd2 RhoGAP proteins from Saccharomyces cerevisiae. FEBS Lett 506, 149-156.

Rout, M. P., Aitchison, J. D., Suprapto, A., Hjertaas, K., Zhao, Y., and Chait, B. T. (2000) The yeast nuclear pore complex: composition, architecture, and transport mechanism. J Cell Biol 148, 635-651.

Salzano, A. M., and Crescenzi, M. (2005) Mass spectrometry for protein identification and the study of post translational modifications. Ann Ist Super Sanita 41, 443-450.

Sambrook and Russell (2001) Molecular Cloning: A Laboratory Manual (3rd ed.). Cold Spring Harbor Laboratory Press.

Schlosser, A., Vanselow, J. T., and Kramer, A. (2005) Mapping of phosphorylation sites by a multi-protease approach with specific phosphopeptide enrichment and NanoLC-MS/MS analysis. Anal Chem 77, 5243-5250.

Schnall, R., Mannhaupt, G., Stucka, R., Tauer, R., Ehnle, S., Schwarzlose, C., Vetter, I., and Feldmann, H. (1994) Identification of a set of yeast genes coding for a novel family of putative ATPases with high similarity to constituents of the 26S protease complex. Yeast 10, 1141-1155.

Schneider, M., Hsiao, H. H., Will, C. L., Giet, R., Urlaub, H., and Lührmann, R. (2010) Human PRP4 kinase is required for stable tri-snRNP association during spliceosomal B complex formation. Nat Struct Mol Biol 17, 216-221.

Schneider, S., Hotz, H. R., and Schwer, B. (2002) Characterization of dominant-negative mutants of the DEAH-box splicing factors Prp22 and Prp16. J Biol Chem 277, 15452-15458.

Schwartz, M. F., Duong, J. K., Sun, Z., Morrow, J. S., Pradhan, D., and Stern, D. F. (2002) Rad9 phosphorylation sites couple Rad53 to the Saccharomyces cerevisiae DNA damage checkpoint. Mol Cell 9, 1055-1065.

Schwer, B., and Gross, C. H. (1998) Prp22, a DExH-box RNA helicase, plays two distinct roles in yeast pre-mRNA splicing. EMBO J 17, 2086-2094.

Sefton, B. M., and Shenolikar, S. (2001) Overview of protein phosphorylation. Curr Protoc Protein Sci, Chapter 13.

Segault, V., Will, C. L., Polycarpou-Schwarz, M., Mattaj, I. W., Branlant, C., and Luhrmann, R. (1999) Conserved loop I of U5 small nuclear RNA is

dispensable for both catalytic steps of pre-mRNA splicing in HeLa nuclear extracts. Mol Cell Biol 19, 2782-2790.

Shi, Y., Reddy, B., and Manley, J. L. (2006) PP1/PP2A phosphatases are required for the second step of Pre-mRNA splicing and target specific snRNP proteins. Mol Cell 23, 819-829.

Shih, J. L., Reck-Peterson, S. L., Newitt, R., Mooseker, M. S., Aebersold, R., and Herskowitz, I. (2005) Cell polarity protein Spa2P associates with proteins involved in actin function in *Saccharomyces cerevisiae*. Mol Biol Cell 16, 4595-4608.

Shirahige, K., Iwasaki, T., Rashid, M. B., Ogasawara, N., and Yoshikawa, H. (1993) Location and characterization of autonomously replicating sequences from chromosome VI of *Saccharomyces cerevisiae*. Mol Cell Biol 13, 5043-5056.

Singh, K. K., Sigala, B., Sikder, H. A., and Schwimmer, C. (2001) Inactivation of *Saccharomyces cerevisiae* OGG1 DNA repair gene leads to an increased frequency of mitochondrial mutants. Nucleic Acids Res 29, 1381-1388.

Small, E. C., Leggett, S. R., Winans, A. A., and Staley, J. P. (2006) The EF-G-like GTPase Snu114p regulates spliceosome dynamics mediated by Brr2p, a DExD/H box ATPase. Mol Cell 23, 389-399.

Smith, C. L., Horowitz-Scherer, R., Flanagan, J. F., Woodcock, C. L., and Peterson, C. L. (2003) Structural analysis of the yeast SWI/SNF chromatin remodeling complex. Nat Struct Biol 10, 141-145.

Staley, J. P., and Guthrie, C. (1998) Mechanical devices of the spliceosome: motors, clocks, springs, and things. Cell 92, 315-326.

Stevens, S. W. and Abelson, J. (1999) Purification of the yeast U4/U6.U5 small nuclear ribonucleoprotein particle and identification of its proteins. Proc Natl Acad Sci USA 96, 7226-7231.

Stevens, S.W., Barta, I., Ge, H. Y., Moore, R. E., Young, M. K., Lee, T. D., and Abelson, J. (2001) Biochemical and genetic analyses of the U5, U6, and U4/U6 x U5 small nuclear ribonucleoproteins from *Saccharomyces cerevisiae*. RNA 7, 1543-1553.

Stoltzfus, A. (2001). Introns and Exons. In Encyclopedia of Genetics (Brenner, S. & Miller, J. H., eds), pp. 1052. London, Elsevier Science Inc.

Strawn, L. A., Shen, T., and Wente, S. R. (2001) The GLFG regions of Nup116p and Nup100p serve as binding sites for both Kap95p and Mex67p at the nuclear pore complex. J Biol Chem 276, 6445-6452.

Swaffield, J. C., and Purugganan, M. D. (1997) The evolution of the conserved

ATPase domain (CAD): reconstructing the history of an ancient protein module. J Mol Evol 45, 549-563.

Takayama, Y., Kamimura, Y., Okawa, M., Muramatsu, S., Sugino, A., and Araki, H. (2003) GINS, a novel multiprotein complex required for chromosomal DNA replication in budding yeast. Genes Dev 17, 1153-1165.

Teigelkamp, S., Newman, A. J, and Beggs, J. D. (1995) Extensive interactions of PRP8 protein with the 5' and 3' splice sites during splicing suggest a role in stabilization of exon alignment by U5 snRNA. EMBO J 14, 2602-2612.

Thireos, G., Penn, M. D., and Greer, H. (1984) 5' untranslated sequences are required for the translational control of a yeast regulatory gene. Proc Natl Acad Sci USA 81, 5096-5100.

Toh GW and Lowndes NF (2003) Role of the Saccharomyces cerevisiae Rad9 protein in sensing and responding to DNA damage. Biochem Soc Trans 31(Pt 1):242-6

Tsai RT, Fu RH, Yeh FL, Tseng CK, Lin YC, Huang YH, Cheng SC. (2005) Spliceosome disassembly catalyzed by Prp43 and its associated components Ntr1 and Ntr2. Genes Dev 19, 2991-3003.

Umen, J. G, and Guthrie, C. (1995) A novel role for a U5 snRNP protein in 3' splice site selection. Genes Dev 9, 855-868.

Ungar, L., Yosef, N., Sela, Y., Sharan, R., Ruppin, E., and Kupiec, M. (2009) A genome-wide screen for essential yeast genes that affect telomere length maintenance. Nucleic Acids Res 37, 3840-3849.

van Nues, R. W., and Beggs, J. D. (2001) Functional contacts with a range of splicing proteins suggest a central role for Brr2p in the dynamic control of the order of events in spliceosomes of *Saccharomyces cerevisiae*. Genetics 157, 1451-1467.

Vijayraghavan, U., Company, M., and Abelson, J. (1989) Isolation and characterization of pre-mRNA splicing mutants of *Saccharomyces cerevisiae*. Genes Dev 3, 1206-1216.

Wachtel, C., and Manley, J. L. (2009) Splicing of mRNA precursors: the role of RNAs and proteins in catalysis. Mol Biosyst 5, 311-316.

Wahl, M. C., Will, C. L., and Lührmann, R. (2009) The spliceosome: design principles of a dynamic RNP machine. Cell 136, 701-718.

Wang, G. S., and Cooper, T. A. (2007) Splicing in disease: disruption of the splicing code and the decoding machinery. Nat Rev Genet 8, 749-761.

Wang, G. S., and Cooper, T. A. (2007) Splicing in disease: disruption of the splicing code and the decoding machinery. Nature Rev Genet 8, 749-761.

Warkocki, Z., Odenwälder, P., Schmitzová, J., Platzmann, F., Stark, H., Urlaub, H., Ficner, R., Fabrizio, P., and Lührmann, R. (2009) Reconstitution of both steps of *Saccharomyces cerevisiae* splicing with purified spliceosomal components. Nat Struct Mol Biol 16, 1237-1243.

Watanabe, M., Chen, C. Y., and Levin, D. E. (1994) *Saccharomyces cerevisiae* PKC1 encodes a protein kinase C (PKC) homolog with a substrate specificity similar to that of mammalian PKC. J Biol Chem 269, 16829-16836.

Waterhouse, A. M., Procter, J. B., Martin, D. M., Clamp, M., Barton, G. J. (2009) Jalview Version 2: a multiple sequence alignment editor and analysis workbench. Bioinformatics 25, 1189-1191.

Werner-Washburne, M., Stone, D. E., and Craig, E. A. (1987) Complex interactions among members of an essential subfamily of hsp70 genes in *Saccharomyces cerevisiae*. Mol Cell Biol 7, 2568-2577.

Whittaker, E., and Beggs J. D. (1991) The yeast PRP8 protein interacts directly with pre-mRNA. Nucleic Acids Res 19, 5483-5489.

Whittaker, E., Lossky, M., and Beggs, J. D. (1990) Affinity purification of spliceosomes reveals that the precursor RNA processing protein PRP8, a protein in the U5 small nuclear ribonucleoprotein particle, is a component of yeast spliceosomes. Proc Natl Acad Sci USA 87, 2216-2219.

Wiederkehr, A., Avaro, S., Prescianotto-Baschong, C., Haguenauer-Tsapis, R., and Riezman, H. (2000) The F-box protein Rcy1p is involved in endocytic membrane traffic and recycling out of an early endosome in *Saccharomyces cerevisiae*. J Cell Biol 149, 397-410.

Will, C. L., and Lührmann, R. (2001) Spliceosomal UsnRNP biogenesis structure and function. Curr Opin Cell Biol 13, 290-301.

Wyrick, J. J., Aparicio, J. G., Chen, T., Barnett, J. D., Jennings, E. G., Young, R. A., Bell, S. P., and Aparicio, O. M. (2001) Genome-wide distribution of ORC and MCM proteins in *S. cerevisiae*: high-resolution mapping of replication origins. Science 294, 2357-2360.

Xu, W., Aparicio, J. G., Aparicio, O. M., and Tavaré, S. (2006) Genome-wide mapping of ORC and Mcm2p binding sites on tiling arrays and identification of essential ARS consensus sequences in *S. cerevisiae*. BMC Genomics 7, 276.

Yamada, M., Hayatsu, N., Matsuura, A., and Ishikawa, F. (1998) Y'-Help1, a DNA helicase encoded by the yeast subtelomeric Y' element, is induced in survivors defective for telomerase. J Biol Chem 273, 33360-33366.

Yang, K., Zhang, L., Xu, T., Heroux, A., Zhao, R. (2008) Crystal structure of the beta-finger domain of Prp8 reveals analogy to ribosomal proteins. Proc Natl Acad Sci USA 105, 13817-13822.

Yeast Resource Center. Fields S., unpublished data. Available at: http://www.yeastrc.org/pdr/viewY2HScreen.do;jsessionid=BE7C258B1333640D9E378A636E0A2380?ID=25 (accessed March 2009).

Zhao, C., Bellur, D., Lu, S., Zhao, F., Grassi, M. A., Bowne, S. J., Sullivan, L. S., Daiger, S. P., Chen, L. J., Pang, C. P., Zhao, K., Staley, J. P., and Larsson, C. (2009) Autosomal-dominant retinitis pigmentosa caused by a mutation in SNRNP200, a gene required for unwinding of U4/U6 snRNAs. Am J Hum Genet 85, 617-627.

Zhu, H., Klemic, J. F., Chang, S., Bertone, P., Casamayor, A., Klemic, K. G., Smith, D., Gerstein, M., Reed, M. A., and Snyder, M. (2000) Analysis of yeast protein kinases using protein chips. Nat Genet 26, 283-289.

Zhuo, S., Clemens, J. C., Hakes, D. J., Barford, D., and Dixon, J. E. (1993) Expression, purification, crystallization, and biochemical characterization of a recombinant protein phosphatase. J Biol Chem 268, 17754-17761.